

คุณลักษณะและบทบาทของสปีชีส์บนพื้นผิวในปฏิกิริยารีดักชันแบบเลือกเกิดของไนตริก  
ออกไซด์โดยใช้โพรพีนบนตัวเร่งปฏิกิริยาซิลเวอร์บนตัวรองรับ อะลูมินาโดยเทคนิค

โปรแกรมอุณหภูมิต



นายณัฐยา เกียจติศิริกุล

สถาบันวิทยบริการ

วิทยานิพนธ์นี้เป็นส่วนหนึ่งของการศึกษาตามหลักสูตรปริญญาวิศวกรรมศาสตรมหาบัณฑิต

สาขาวิชาวิศวกรรมเคมี ภาควิชาวิศวกรรมเคมี

คณะวิศวกรรมศาสตร์ จุฬาลงกรณ์มหาวิทยาลัย

ปีการศึกษา 2546

ISBN 974-17-4518-4

ลิขสิทธิ์ของจุฬาลงกรณ์มหาวิทยาลัย

**CHARACTERISTICS AND ROLES OF SURFACE SPECIES IN C<sub>3</sub>H<sub>6</sub>-SCR  
OF NO OVER A Ag/Al<sub>2</sub>O<sub>3</sub> CATALYST BY TEMPERATURE  
PROGRAMMED TECHNIQUE**



Mr. Natthaya Kiattisirikul

A Thesis Submitted in Partial Fulfillment of the Requirements  
for the Degree of Master of Engineering in Chemical Engineering  
Department of Chemical Engineering

Faculty of Engineering  
Chulalongkorn University

Academic Year 2003

ISBN 974-17-4518-4

Thesis Title           CHARACTERISTICS AND ROLES OF SURFACE SPECIES IN  
C<sub>3</sub>H<sub>6</sub>-SCR OF NO OVER A Ag/Al<sub>2</sub>O<sub>3</sub> CATALYST BY  
TEMPERATURE PROGRAMMED TECHNIQUE

By                       Mr. Natthaya Kiattisirikul

Field of Study        Chemical Engineering

Thesis Advisor       Professor Piyasan Praserthdam, Dr.Ing.

---

Accepted by the Faculty of Engineering, Chulalongkorn University in Partial  
Fulfillment of the Requirements for the Master's Degree

.....Dean of Faculty of Engineering  
(Professor Somsak Panyakeow, D.Eng.)

#### THESIS COMMITTEE

..... Chairman  
(Montree Wongsri, D.Sc.)

.....Thesis Advisor  
(Professor Piyasan Praserthdam, Dr.Ing.)

.....Thesis Co-Advisor  
(Choowong Chaisuk, D.Eng.)

.....Member  
(Suphot Phatanasri, D.Eng.)

.....Member  
(Bongkot Ngamsom, D.Eng.)

นัสธยา เกียรติศิริกุล : คุณลักษณะและบทบาทของสปีชีส์บนพื้นผิวในปฏิกิริยารีดักชันแบบเลือกเกิดของไนตริกออกไซด์โดยใช้โพรพีนบนตัวเร่งปฏิกิริยาซิลเวอร์บนตัวรองรับอะลูมินาโดยเทคนิคโปรแกรมอุณหภูมิ (CHARACTERISTICS AND ROLES OF SURFACE SPECIES IN C<sub>3</sub>H<sub>6</sub>-SCR OF NO OVER A Ag/Al<sub>2</sub>O<sub>3</sub> CATALYST BY TEMPERATURE PROGRAMMED TECHNIQUE.)

อ. ที่ปรึกษา : ศ.ดร.ปิยะสาร ประเสริฐธรรม, อ.ที่ปรึกษาร่วม : ดร.ชูวงศ์ ชัยสุข, 79 หน้า.

ISBN 947-17-4518-4

ในงานวิจัยนี้ พฤติกรรมของสารบนพื้นผิวที่เกิดขึ้นบนตัวเร่งปฏิกิริยาซิลเวอร์บนตัวรองรับอะลูมินาในปฏิกิริยารีดักชันแบบเลือกเกิดของไนตริกออกไซด์โดยใช้ไฮโดรคาร์บอนได้ถูกศึกษาผ่านเทคนิคโปรแกรมอุณหภูมิ เมื่อใช้โพรพีนเป็นแบบของสารรีดิวซ์ ชุดการทดลองที่มี 3 ขั้นตอนต่อเนื่องกัน ประกอบด้วย ขั้นตอนการเกิดปฏิกิริยา ขั้นตอนทำให้หลุดออกแบบโปรแกรมอุณหภูมิ และขั้นตอนการออกซิเดชันแบบโปรแกรมอุณหภูมิ แสดงให้เห็นว่ามีสารบนพื้นผิวอย่างน้อย 5 สปีชีส์ซึ่งเกิดขึ้นทั้งในขั้นตอนทำให้หลุดออกแบบโปรแกรมอุณหภูมิ และขั้นตอนการออกซิเดชันแบบโปรแกรมอุณหภูมิ จากการทดสอบรีแอคทีวิตีของสารบนพื้นผิวบนตัวเร่งปฏิกิริยาซิลเวอร์บนตัวรองรับอะลูมินาและซิลเวอร์บนตัวรองรับซิลิกาแสดงให้เห็นว่ามีเพียงสารบนพื้นผิวเพียง 2 ชนิด คือ สารที่สามารถหลุดออกที่อุณหภูมิต่ำและสารที่ต้องถูกออกซิไดซ์ด้วยออกซิเจนที่อุณหภูมิสูง ที่แสดงบทบาทสำคัญในการสร้างไนโตรเจน ดังนั้นกลไกการเกิดปฏิกิริยาประกอบด้วย 2 กลไกหลัก คือ การสลายตัวและการเกิดรีดักชันของไนตริกออกไซด์ นอกจากนี้ผลที่ได้ยังแสดงให้เห็นว่าสารที่ต้องถูกออกซิไดซ์ด้วยออกซิเจนที่อุณหภูมิสูงปรากฏครั้งแรกบนบริเวณเร่งของซิลเวอร์หลังจากนั้นมีการย้ายไปอยู่บนบริเวณเร่งของอะลูมินา และเกิดปฏิกิริยากับแก๊สผสมของไนตริกออกไซด์กับออกซิเจนเพื่อสร้างสารที่สามารถหลุดออกที่อุณหภูมิต่ำ ดังนั้นเทคนิคโปรแกรมอุณหภูมิไม่ได้ใช้เพื่อศึกษาพฤติกรรมของสารบนพื้นผิวเพียงอย่างเดียวแต่ยังนำมาประยุกต์ในการศึกษาถึงตำแหน่งของสารบนพื้นผิวที่เกิดขึ้น

ภาควิชา.....วิศวกรรมเคมี..... ลายมือชื่อนิสิต.....

สาขาวิชา.....วิศวกรรมเคมี..... ลายมือชื่ออาจารย์ที่ปรึกษา.....

ปีการศึกษา.....2545..... ลายมือชื่ออาจารย์ที่ปรึกษาร่วม.....

##4570386321: MAJOR CHEMICAL ENGINEERING

KEY WORD: Ag/Al<sub>2</sub>O<sub>3</sub> / SURFACE SPECIES / SCR

NATTHAYA KIATTISIRIKUL: CHARACTERISTICS AND ROLES OF SURFACE SPECIES IN C<sub>3</sub>H<sub>6</sub>-SCR OF NO OVER A Ag/Al<sub>2</sub>O<sub>3</sub> CATALYST BY TEMPERATURE PROGRAMMED TECHNIQUE. THESIS ADVISOR: PROF. PIYASAN PRASERTHDAM, Dr.Ing., THESIS COADVISOR: DR.CHOOWONG CHAISUK, Dr.ENG., 76 pp. ISBN 974-17-4518-4

### Abstract

In this thesis, the behavior of surface species which occur in the selective catalytic reduction of nitric oxide by hydrocarbon over Ag/Al<sub>2</sub>O<sub>3</sub> catalyst under excess oxygen was investigated through the Temperature Programmed Technique. With propene as a model reductant, and experimental set of three continuous steps containing reaction step, temperature programmed desorption step and temperature programmed oxidation step shows that there are at least five types of surface species occurred on Ag/Al<sub>2</sub>O<sub>3</sub> both TPD and TPO step. From the reactivity tests of surface species on Ag/Al<sub>2</sub>O<sub>3</sub> and Ag/SiO<sub>2</sub> indicate that only two surface species, S<sub>TPDL</sub> and S<sub>TPOH</sub>, play an important role in the production of N<sub>2</sub>. Hence, the reaction mechanisms consist of two pathways including the decomposition of S<sub>TPDL</sub> species and the NO reduction of S<sub>TPOH</sub> species. Moreover, the results show that the S<sub>TPOH</sub> species first occurred on silver active site after expose to the reactant gases and then move to the alumina active site. In addition, some of S<sub>TPOH</sub> species can react with NO+O<sub>2</sub> to form the other surface species (S<sub>TPDL</sub>). Therefore, the Temperature Programmed Techniques do not use only to characterize the behavior of surface species but also apply to investigate the appeared position of surface species.

Department.....Chemical Engineering... Student's signature.....

Field of study...Chemical Engineering... Advisor's signature.....

Academic year.....2002..... Co-Advisor's signature.....

## ACKNOWLEDGEMENTS

The author would like to express his greatest gratitude to Professor Dr. Piyasan Prasertdam, his thesis advisor, for his perceptive questions, continuous guidance, kind suggestion and encouragement during his study. He is similarly grateful for the heartfelt assistance, encouragement and friendship that he has received from Dr. Choowong Chaisuk, his co-advisor. In particular, he is also grateful to Dr. Montree Wongsri, as Chairman and, Dr. Suphot Phatanasri and Dr. Bongkot Ngamsom as the members of thesis committee.

Special thank to Miss Tananya Vongthaworn who has encouraged him over the year of this study. To the many other not specially named who have provide him with information, support and encouragement, please be assured that he thinks of them.

Finally, he would also like to manifest his greatest gratitude to his parent and his family for their supported and encouragement.

สถาบันวิทยบริการ  
จุฬาลงกรณ์มหาวิทยาลัย

# CONTENTS

	page
ABSTRACT (IN THAI).....	iv
ABSTRACT (IN ENGLISH).....	v
ACKNOWLEDGMENTS.....	vi
CONTENTS.....	vii
LIST OF TABLES.....	x
LIST OF FIGURES.....	xi
CHAPTER	
I    INTRODUCTION.....	1
II   SELECTIVE REDUCTION OF NO <sub>x</sub> WITH HYDROCARBON OVER Ag-BASED CATALYST UNDER LEAN-BURN CONDITION AND OVERALL MECHANISM STUDIES.....	7
2.1 Overview of SCR over Ag-Based Catalyst.....	9
2.2 Mechanism Studies.....	16
III  EXPERIMENTAL.....	24
3.1 Catalyst Preparation.....	24
3.1.1 Chemicals.....	24
3.1.2 Preparation of Support.....	25
3.1.3 Preparation of Silver Catalyst.....	25
3.2 Catalyst Characterization.....	26
3.2.1 X-ray Diffraction .....	26
3.2.2 Silver Metal Active Sites Measurement by N <sub>2</sub> O Decomposition Method.....	26
3.2.3 Basicity by CO <sub>2</sub> TPD.....	29
3.3 Catalyst Activities and Characterization of Surface Species.....	30

## CONTENTS (CONT.)

	page
IV RESULTS AND DISCUSSION.....	35
4.1 The Characterization of Ag/Al <sub>2</sub> O <sub>3</sub> Catalyst.....	35
4.1.1 X-ray Diffraction Analysis .....	35
4.1.2 The Basicity by CO <sub>2</sub> -TPD.....	36
4.2 Evaluation of Surface Species.....	37
4.2.1 The Nature of Surface Species.....	39
4.2.2 The Nature Study by Using Physical Mixture of Ag/SiO <sub>2</sub> and Al <sub>2</sub> O <sub>3</sub> .....	51
V CONCLUSIONS AND RECOMMENDATIONS.....	59
REFERENCES.....	61
APPENDICES.....	69
APPENDIC A SPECIFICATION OF ALUMINA SUPPORT (Al <sub>2</sub> O <sub>3</sub> ) TYPE NKH-3.....	70
APPENDIC B CALIBRATION CURVES.....	71
APPENDIC C CALCULATION OF CATALYST PREPARATION.....	77
APPENDIC D CALCULATION OF SILVER METAL ACTIVE SITE ON CATALYST.....	78
VITA.....	79



## LIST OF TABLES

Table	page
1.1 Operating characteristics of different SCR catalyst.....	3
3.1 Details of chemical reagents used for catalyst preparation.....	24
3.2 Operating condition of a thermal conductivity detector within a gas chromatograph (GOW-MAC) for measurement of the metal active sites..	27
3.3 Operating condition of a thermal conductivity detector within a gas chromatograph (GOW-MAC) for measurement of CO <sub>2</sub> TPD.....	29
3.4 The details of gases used in the catalyst activity test.....	30
3.5 Operating conditions of gas chromatographs for the catalytic activity test..	32
4.1 Metal Active Sites Measurement of Silver.....	57
5.1 The reactivity of surface species with oxidizing gases.....	60
A.1 Chemical composition of alumina support type NKH-3.....	70
A.2 Physical properties of alumina support type NKH-3.....	70

## LIST OF FIGURES

Figure	page
1.1 Three major families of SCR catalyst .....	3
2.1 C <sub>3</sub> H <sub>6</sub> -SCR of NO over (×) γ-Al <sub>2</sub> O <sub>3</sub> , (○) 1.2% Al <sub>2</sub> O <sub>3</sub> , and (●) 10% Ag/Al <sub>2</sub> O <sub>3</sub> catalysts as a function of temperature. Feed: 500 ppm. NO + 500 ppm. C <sub>3</sub> H <sub>6</sub> + 2.5% O <sub>2</sub> /He, W/F = 0.06g s cm <sup>-3</sup> (GHSV ~ 50000 h <sup>-1</sup> ). The dotted line in the plot giving the NO <sub>2</sub> yield represents the thermodynamic limit associated with the reaction NO + ½ O <sub>2</sub> ⇌ NO <sub>2</sub> ..	8
2.2 N <sub>2</sub> yield (●), N <sub>2</sub> O yield (○), NO <sub>2</sub> yield (△) and propene conversion (×) during the propene-SCR of NO over Ag /Al <sub>2</sub> O <sub>3</sub> as a function of the time of exposure to 100 ppm of SO <sub>2</sub> . T = 486°C, GHSV= 10 <sup>5</sup> h <sup>-1</sup> , 0.1% NO+ 0.1% C <sub>3</sub> H <sub>6</sub> +5% O <sub>2</sub> in helium, total flow= 100 ml min <sup>-1</sup> , 50 mg of catalyst.....	11
2.3 N <sub>2</sub> yield % (a) and NO <sub>2</sub> yield % (b) as a function of time-on-stream at various SO <sub>2</sub> feed concentrations between 0 and 100 % ppm (1000 vppm NO, 500 vppm C <sub>3</sub> H <sub>6</sub> , 500 vppm C <sub>3</sub> H <sub>8</sub> , 10% (v/v) O <sub>2</sub> , balance He, 0.66 g of catalyst, flow rate 500 ml min. <sup>-1</sup> ). The dashed line in (b) represents the NO <sub>2</sub> produced in the dead volume of the apparatus.....	12
2.4 Propene-SCR of NO: effect of the loading of silver over Al <sub>2</sub> O <sub>3</sub> (Al <sub>2</sub> O <sub>3</sub> : 115m <sup>2</sup> g <sup>-1</sup> ). The Tmax is given at the top of the bars for each silver loading. Feed: 0.1% NO+0.1% C <sub>3</sub> H <sub>6</sub> +5% O <sub>2</sub> in He; W/F = 0.12 g s cm <sup>-3</sup> , GHSV = 25,000 h <sup>-1</sup> .....	12
2.5 Propene-SCR of NO: effect of the loading of silver over Al <sub>2</sub> O <sub>3</sub> (Al <sub>2</sub> O <sub>3</sub> : 115m <sup>2</sup> g <sup>-1</sup> ). The Tmax is given at the top of the bars for each silver loading. Feed: 0.1% NO+0.1% C <sub>3</sub> H <sub>6</sub> +5% O <sub>2</sub> in He; W/F = 0.12 g s cm <sup>-3</sup> , GHSV = 25,000 h <sup>-1</sup> .....	13
2.6 NO conversion to N <sub>2</sub> on Ag–Al <sub>2</sub> O <sub>3</sub> catalyst using various <i>n</i> -alkanes: (●) methane, (○) ethane, (△) propane, (▲) <i>n</i> -butane, (◆) <i>n</i> -hexane, (◇) <i>n</i> -octane. Conditions: NO =1000 ppm, <i>n</i> -alkane = 6000 ppm, O <sub>2</sub> = 10%, H <sub>2</sub> O = 2%, and W/F = 0.12 g s cm <sup>-3</sup> except for methane-SCR (W/F = 0.9 g s cm <sup>-3</sup> ).....	14

## LIST OF FIGURES

Figure	page
2.7 NO to N <sub>2</sub> conversions over fresh Ag/Al <sub>2</sub> O <sub>3</sub> as a function of temperature using different hydrocarbons as reductants. HC/NO = 6 and GHSV = 60,000 h. <sup>-1</sup> . (□) Propane + propene, (▲) octane, (●) isooctane, (▼) 1-octene, (○) octanal, (■) octanol, and (△) octanoic acid.....	15
2.8 Thermogravimetric analysis of the formation of ad-NO <sub>x</sub> species at 400 °C over (×) Al <sub>2</sub> O <sub>3</sub> , (●) 1.2% Ag/Al <sub>2</sub> O <sub>3</sub> , (○) 10% Ag/Al <sub>2</sub> O <sub>3</sub> , and (△) 0.4% Co/Al <sub>2</sub> O <sub>3</sub> as a function of time. Feed: 0.05% NO + 2.5% O <sub>2</sub> .....	19
2.9 Simplified reaction scheme of the C <sub>3</sub> H <sub>6</sub> -SCR of NO over oxide catalysts giving the nature of the different species likely to be involved. It is proposed that the reduction to N <sub>2</sub> occurs through the reaction of oxidised and reduced (species in shaded circle) nitrogen compounds.....	21
2.10 The different roles of Ag during the C <sub>3</sub> H <sub>6</sub> -SCR over Ag/Al <sub>2</sub> O <sub>3</sub> : large Ag <sub>0</sub> particles catalyze the decomposition–reduction of NO, whereas Ag <sup>+</sup> species favors the oxidation of NO to ad-NO <sub>x</sub> species which subsequently react through the intermediacy of organo-nitrogen compounds.....	23
3.1 Flow diagram of measurement of N <sub>2</sub> O decomposition and CO <sub>2</sub> -TPD.....	28
3.2 Schematic diagram of the reaction line for NO and HC conversions analyzed by gas chromatographs equipped with molecular sieve 5A and porapak QS columns.....	31
4.1 X-ray diffraction pattern of 2% and 10%Ag/Al <sub>2</sub> O <sub>3</sub> catalyst: (●) γ-Al <sub>2</sub> O <sub>3</sub> .....	36
4.2 Carbon dioxide TPD spectrum of Ag/Al <sub>2</sub> O <sub>3</sub> catalyst.....	37
4.3 The temperature programmed reaction profiles of 2 wt% Ag/Al <sub>2</sub> O <sub>3</sub> for the selective catalytic reduction of NO by C <sub>3</sub> H <sub>6</sub> under excess oxygen: (●) C <sub>3</sub> H <sub>6</sub> conversion and (△) total NO conversion.....	38

## LIST OF FIGURES

Figure	page
4.4 The temperature programmed reaction profiles of 10 wt% Ag/Al <sub>2</sub> O <sub>3</sub> for the selective catalytic reduction of NO by C <sub>3</sub> H <sub>6</sub> under excess oxygen: (●) C <sub>3</sub> H <sub>6</sub> conversion, (△) total NO conversion to N <sub>2</sub> and N <sub>2</sub> O as well as (◇) NO conversion to N <sub>2</sub> O.....	39
4.5 The temperature programmed desorption profiles of 2 wt% Ag/Al <sub>2</sub> O <sub>3</sub> after dosing 1000 ppm C <sub>3</sub> H <sub>6</sub> + 1000 ppm NO + 5% O <sub>2</sub> at 370°C for 2 h: (△) N <sub>2</sub> , (●) CO <sub>2</sub> and (×) CH <sub>4</sub> .....	41
4.6 The temperature programmed oxidation profiles of 2 wt% Ag/Al <sub>2</sub> O <sub>3</sub> by using 1% O <sub>2</sub> as the oxidizing gas after the two steps, reaction and TPD steps: (△) N <sub>2</sub> and (●) CO <sub>2</sub> .....	41
4.7 The temperature programmed desorption profiles of 10 wt% Ag/Al <sub>2</sub> O <sub>3</sub> after dosing 1000 ppm C <sub>3</sub> H <sub>6</sub> + 1000 ppm NO + 5% O <sub>2</sub> at 210°C for 2 h: (△) N <sub>2</sub> , (●) CO <sub>2</sub> and (×) CH <sub>4</sub> .....	44
4.8 The temperature programmed oxidation profiles of 10 wt% Ag/Al <sub>2</sub> O <sub>3</sub> by using 1% O <sub>2</sub> as the oxidizing gas after the two steps, reaction and TPD steps: (△) N <sub>2</sub> and (●) CO <sub>2</sub> .....	45
4.9 The temperature programmed oxidation profiles of 2 wt% Ag/Al <sub>2</sub> O <sub>3</sub> by using 1% O <sub>2</sub> as the oxidizing gas after dosing 1000 ppm NO + 1000 ppm C <sub>3</sub> H <sub>6</sub> + 5% O <sub>2</sub> at 370°C for 2 h: (△) N <sub>2</sub> and (●) CO <sub>2</sub> .....	46
4.10 The temperature programmed oxidation profiles of 2 wt% Ag/Al <sub>2</sub> O <sub>3</sub> by using 1% O <sub>2</sub> +1000 ppm. NO without TPD as the oxidizing gas after dosing 1000 ppm C <sub>3</sub> H <sub>6</sub> + 5% O <sub>2</sub> at 370°C for 2 h: (△) N <sub>2</sub> and (●) CO <sub>2</sub> .....	47
4.11 The temperature programmed oxidation profiles of 2 wt% Ag/Al <sub>2</sub> O <sub>3</sub> by using 1% O <sub>2</sub> +1000 ppm. NO as the oxidizing gas after dosing 1000 ppm C <sub>3</sub> H <sub>6</sub> + 5% O <sub>2</sub> at 370°C for 2 h: (△) N <sub>2</sub> and (●) CO <sub>2</sub> .....	47
4.12 The temperature programmed oxidation profiles of 10 wt% Ag/Al <sub>2</sub> O <sub>3</sub> by using 1% O <sub>2</sub> +1000 ppm. NO TPD as the oxidizing gas after dosing 1000 ppm C <sub>3</sub> H <sub>6</sub> + 5% O <sub>2</sub> at 210°C for 2 h: (△) N <sub>2</sub> and (●) CO <sub>2</sub> .....	49

## LIST OF FIGURES

Figure	page
4.13 The temperature programmed oxidation profiles of 10 wt% Ag/Al <sub>2</sub> O <sub>3</sub> by using 1% O <sub>2</sub> +1000 ppm. NO as the oxidizing gas after dosing 1000 ppm C <sub>3</sub> H <sub>6</sub> + 5% O <sub>2</sub> at 210°C for 2 h: (Δ) N <sub>2</sub> and (●) CO <sub>2</sub> .....	49
4.14 The temperature programmed reaction profiles of 2 wt% Ag/SiO <sub>2</sub> and Al <sub>2</sub> O <sub>3</sub> for the selective catalytic reduction of NO by C <sub>3</sub> H <sub>6</sub> under excess oxygen: (●) C <sub>3</sub> H <sub>6</sub> conversion, (Δ) NO conversion and (◇) NO conversion to N <sub>2</sub> O.....	52
4.15 The temperature programmed reaction profiles of 10 wt% Ag/SiO <sub>2</sub> and Al <sub>2</sub> O <sub>3</sub> for the selective catalytic reduction of NO by C <sub>3</sub> H <sub>6</sub> under excess oxygen: (●) C <sub>3</sub> H <sub>6</sub> conversion and (Δ) NO conversion .....	52
4.16 The temperature programmed reaction profiles of Al <sub>2</sub> O <sub>3</sub> for the selective catalytic reduction of NO by C <sub>3</sub> H <sub>6</sub> under excess oxygen: (●) C <sub>3</sub> H <sub>6</sub> conversion and (Δ) NO conversion.....	53
4.17 The temperature programmed reaction profiles of 2 wt% Ag/SiO <sub>2</sub> for the selective catalytic reduction of NO by C <sub>3</sub> H <sub>6</sub> under excess oxygen: (●) C <sub>3</sub> H <sub>6</sub> conversion to CO <sub>2</sub> , (x) total C <sub>3</sub> H <sub>6</sub> conversion and (□) C <sub>3</sub> H <sub>6</sub> conversion to CO.....	54
4.18 The temperature programmed desorption profiles of 2 wt% Ag/SiO <sub>2</sub> and Al <sub>2</sub> O <sub>3</sub> after dosing 1000 ppm C <sub>3</sub> H <sub>6</sub> + 1000 ppm NO + 5% O <sub>2</sub> at 370°C for 2 h.....	55
4.19 The temperature programmed oxidation profiles of 2 wt% Ag/SiO <sub>2</sub> and Al <sub>2</sub> O <sub>3</sub> by using 1% O <sub>2</sub> as the oxidizing gas after dosing 1000 ppm C <sub>3</sub> H <sub>6</sub> + 5% O <sub>2</sub> at 370°C for 2 h.....	56
4.20 The temperature programmed oxidation profiles of 2 wt% Ag/SiO <sub>2</sub> and Al <sub>2</sub> O <sub>3</sub> by using NO+O <sub>2</sub> as the oxidizing gas after dosing 1000 ppm C <sub>3</sub> H <sub>6</sub> + 5% O <sub>2</sub> at 370°C for 2 h.....	57

## LIST OF FIGURES

Figure	page
4.21 The temperature programmed desorption profiles of $S_{TPOH}$ surface species over 10 wt% Ag/ $Al_2O_3$ after dosing 1% $O_2$ + 1000 ppm NO at 210°C for 30 s:(●) $CO_2$ .....	58
B.1 The calibration curve of oxygen from TCD of GC 8ATP.....	71
B.2 The calibration curve of nitrogen.....	72
B.3 The calibration curve of carbon monoxide.....	72
B.4 The calibration curve of oxygen from TCD of GC 8AIT.....	73
B.5 The calibration curve of methane.....	73
B.6 The calibration curve of carbon dioxide.....	74
B.7 The calibration curve of nitrous oxide.....	74
B.8 The calibration curve of propene.....	75
B.9 The calibration curve of propane.....	75
B.10 The calibration curve of sulfur dioxide.....	76

## CHAPTER I

### INTRODUCTION

Air pollution is a problem of general interest because polluted sources have sharply increased in many years ago. The origins of pollutants that are cause of this problem divided into two kinds of sources dependent on characteristic movement, i.e. mobile source and stationary source [1]. The pollutants and other compounds in exhaust gases consist of principally primary pollutants, unburned hydrocarbon (HCs), carbon monoxide (CO), sulphur oxides (SO<sub>x</sub>) and nitrogen oxides (NO<sub>x</sub>), in addition to the other compounds such as water, hydrogen, nitrogen and etc.

Emissions of nitrogen oxides that are generated primarily from both stationary and mobile sources are important air pollutants. Their effects are reported to contribute to a variety of environmental problems, including acid rain and acidification of aquatic systems, because it is a strong oxidant and soluble in water and can be oxidized within the atmosphere to form nitric acid (HNO<sub>3</sub>). Moreover, it is cause of the harmful impact for the respiratory system of human. The formation of NO<sub>x</sub> is occurred in combustion process by combining the N<sub>2</sub> and O<sub>2</sub> present in the air at high temperature [1], as the equation 1.1. However, if a compound in combustion process has bound nitrogen, NO<sub>x</sub> is readily formed at much lower temperature through an oxidation process.



Nitrogen oxides are formed at two stages during combustion:

1. The reaction of oxygen with nitrogen compounds in the fuel - this is termed fuel NO<sub>x</sub>;

2. The reaction of nitrogen with oxygen in the combustion air - this is termed thermal NO<sub>x</sub>;

The relative contribution of fuel and thermal  $\text{NO}_x$  depends on the type of fuel being used and the operating conditions.

It is not possible to reduce the nitrogen content of the fuel by physical cleaning as it is combined within the organic matter of the fuel, and at present there are no commercially available methods to reduce organic nitrogen. Hence, the emissions of  $\text{NO}_x$  generated during the combustion process can be reduced, as with  $\text{SO}_2$ , by treating the flue gases. For the above reasons,  $\text{NO}_x$  emissions are regulated in two ways before the flue gases release to environment.

- Preventing the production and release of nitrogen oxides during combustion, i.e. stages combustion and fluidized bed combustion (FBC)
- Removal of nitrogen oxides after combustion, i.e. selective catalytic reduction (SCR), non-selective catalytic reduction (NSCR) and activated carbon process.

However, the major disadvantages of regulations during combustion are the loss of energy consumption to eliminate  $\text{NO}_x$  at high temperature, and these processes are used with only stationary source. Therefore, the other method such as catalytic technology has been developing in the present time, because it is applied to control the emissions of  $\text{NO}_x$  both stationary and mobile sources. The SCR of  $\text{NO}_x$  using  $\text{NH}_3$  was first discovered in 1957 [2]. It was discovered that  $\text{NH}_3$  can react selectively with  $\text{NO}_x$  to produce  $\text{N}_2$ . Nonetheless, applied  $\text{NH}_3$  for management of  $\text{NO}_x$  has some disadvantage including undesirable product, i.e.  $\text{NO}_2$ , corrosion and fouling [1]. Until the early 1970, the reduction of the emission of  $\text{NO}_x$  by using HC became an important control issue. The other catalysts were investigated for use in SCR and the catalysts are divided into three major groups dependent on catalyst performance as shown in Fig.1.1 [3].



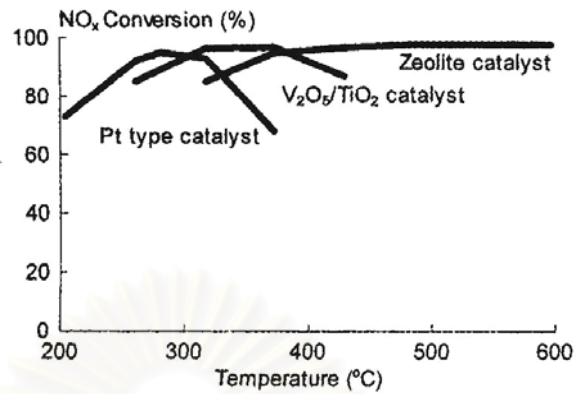


Figure 1.1 Three major families of SCR catalyst [2].

The various characteristics of these catalyst families as described manufacture are given in Table 1.1 [2].

Table 1.1 Operating characteristics of different SCR catalyst.

---

Medium temperature - VNX<sup>TM</sup> catalyst (V<sub>2</sub>O<sub>5</sub>/TiO<sub>2</sub>)

- 260-425°C
- most broadly used
- sulfur tolerant

High temperature - ZNX<sup>TM</sup> catalysts (zeolite)

- 345-590°C
- very high NO conversion
- sulphur tolerant above 425°C

Low temperature - LT catalyst (Pt-based)

- 150-300°C
  - narrow temperature window
  - temperature window shifts
  - no sulphur tolerant
-

Certainly, no suitable catalyst is used to control the emission of  $\text{NO}_x$ , because each catalyst shows both advantage and disadvantage [4]. Therefore, the procedures of research about SCR are separated to two parts: (1) to study and improve the conventional catalysts and (2) to develop and design the modern catalyst for the SCR of  $\text{NO}_x$ . From the literature reviews, although the development of catalyst is achieved by using promoter to improve the stability with  $\text{H}_2\text{O}$  and sulphur, but the selectivity and activity of this is decreased [5]. Nonetheless, after testing nine different classes of promising catalysts was reported, the other concluded that despite the fact that some NM-containing catalysts, there is no single phase catalyst capable of satisfying the practical demands for  $\text{NO}_x$  removal. Although the unsuccessful management to control  $\text{NO}_x$  removal was reported, but the developments are continually studied to select the suitable catalysts which show both high activity and stability for  $\text{NO}_x$  removal.

In recent year, silver (Ag) is a promising catalyst for HC-SCR of  $\text{NO}_x$ , because the silver-based formulation is an effective catalyst for  $\text{NO}_x$  removal from exhaust gases under lean-burn conditions. It shows a good activity and selectivity for the SCR of NO by various hydrocarbons. Several organic compounds such as methane [6-8], methanol [5,10], ethane [7-8], hexane [7], butane [7], propene [9-19], methane [AB25,CT45], ethane [Ab 25,CT45], propane [ab25],CT45, ethanol [11,20-23], decane [24], propane [7-8,19,25-28], octane [7,29] were used as the reductant. Moreover, the other advantageous performance is a broad temperature window and a lower selective harmful product. Also, several studies investigated the activity, selectivity and stability of the silver-based material. At the present time, although many authors have reported to advantages of the silver-based catalyst in the HC-SCR of NO under excess oxygen, the reaction mechanism and active intermediate species are rather complicated and have not been fully elucidated. Typically, application of *in situ* Fourier transform infrared spectroscopy has been only used to predict the reaction mechanism and identify the intermediates [30-39]. The possible simultaneous occurrence of at least two reaction pathways results in complication of the analysis and therefore other procedures have to be made in order to obtain more information.

Temperature programmed technique is one of many methods that is useful for investigation of surface species [40-42]. It is noted that IR and TP techniques show different information. The spectra of IR technique exhibit the formation of surface species but do not show the quantity of each species. On the other hand, temperature programmed techniques give overall information such as quantity, containing species and etc. Examples of the characterization include the observation of the nature of surface species using an experimental set of three steps consisting of reaction step, temperature programmed desorption step and temperature programmed oxidation step. Prasertthadan et al. [40] and Isarangura Na Ayuthatya et al. [41] have used the temperature programmed technique to investigate the nature of the surface species in the SCR of NO by C<sub>3</sub>H<sub>6</sub> over zeolite- and platinum-based catalysts and they confirm that this method can be employed to indicate the classification of the surface species. However, only these methods cannot show all information of the surface species. The other method was added to fulfill the result of surface species. Srihiranpullop et al. [43] reported the application of physical mixture method to investigate coke formation and found that this method can be used to determine the appeared position of coke. From this report, the physical mixture may be used to investigate the position of surface species that occur on Ag active sites, interface or alumina active sites.

Hence, in this work we have applied temperature programmed techniques to study the nature and reactivity of the surface species on Ag/Al<sub>2</sub>O<sub>3</sub> in the SCR of NO by C<sub>3</sub>H<sub>6</sub> under lean-burn condition.

Following the above motivation, the scopes of this study have to be taken into account.

1. Prepare and characterize Ag/Al<sub>2</sub>O<sub>3</sub> in order to use for investigation of the surface species.

2. Study the catalytic behavior in the selective catalytic reduction of NO by propene under excess oxygen over Ag/Al<sub>2</sub>O<sub>3</sub> catalyst towards temperature programmed

reaction in order to determine a range of the operating temperature for production of the surface species.

3. Investigate the surface species produced on a Ag/Al<sub>2</sub>O<sub>3</sub> catalyst in the selective catalytic reduction of NO with propene under excess oxygen by emphasizing on the temperature programmed techniques as follows:

- Study the nature of surface species by an experimental set consisting of three continuous steps including reaction step, temperature programmed desorption step and temperature programmed oxidation step.
- Study the reactivity of surface species to various oxidizing gases by application of temperature programmed oxidation technique
- Study the characteristic of surface species using the physical mixture.

The present research work is divided into five chapters. To accommodate a variety of background of readers, it begins with introduction that is necessary for the understanding of emission control of NO<sub>x</sub> in chapter I. Chapter II is concerned with literature reviews of HC-SCR of NO<sub>x</sub> over Ag-based catalyst under lean burn condition. An experimental system including catalyst preparation, catalyst characterization and catalyst activities and characterization of surface species is reported in chapter III. Chapter IV demonstrates the experimental results and discussion. Finally, the conclusions and recommendations are shown in chapter V.

จุฬาลงกรณ์มหาวิทยาลัย

## CHAPTER II

### SELECTIVE REDUCTION OF NO<sub>x</sub> WITH HYDROCARBON OVER Ag-BASED CATALYST UNDER LEAN-BURN CONDITION

The SCR of nitrogen oxides by hydrocarbons has attracted much attention recently because it has the potential ability to remove nitrogen oxides from diesel exhaust and oxygen rich flue gases. Held et al. [44] and Iwamoto [45] first reported some success using zeolite-based catalyst for lean de-NO<sub>x</sub>. However, the hydrothermal resistance of these materials is usually unsatisfactory. After that, the other active catalysts such as platinum group materials (PGMs) [46], based oxide/metals have been investigated as de-NO<sub>x</sub> catalyst to improve the stability problem. PGMs are inefficient at moderate and high temperatures, pioneering work by Hamada et al. [47] and Obuchi et al. [46] described that these metals could catalyze NO<sub>x</sub> reduction by hydrocarbon at low temperature (typically below 300°C). Although these catalysts exhibited significant activities for the same reaction, but the problem of selectivity was observed. At low temperature, a significant amount of NO is converted to N<sub>2</sub>O rather than N<sub>2</sub>. The others base oxides/metals (e.g. Al<sub>2</sub>O<sub>3</sub>, TiO<sub>2</sub>, ZrO<sub>2</sub>, MgO and these oxides promoted by, e.g. Co, Ni, Cu, Fe, Sn, Ga, In as well as Ag compounds) are active catalysts for HC-SCR of NO<sub>x</sub> [48-52].

Even though some interesting activities were claimed, there is not sufficient evidence for possible application of such systems under real exhaust condition. In fact, even though some increase of thermal/hydrothermal stability could be achieved, the activities generally poorer compared to the Cu-ZSM5 system. Therefore, many works are focus to find the new catalyst or improve the properties of primary catalysts. Within several materials, Ag-based catalysts appear to be the most promising materials because they show high activity and selectivity to produce N<sub>2</sub> [36]. These include: (1) appreciable activity between 300-600°C and wide temperature windows as shown in Figure 2.1; (2) stability with water and (3) a little selectivity towards dinitrogen formation.

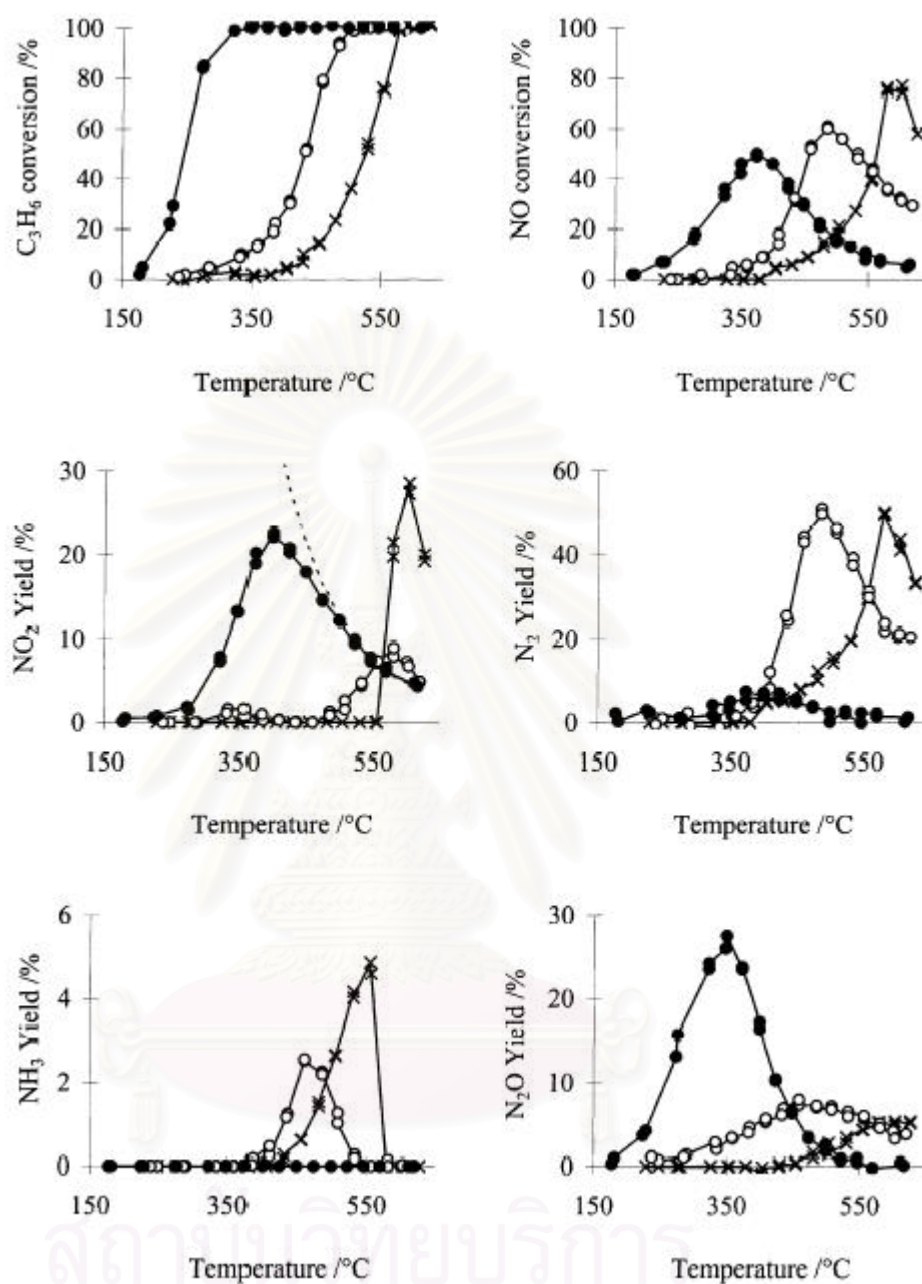


**Figure 2.1** C<sub>3</sub>H<sub>6</sub>-SCR of NO over (x)  $\gamma$ -Al<sub>2</sub>O<sub>3</sub>, (o) 1.2% Al<sub>2</sub>O<sub>3</sub>, and (●) 10% Ag/Al<sub>2</sub>O<sub>3</sub> catalysts as a function of temperature. Feed: 500 ppm. NO + 500 ppm. C<sub>3</sub>H<sub>6</sub> + 2.5% O<sub>2</sub>/He, W/F = 0.06g s cm<sup>-3</sup> (GHSV ~ 50000 h<sup>-1</sup>). The dotted line in the plot giving the NO<sub>2</sub> yield represents the thermodynamic limit associated with the reaction  $\text{NO} + \frac{1}{2} \text{O}_2 \rightleftharpoons \text{NO}_2$  [36].

At the present time, although many authors have reported to advantages of the silver-based catalyst in the HC-SCR of NO under excess oxygen, the reaction mechanism and active intermediate species are rather complicated and have not been fully elucidated. Although the success of HC-SCR still lies somewhere in future, it is now timely to assess the state-of-the-art in terms of our fundamental understanding. In this review, we critically evaluate the published work on the experiment information currently available on Ag-based catalysts including basic concept in the selective catalytic reduction of NO under lean-burn condition over this catalysts and the mechanistic studies of such reaction.

## 2.1 Overview of SCR over Ag-Based Catalyst

Ag-based catalysts are also among those extensively studies since high activity was reported, particularly when hydrocarbons such as alcohol, alkane, alkene and etc. are employed as reducing agent. The continuous developments of this catalyst have been performed to improve the stability and activity problems.

Originally, the various promoters including Ag were studied to increase the stability and activity of primary catalysts (zeolite based catalyst)). From the literature, clearly the temperatures of highest activity are greatly different dependent on the cations while the maximum activities differed slightly. The order of active temperature regions was  $\text{Cu} < \text{Co} < \text{H} < \text{Ag} < \text{Zn}$ . It was also noted that the wide temperature window over Ag was observed. Moreover, the other metals such as Pd-, Cu- and Au- catalysts are also compared with Ag-based catalyst [49]. In addition, some literature reported regarding unsuccessful improvement of SCR by using single phase catalyst [51]. A variety of catalysts including, which can be classified into: zeolites exchanged with metals ions or just a proton types, alumina and its combination with supported metals or metal oxides, metal oxides other than alumina, metal silicates, and ion exchanged materials other than zeolites. Except for emphasizing differences in the activity among catalysts, general behaviors of the catalysts, such as the active temperature range and the selectivity to  $\text{N}_2\text{O}$ , were similar to that investigates under model gas mixture condition. These results led us to the conclusion that the use of any single phase catalyst, including uniformly mixed

catalysts composed of two different types of catalyst, does not satisfy the practical demand.

While the improvement of activity is executed, the other study about the stability is made [52-55]. Many works attempted to test the stability, because of the typical exhausts to be treated by lean- $\text{NO}_x$  catalysts contain up to 10 vol. % of water and up a few hundred parts per million of  $\text{SO}_2$ . The effect of water on HC-SCR over Ag and other metal promoted on alumina catalyst was investigated. Alumina-supported silver catalyst exhibited extremely high activities in reducing nitric oxide by organic compound in the presence of water [54]. Normally, high concentrations of water in the feed induce a significant deactivation of most catalysts when using light alkenes or alkanes as reductants; however, a high activity can be maintained when oxygenated molecules are used. The inhibition by water is most likely to be due to competitive adsorption between water and one or more of the reactants. The high polarity of oxygenates probably explains their greater ability to compete with water for adsorption when compared to hydrocarbons. Nonetheless, silver has been chosen to study the effect of cocation in order to limit the migration and the subsequent agglomeration of zeolite based catalyst [53]. The presence of silver is possible to partly prevent the catalyst deactivation and in particular to decrease the inhibiting water effect.

In case of sulphur-tolerance,  $\text{SO}_2$  is typically found in lean exhaust streams as a result tolerance of several catalysts. Many published research works reported regarding the SCR of  $\text{NO}_x$  in the presence of  $\text{SO}_x$ . An inhibition of the SCR of NO by sulphur dioxide is observed in essentially cases, but its extent dramatically depends on the nature of the reductants and the sulphur concentration.  $\text{SO}_2$  is known to react with  $\text{O}_2$  and the catalyst surface to form stable sulphate phases under reaction conditions. The formation of these sulphate species brings about a reduction in the number of 'strong' chemisorption sites for  $\text{NO}_x$ . For Ag-based catalyst, the literature reported both advantage and disadvantage of  $\text{SO}_2$ . Mostly, the loss of activity for SCR over these catalysts was observed as shown in Figure 2.2 when the  $\text{SO}_2$  was introduced in to a system. From the DRIFT studies, the spectra of deactivated silver-alumina material showed the formation of two different types of surface sulphate species. One of surface species was a surface aluminium sulphate whereas the other corresponded



to a sulphate associated with the silver phases [55]. However, the sulphate species was removed by using the thermal decomposition process. On the other hand, some work [19] found that the  $N_2$  yield in the absence of  $SO_2$  is reached almost instantaneously a constant level, which is considerably lower than in the presence of  $SO_2$ . A promotion effect on the catalytic activity was shown in Figure 2.3.

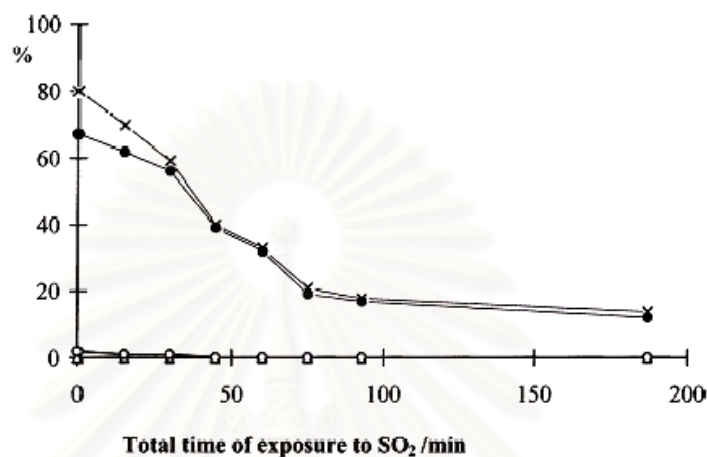


**Figure 2.2**  $N_2$  yield (●),  $N_2O$  yield (○),  $NO_2$  yield (△) and propene conversion (×) during the propene-SCR of NO over Ag / $Al_2O_3$  as a function of the time of exposure to 100 ppm of  $SO_2$ .  $T = 486^\circ C$ ,  $GHSV = 10^5 h^{-1}$ , 0.1% NO+ 0.1%  $C_3H_6$  +5%  $O_2$  in helium, total flow= 100 ml  $min^{-1}$ , 50 mg of catalyst [55].

Focusing on the activity of Ag-based catalyst, the effectiveness of this catalyst for the SCR reaction depends markedly on the nature of reducing agent, its concentration and etc. The effect of the loading of silver on alumina based catalysts for the  $C_3H_6$ -SCR of NO has been studied by using loading of silver ranging from 0.5-4wt%. The NO and propene conversions and yields of  $N_2$  and  $N_2O$  of these sample at the temperature at which the maximum of NO conversion was obtained in each case are show in Figure 2.4. The  $T_{max}$  steadily decreased with increasing silver loading. The highest  $N_2$  yield was obtained with 1% loading. The samples with a loading lower than 2% showed selectivities to  $N_2$  whereas that a higher silver loading also gave significant proportions of  $N_2O$ .

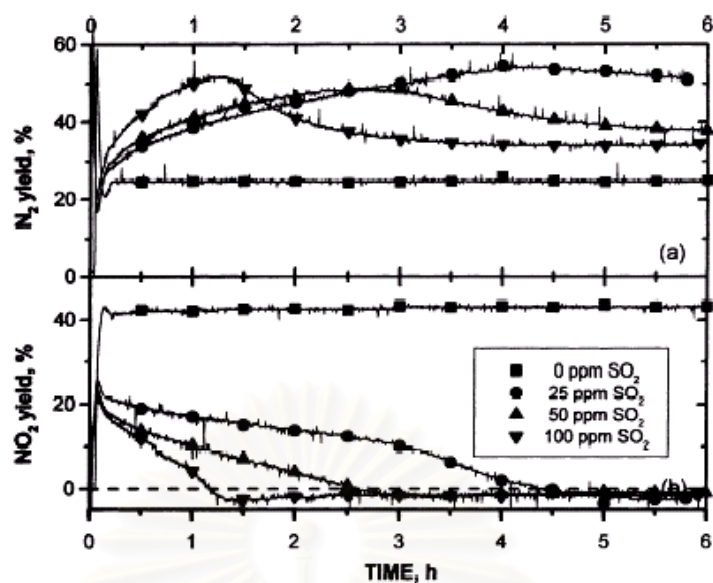


**Figure 2.3** N<sub>2</sub> yield % (a) and NO<sub>2</sub> yield % (b) as a function of time-on-stream at various SO<sub>2</sub> feed concentrations between 0 and 100 % ppm (1000 vppm NO, 500 vppm C<sub>3</sub>H<sub>6</sub>, 500 vppm C<sub>3</sub>H<sub>8</sub>, 10% (v/v) O<sub>2</sub>, balance He, 0.66 g of catalyst, flow rate 500 ml/min). The dashed line in (b) represents the NO<sub>2</sub> produced in the dead volume of the apparatus [19].

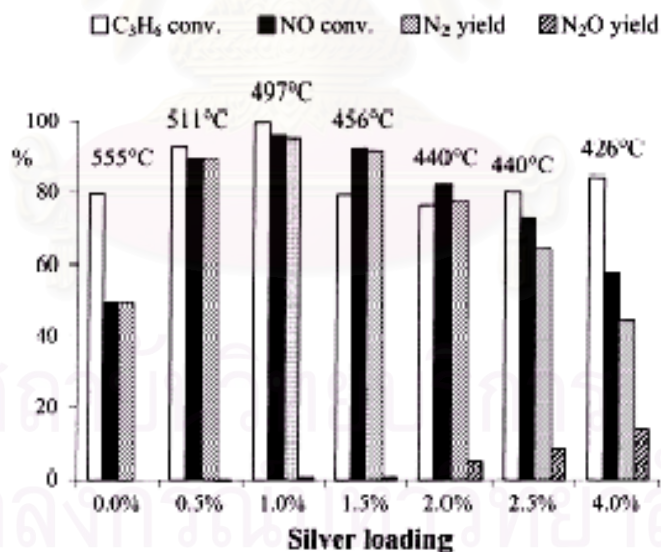
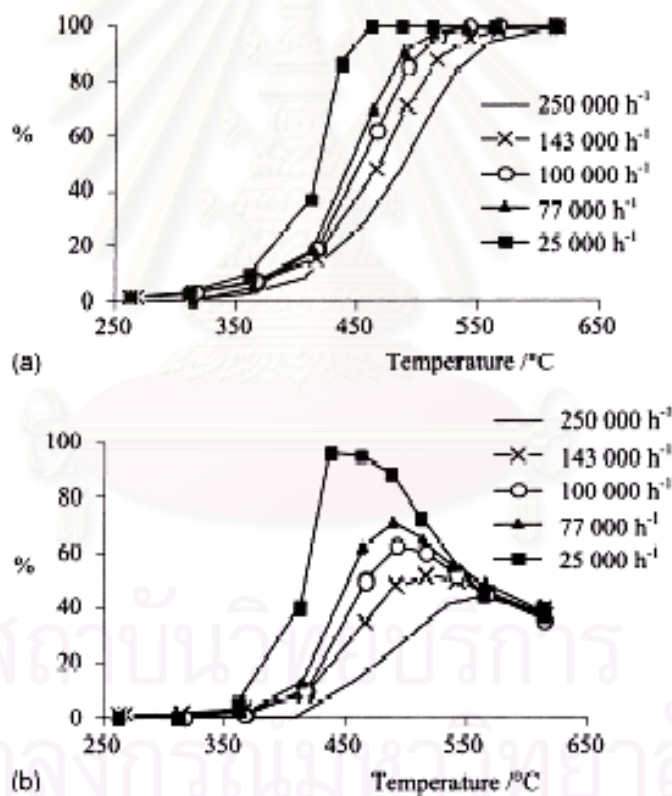


**Figure 2.4** Propene-SCR of NO: effect of the loading of silver over Al<sub>2</sub>O<sub>3</sub> (Al<sub>2</sub>O<sub>3</sub>: 115m<sup>2</sup>/g). The T<sub>max</sub> is given at the top of the bars for each silver loading. Feed: 0.1% NO+0.1% C<sub>3</sub>H<sub>6</sub>+5% O<sub>2</sub> in He; W/F = 0.12 g s cm<sup>-3</sup>, GHSV = 25,000 h<sup>-1</sup>[56]

In addition, the above results indicate the promoting effect of silver at intermediate loadings on the SCR reaction. Thus, low Ag samples are active for  $\text{NO}_x$  reduction, showing  $\text{NO}_x$  and  $\text{C}_3\text{H}_6$  conversion profiles at high temperature. On the other hand, the catalytic behavior of the sample with the highest silver loading shows similarities with several studies [56], indicating that low  $\text{NO}_x$  conversion levels are achieved over alumina-supported samples with relatively high silver loadings, while a relatively higher rate for the non-selective  $\text{C}_3\text{H}_6$  combustion occurs.

The effect of the other parameter such as space velocity is shown in Figure 2.5. The space velocity affect to both  $\text{NO}$  and  $\text{C}_3\text{H}_6$  conversion. When the space velocity increase, both  $\text{NO}$  and  $\text{C}_3\text{H}_6$  conversion readily decrease. It indicates that the retention time has great effect to  $\text{NO}$ -SCR.



In case of reducing gases, the different catalytic behavior towards temperature programmed reaction obtained by changing types of reductant, typically results for Ag catalysts tested with a wide range of different organic compounds in some literature are interestingly pronounced. Figure 2.6 shows the conversion of NO in the presence of water vapor when linear alkanes are used as a reductant. Clearly, the carbon number in the hydrocarbon reductant significantly affects NO reduction activity. As the carbon number increased, the temperature range at which NO reduction occurs shifted to the lower temperature region.

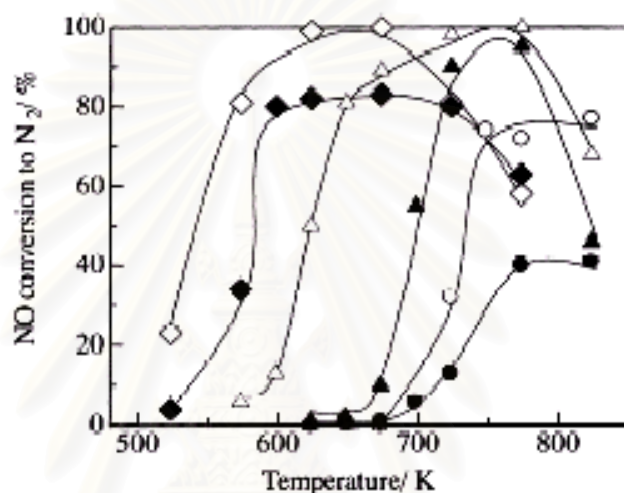


**Figure 2.6** NO conversion to  $N_2$  on Ag- $Al_2O_3$  catalyst using various *n*-alkanes: (●) methane, (○) ethane, (△) propane, (▲) *n*-butane, (◆) *n*-hexane, (◇) *n*-octane. Conditions: NO = 1000 ppm, *n*-alkane = 6000 ppm,  $O_2$  = 10%,  $H_2O$  = 2%, and  $W/F$  = 0.12 g s  $cm^{-3}$  except for methane-SCR ( $W/F$  = 0.9 g s  $cm^{-3}$ ) [7].

In addition, the effects of kind of organic compounds were tested. The results in which the hydrocarbon (number of carbon = 8) have varied to alkane, alkene, aldehyde, alcohol and acid are shown graphically in Figure 2.8. Octane is much more effective at high temperature while octanol shows high activity at low temperature. The others show moderate NO conversion.

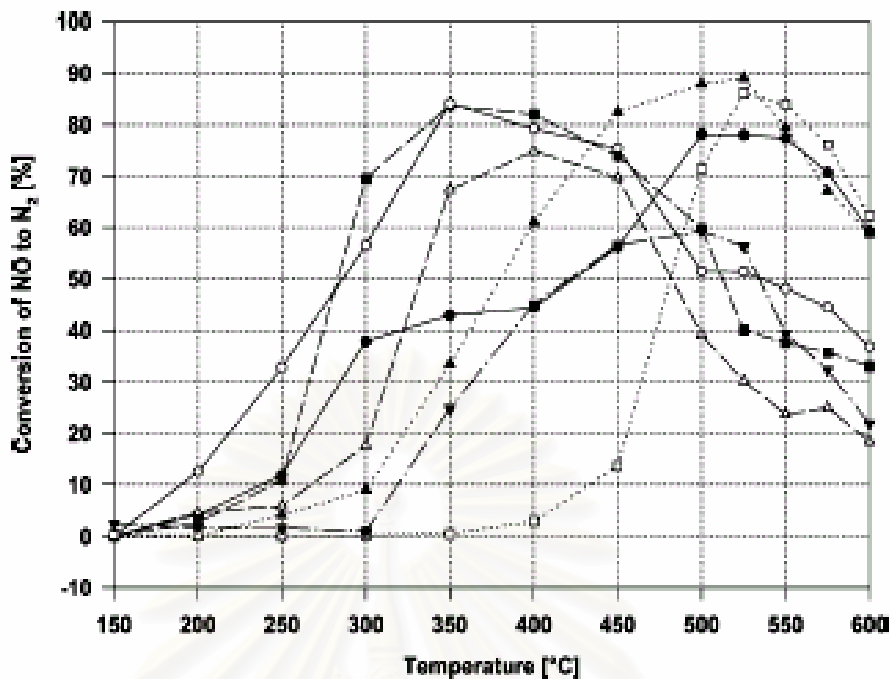


**Figure 2.8** NO to N<sub>2</sub> conversions over fresh Ag/Al<sub>2</sub>O<sub>3</sub> as a function of temperature using different hydrocarbons as reductants. HC/NO = 6 and GHSV = 60,000 h<sup>-1</sup>. (□) Propane + propene, (▲) octane, (●) isooctane, (▼) 1-octene, (○) octanal, (■) octanol, and (△) octanoic acid [29].

From described above, this information is some reported regarding the development of SCR over Ag-based catalyst. The obtained available about this basic catalytic behavior encourage in the development of new catalyst formulations sufficiently active and select for the proposed process capable to meet the continuously increased requirement for the clean environment. To improve the catalytic performance, the clarification of the reaction mechanism is essential for future improvement of this catalytic process. Hence, the mechanistic studies of such reaction on Ag-based catalyst are individually in the next section.

## 2.2 Reaction Mechanistic Studied

There have been a number of studies in which the mechanistic aspects of the selective catalytic reduction of NO by hydrocarbon under excess oxygen on a Ag-based catalyst have been considered but yet there is little definitive evidence in support of one model rather than another and as a consequence several mechanisms have been proposed. In general, the reaction mechanism can be subdivided into decomposition mechanism and reduction mechanism. However, the overall reaction mechanism and the rate-determining step of the selective reduction of NO over a given catalyst depend on the nature of the reductant and the experimental conditions. The mechanism is rather complicated and has not been fully elucidated for any given SCR system. Nevertheless, a general picture of the most significant steps likely to occur during the reaction can be drawn from the vast amount of data generated. Alumina and alumina-supported samples have been the focus of most of the studies of reaction mechanisms, generally using propene as reductant.

The role of dioxygen is quite intricate, as it strongly favours the reduction process over most catalytic formulations [58-59]. Most authors acknowledge that the two main functions of O<sub>2</sub> are the oxidation of NO and of the reductant to form various reaction intermediates. Oxygen may also have a role to play in preventing coking of the catalyst surface, especially in the case of strongly adsorbing hydrocarbons such as alkenes.

Since the reaction orders for N<sub>2</sub> formation with respect to both NO and propene are usually close to zero on alumina-based materials [60], the formation of strongly bound reaction intermediates is expected.

### **Reaction mechanism over oxides: NO reaction pathway**

In the absence of O<sub>2</sub>, NO only weakly adsorbs on most catalysts surfaces [61-62]. On the contrary, strongly bound nitrite and nitrates are formed in NO/O<sub>2</sub> mixtures. Several literatures reported regarding the reduction of surface species with nitric oxide. Sadykov et al. [63] showed that the decomposition temperatures of strongly bound ad-NO<sub>x</sub> species corresponded well to the onset of propane-SCR

activity over numerous catalytic formulations. For alumina and silver/alumina, Shimizu et al. [35,64-65] clearly showed that nitrate species were converted to  $N_2$  during exposure to the reductant at rates that were similar to those of the steady-state reduction of NO. These data strongly support the conclusions reached by many research teams on the role of nitrate species as true reaction intermediates in the SCR process over oxides. The formation of ad- $NO_x$  species on surface sites S is therefore proposed to be the first reaction step of NO as shown in equation 2.1.



The formation of  $NO_2$  and its role as a reaction intermediate during the SCR reaction has generated much interest. Although the conversion of NO to  $NO_2$  could conceivably be the first step of the  $CH_4$ -SCR on some zeolitic materials (e.g. Co/H-ZSM-5 [66]), most selective oxides are not sufficiently active for this reaction to support the formation of  $NO_2$  as a main reaction intermediate.



Meunier et al. [36] clearly showed that selective SCR catalysts, e.g. low loading (< 2 wt.%) Co or Ag supported on alumina, are not significantly active for either the oxidation of NO to  $NO_2$  or the reverse reaction at the temperatures at which these materials are active for the SCR reaction. The reverse is true for high loading catalysts (e.g. 10 wt.%), which show good activity for NO oxidation, but are nonselective for the SCR reaction. The high rate of  $NO_2$  formation observed over high loading samples is clearly related to their high activity for hydrocarbon combustion. Furthermore, the ratio of  $NO_2/NO$  observed during the course of the SCR reaction over selective catalysts sometimes exceeds that associated with the thermodynamic equilibrium value of equation 2.2, clearly discarding it as the main route to  $NO_2$  [34,36,67]. High yields of  $NO_2$  can be obtained by the oxidation of organo-nitrito compounds and this rather than the direct oxidation of NO to  $NO_2$  is proposed as the most likely route to gas-phase  $NO_2$  [34,36].

Most of the confusion regarding the role of  $NO_2$  originates from the fact that the SCR of  $NO_2$  is much faster than the reaction with NO over unpromoted oxides

such as  $\text{Al}_2\text{O}_3$  [68].  $\text{NO}_2$  is more reactive than  $\text{NO}$  and as a result is more likely to react more quickly with the surface of the catalyst to form ad- $\text{NO}_x$  species which have been proposed as key intermediates in the reaction. Metals such as cobalt were proposed to promote the oxidation of  $\text{NO}$  to  $\text{NO}_2$ , with the reduction of  $\text{NO}_2$  then occurring on the  $\text{Al}_2\text{O}_3$ . However, low rates of  $\text{NO}_2$  formation have been observed in the absence of reductant over selective SCR catalysts such as low loading  $\text{Co}/\text{alumina}$ . In addition, in situ IR and thermogravimetric data (Figure 2.8) stressed the inability of isolated cobalt ions to promote the formation of ad- $\text{NO}_x$  species on alumina [36]. Instead, the key to the high selectivity and activity of promoted alumina catalyst could be attributed to the reactivity of the ad- $\text{NO}_x$  species. Note that these highly reactive nitrate species do not migrate onto the support, in contrast to silver-promoted alumina, which promotes the formation of ad- $\text{NO}_x$  species on the support [34].

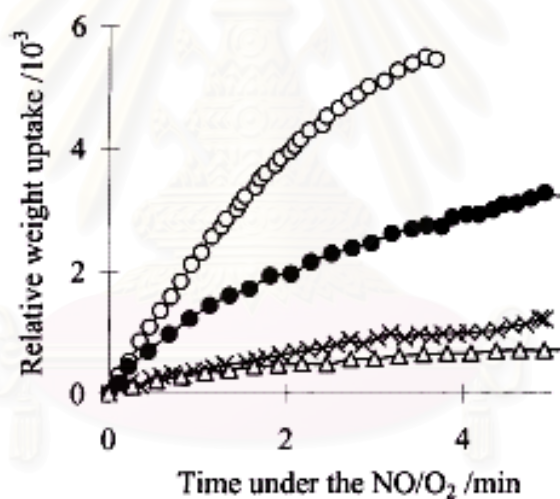


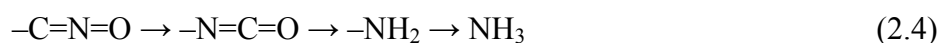
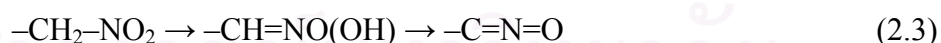
**Figure 2.8.** Thermogravimetric analysis of the formation of ad- $\text{NO}_x$  species at 400 °C over (x)  $\text{Al}_2\text{O}_3$ , (●) 1.2%  $\text{Ag}/\text{Al}_2\text{O}_3$ , (○) 10%  $\text{Ag}/\text{Al}_2\text{O}_3$ , and (Δ) 0.4%  $\text{Co}/\text{Al}_2\text{O}_3$  as a function of time. Feed: 0.05%  $\text{NO}$  + 2.5%  $\text{O}_2$  [34].

### Reaction mechanism over oxides: hydrocarbon reaction pathway

Similarly to the case of  $\text{NO}$ , most authors have proposed the formation of strongly bound oxidized species as the first reaction step in the reaction of the hydrocarbon. In addition to the low reaction order for  $\text{N}_2$  formation with respect to hydrocarbons [60], this proposition is supported by the fact that oxygenated molecules



react much faster and efficiently than hydrocarbons. For the C<sub>3</sub>H<sub>6</sub>-SCR of NO over alumina and silver/alumina, Shimizu et al. [35,64,65] clearly showed that acetate surface species were formed by the oxidation of various hydrocarbons and were thereafter consumed at rates similar to that of the reduction of NO. The acetate species or other adsorbed oxidised hydrocarbon species are then believed to react with the surface nitrates (and possibly with gas-phase NO<sub>x</sub>) to yield organo-nitrogen species, the exact nature of the organo-nitrogen species remains unclear [69-72]. The formation of the organo-nitrogen species is likely to be the rate-determining step of the reaction. These species are not readily detectable but can be observed during carefully designed transient experiments such as temperature-programmed surface reaction monitored by in situ IR. Organo-nitrogen species can be readily formed non-catalytically by reaction of hydrocarbon, dioxygen and nitric oxide in the liquid or gas phase [70]. In addition, the decomposition products of organo-nitrogen species yield similar products to those observed during the SCR reactions (e.g. cyanide, isocyanates), supporting their role as intermediates. The reactivity of nitromethane has been studied over alumina, over which it is readily decomposed below 200 °C forming isocyanate and ammonia species. NH<sub>3</sub> can be obtained from nitromethane through the tautomerisation to the corresponding oxime followed by dehydration to a nitrile N-oxide (equation 2.3), which isomerise to an isocyanate before yielding a primary amine and NH<sub>3</sub> by hydrolysis (equation 2.4), as suggested over zeolitic materials [72]. Over alumina, the possibility of forming NH<sub>3</sub> from reaction of organo-nitrile N-oxides species was confirmed by Obuchi et al. [73]. The same authors proposed that the organo-nitrile N-oxide were formed from organo-nitroso compounds, via enol and cyanide formation (equation 2.5).



The selective reduction of NO with ammonia is an efficient reaction over many catalysts, including alumina and other base oxides and metals. The

intermediacy of  $\text{NH}_3$  in the hydrocarbon-SCR reaction has been suggested over zeolites and alumina-based materials [34]. In addition, isocyanate species, readily formed when hydrocarbon reductants were used, were also shown to yield  $\text{N}_2$  in the presence of  $\text{O}_2$  or  $\text{NO} + \text{O}_2$  [30-31,74].

### **Conclusions on the lean-de $\text{NO}_x$ reaction mechanism over Ag-based catalyst**

The amount of evidence for the intermediacy of strongly bound nitrates and acetates during the SCR of  $\text{NO}$  with various hydrocarbons or oxygenated reductants is now substantial. However, the other mechanistic steps are still controversial, the reaction between nitrates and acetates appears to be the rate-determining step and, therefore, the surface or gas-phase concentrations of subsequent intermediates are minute.

Nevertheless, the use of transient experiments has shown that reduced species of nitrogen such as  $-\text{NCO}$  and  $\text{NH}_3$  were readily formed, via organo-nitrogen species. Several authors have therefore proposed that the coupling of nitrogen atoms to form  $\text{N}_2$  could simply occur via the reaction between the and reduced forms of nitrogen [34]. This observation stresses that the reaction mechanism is very complex since  $\text{NO}$  will react through a series of parallel and consecutive pathways to form numerous intermediates. Figure 2.10 gives a simplified scheme of a global reaction scheme over oxides/base metal catalysts.

It should be noted that the relevance and rate of each step of the scheme represented in Figure 2.9 depends on the nature of the reductant, the catalyst and experimental conditions. The overall rate-determining step and the surface concentrations of each species may vary accordingly. For instance, Shimizu et al. showed that the chain length of the alkane influences their adsorption reaction properties and therefore the rate at which acetates form [65]. As a result, the proportion of the surface coverage of acetates and nitrate species, which compete for surface sites, varies.

Similar changes in the balance of acetates and nitrates applies in the case of using propene or ethanol over Ag/Al<sub>2</sub>O<sub>3</sub>, as more acetates and less nitrates are observed in the case of the strongly adsorbing alcohol [75]. This probably explains why isocyanates are more easily observed when using alcohols, as the surface coverage of oxidised ad-NO<sub>x</sub> species is lower.

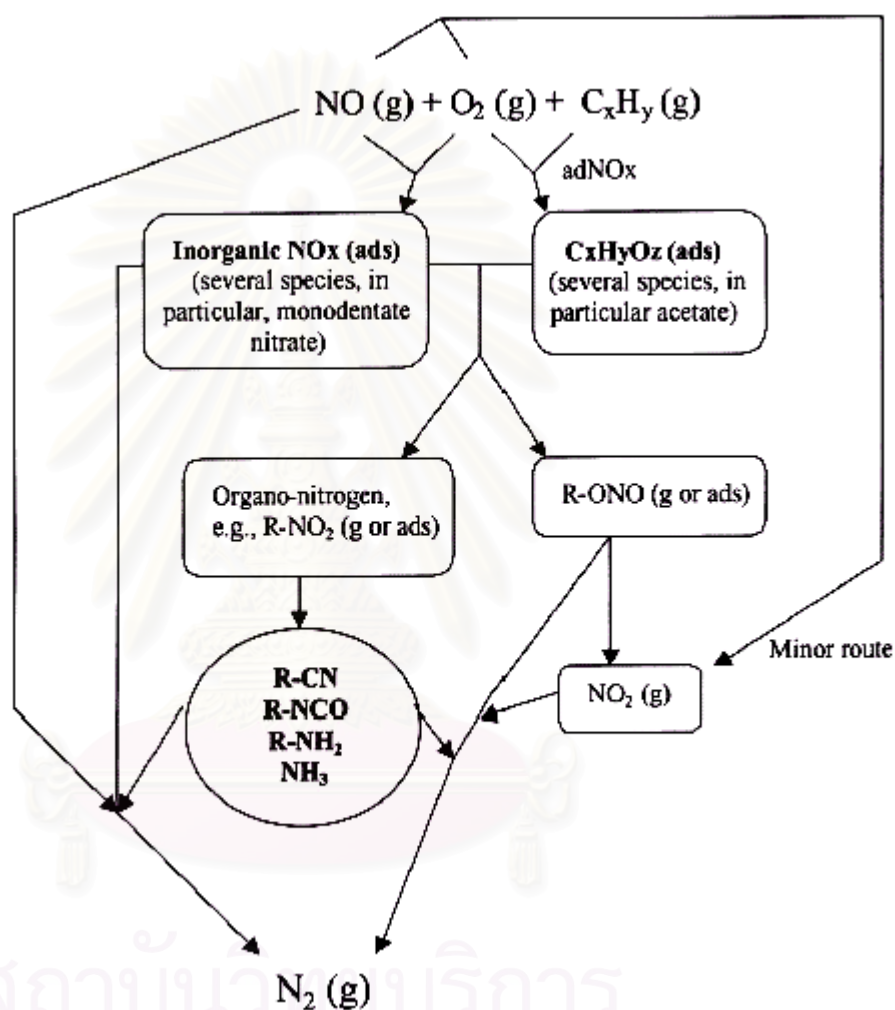


**Figure 2.9** Simplified reaction scheme of the C<sub>3</sub>H<sub>6</sub>-SCR of NO over oxide catalysts giving the nature of the different species likely to be involved. It is proposed that the reduction to N<sub>2</sub> occurs through the reaction of oxidised and reduced (species in shaded circle) nitrogen compounds [34].

In the case of the C<sub>3</sub>H<sub>6</sub>-SCR of NO over Al<sub>2</sub>O<sub>3</sub>, the rate of nitrate formation is slower than their rate of consumption, and mostly acetates are observed [34-35]. One of the roles of Ag in Ag/Al<sub>2</sub>O<sub>3</sub> catalysts is to promote the oxidation of NO to ad-NO<sub>x</sub> species [34], which reside on both the Al<sub>2</sub>O<sub>3</sub> and Ag. Yamaguchi [34] observed that too

large an increase in the partial pressure of NO over Ag/Al<sub>2</sub>O<sub>3</sub> saturated the surface with nitrates, effectively poisoning the sample. Note that such a deactivation was not observed in the case of Co/Al<sub>2</sub>O<sub>3</sub> because the Co does not appear to promote the formation of ad-NO<sub>x</sub> on Al<sub>2</sub>O<sub>3</sub>. This may be due to the formation of strongly bound ad-NO<sub>x</sub> species on the Co which do not readily migrate to the Al<sub>2</sub>O<sub>3</sub> support.

Kameoka et al. [75] also emphasised that nitrates do not all have the same reactivity, and proposed that a monodentate species was the most reactive ad-NO<sub>x</sub> species over Ag/Al<sub>2</sub>O<sub>3</sub>. One of the various roles of nitrates is also to facilitate the initial oxidation of the hydrocarbon, as shown by an increase in oxidation rate by ad-NO<sub>x</sub> species [35]. Regarding potential intermediates, Zuzaniuk et al. [36] reported that organo-nitro and organo-nitrito needed to be considered differently, since the latter mostly yielded NO<sub>2</sub> as oxidation product, rather than the NH<sub>3</sub> derived from the nitrocompound. Other experimental parameters such as temperature, water vapour pressure will affect the priority of the reactions as reported in Figure 2.9. The possible participation of homogeneous reactions must also be considered, especially at the higher temperatures and bearing in mind that NO and NO<sub>2</sub> are radical. Yet, it appears the majority of data reported on oxides/base metals are consistent with this scheme. In addition to the possible simultaneous occurrence of parallel reaction pathways over a given type of catalytic sites, it has also to be born in mind that various catalytic phases may be present on a given materials, complicating further the analysis of the system. This is likely to be the case over, e.g. silver/alumina materials with intermediate loadings, as suggested by Meunier et al. [56] as shown in Figure 2.10.

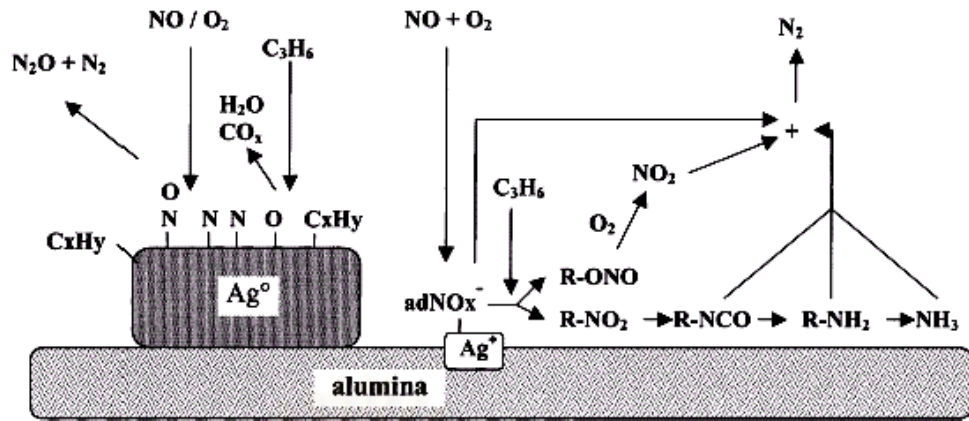


**Figure 2.10** The different roles of Ag during the C<sub>3</sub>H<sub>6</sub>-SCR over Ag/Al<sub>2</sub>O<sub>3</sub>: large Ag<sup>0</sup> particles catalyze the decomposition–reduction of NO, whereas Ag<sup>+</sup> species favors the oxidation of NO to ad-NO<sub>x</sub> species, which subsequently react through the intermediacy of organo-nitrogen compounds [34].

## CHAPTER III

### EXPERIMENTAL

This chapter consists of experimental systems and procedures used in this work, which is divided into three parts: 1) catalyst preparation, 2) catalyst characterization and 3) catalyst activities and characterization of surface species. The section 3.1 describes the procedure for catalyst preparation. The catalyst characterizations by various techniques including N<sub>2</sub>O decomposition method, CO<sub>2</sub> TPD procedure and XRD are explained in section 3.2. Finally, the last section shows the procedures to obtain the catalyst activity and the nature of surface species in SCR of NO by propene.

#### 3.1 Catalyst Preparation

This section is divided into three parts including chemicals, support preparation and preparation of Ag catalyst.

##### 3.1.1 Chemicals

For the preparation of Ag/Al<sub>2</sub>O<sub>3</sub> and Ag/SiO<sub>2</sub>, analytical grades materials were used in these experiments. Alumina and silica support used in this study are listed in table 3.1.

**Table 3.1** Details of chemical reagents used for catalyst preparation

Chemical	Formula	Manufacture
1. Alumina	Al <sub>2</sub> O <sub>3</sub>	Sumitomo Aluminum Smelting Co., Ltd., Japan (type NKH-3)
2. Silver nitrate	AgNO <sub>3</sub>	Sigma-Aldrich Chemical Co., U.S.A.
3. Silica	SiO <sub>2</sub>	

### 3.1.2 Preparation of Support

Alumina and silica pellets, spherical shape, were grounded to a required mesh size of 40-60 mesh and then washed by distilled water for 2-3 times to remove the very fine particles and other impurities. Subsequently, they were dried at 110°C overnight and then calcined at 300°C for 2 h in air atmosphere.

### 3.1.3 Preparation of Silver Catalyst

Ag/Al<sub>2</sub>O<sub>3</sub> and Ag/SiO<sub>2</sub> were prepared by the impregnation technique detailed as follows:

1. The amount of silver was calculated just enough for 2 g of the alumina or silica support and then de-ionized water was added until the total volume of the solution became 2 and 1.8 ml for alumina and silica, respectively.

2. 2 g of support was placed in a 50 ml Erlenmeyer flask and then the impregnation solution was gradually dropped into this support using a dropper. Shaking the flask continuously during impregnation was required to ensure the homogenous distribution of metal component on the support.

3. After the incipient wetness impregnation, the mixture of the impregnation solution and the alumina support was left in the atmosphere for 6 h to make a good distribution of metal complex. Subsequently, the impregnated sample was dried at 110 °C overnight in an oven.

4. The dried sample was purged under nitrogen at a flow rate of 60 ml/min with a heating rate of 10°C/min from room temperature to 600°C. When the temperature was reached to 600°C, 100 ml/min of air flow was instead of nitrogen in order to make silver complex become silver oxide, which was in a stable form. The temperature was held at 600°C for 2 h in air atmosphere.

5. After the calcined sample was cooled down, it was stored in a glass bottle into a dessicator for further use.

### 3.2 Catalyst characterization

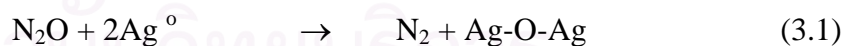
This section explains the characterization of Ag-based catalyst including the crystal structure by XRD analysis, the metal active sites by N<sub>2</sub>O decomposition and the basicity measurement by CO<sub>2</sub>-TPD procedure.

#### 3.2.1 X-ray Diffraction

X-ray diffraction analysis was used to analyze the crystallinity and the structure of a catalyst. The refraction or diffraction of the X-rays was monitored at various angles with respect to the primary beam X-ray diffraction analysis using an X-ray refractometer, SIEMENS XRD D5000, with Ni-filtered CuK $\alpha$  radiation in the 2 $\theta$  range of 10 to 80°.

#### 3.2.2 Silver Metal Active Sites Measurement by N<sub>2</sub>O Decomposition Method

The number of metal active sites were measured by N<sub>2</sub>O decomposition technique on the assumption that only one N<sub>2</sub>O molecule adsorbed and reacted with two silver metal sites, as the equation 3.1



##### A. Materials

Helium in ultra high purity grade, hydrogen in ultra high purity grade and nitrous oxide in purity grade were used as a carrier gas, a reducing agent and an adsorbent gas, respectively. All gases used in this experiment were supplied by Thai Industrial Gas Limited.



## B. Apparatus

The extensive diagram of instruments in measurement of the metal active sites is included in Figure 3.1. The amount of the effluent gases was measured by a thermal conductivity detector within a gas chromatograph (GOW-MAC). An operating condition of the gas chromatograph is illustrated in Table 3.2.

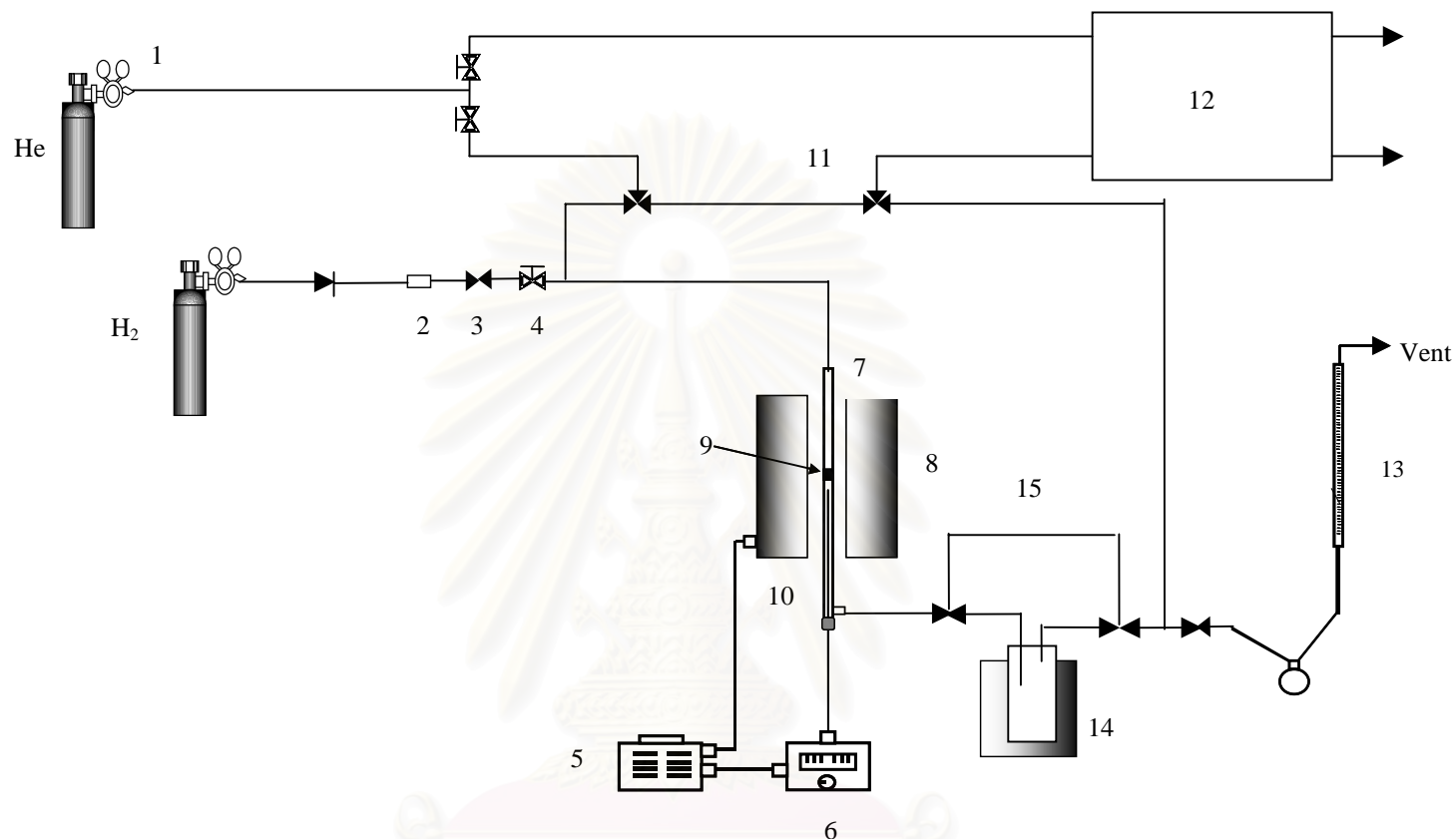
**Table 3.2** Operating condition of a thermal conductivity detector within a gas chromatograph (GOW-MAC) for measurement of the metal active sites

Model	GOW-MAC
Detector type	TCD
Helium flow rate	30 ml/min
Detector temperature	30°C
Detector current	80 mA
Packed column	Porapak-QS

## C. Procedure

1. 0.1 g of a catalyst sample was placed in a stainless steel tubular reactor. Helium gas was introduced into the reactor at a flow rate of 30 ml/min. The catalyst sample was heated at an increasing rate of 10°C/min until a temperature reached to 300°C, then helium was substituted by hydrogen at a flow rate of 50 ml/min and held at this temperature for 1 h. Subsequently, the catalyst sample was cooled down to room temperature in helium flow.

2. At 150°C at which the catalyst sample was ready to be measured the metal active sites, 50 µl of the purity nitrous oxide gas was injected into the injection port to decompose on the metal surface of the catalyst sample. Injection of nitrous oxide was continuously repeated until the nitrous oxide did not any longer decompose on the



- |                           |               |                       |                 |                                 |
|---------------------------|---------------|-----------------------|-----------------|---------------------------------|
| 1. Pressure Regulator     | 2. Gas Filter | 3. On-Off Valve       | 4. Needle Valve | 5. Variable Voltage Transformer |
| 6. Temperature Controller | 7. Reactor    | 8. Furnace            | 9. Catalyst Bed | 10. Thermocouple                |
| 11. Three-way Valve       | 12. TCD       | 13. Bubble Flow Meter | 14. Saturator   | 15. Three-way Valve             |

**Figure 3.1** Flow diagram of measurement of  $N_2O$  decomposition and  $CO_2$ -TPD

catalyst sample. This situation was occurred when an obtained chromatogram area of any injection, after decomposition of the nitrous oxide pulse in the first injection had proceeded, was kept nearly constant compared with that of the former injection or no nitrogen product was released.

3. The amount of the metal active sites of the catalyst sample will be calculated according to description in Appendix C.

### 3.2.3 Basicity by CO<sub>2</sub> TPD

#### A. Materials

Helium in ultra high purity grade and carbon dioxide in purity grade were used as a carrier gas and an adsorbent gas, respectively. All gases used in this experiment were supplied by Thai Industrial Gas Limited.

#### B. Apparatus

The instruments and the flow diagram of the system to study the CO<sub>2</sub> TPD are shown in Figure 3.1. An operating condition of the gas chromatograph is illustrated in Table 3.3.

**Table 3.3** Operating condition of a thermal conductivity detector within a gas chromatograph (GOW-MAC) for measurement of CO<sub>2</sub> TPD

Model	GOW-MAC
Detector type	TCD
Helium flow rate	30 ml/min
Detector temperature	30°C
Detector current	80 mA

### C. Procedure

1. 0.1 g of a catalyst sample was packed in a stainless steel tubular reactor. Helium was introduced at a flow rate of 50 ml/min, the catalyst sample was heated up to 500°C at a heating rate of 10°C/min and held for 1 h at this temperature in order to eliminate the adsorbed water. Then, the system was cooled down to room temperature.

2. The sample was purged with 30 ml/min of CO<sub>2</sub> at room temperature for 1 h, and then helium gas was substituted into the reactor at a flow rate of 30 ml/min. After CO<sub>2</sub> adsorption, this sample was heated from room temperature to 500 °C in He atmosphere. The heating rate used in this study is 5°C/min.

### 3.3 Catalyst Activities and Characterization of Surface Species

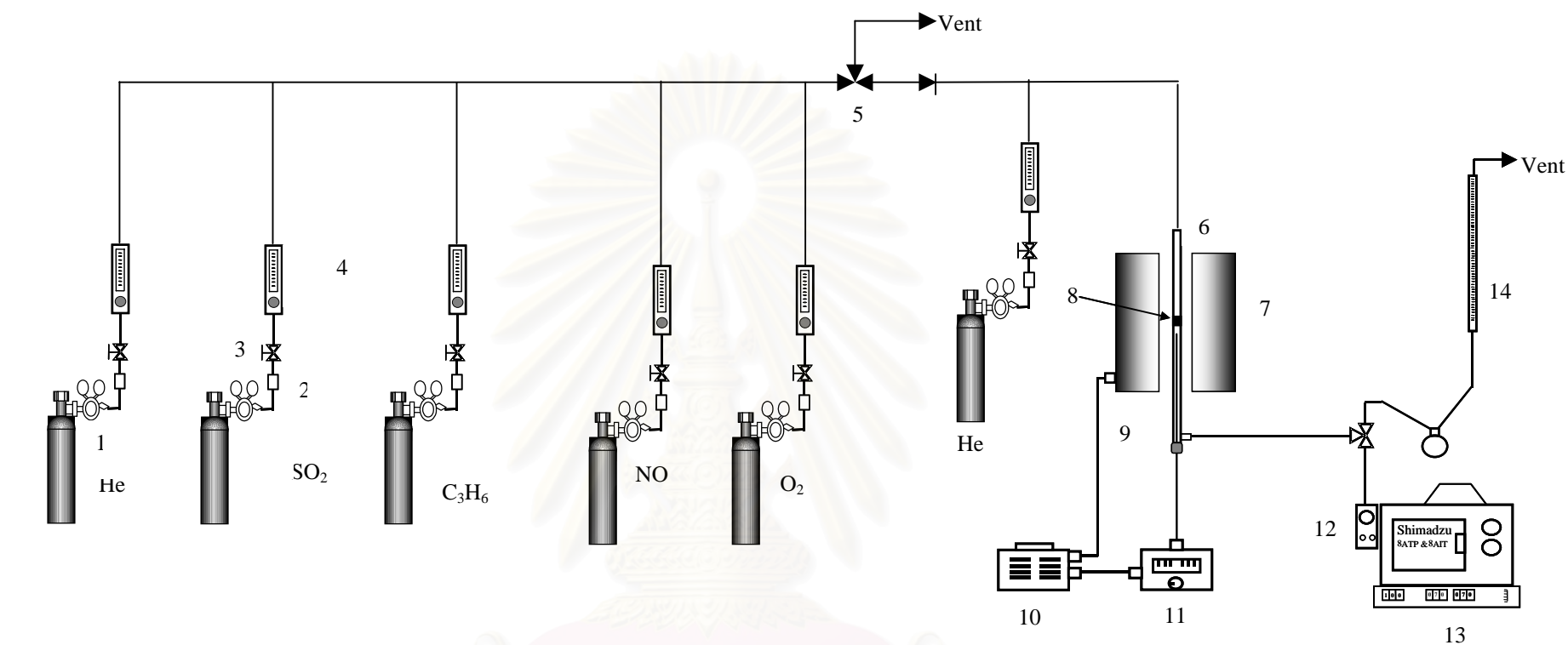
For section 3.3, the activity and characteristic of surface species in SCR of NO by propene were studied using temperature programmed techniques.

#### A. Materials

The gases used in the catalytic activity test are listed in Table 3.4. They were all supplied by Thai Industrial Gas Limited.

**Table 3.4** The details of gases used in the catalyst activity test

Gases	Formula	Grade
Helium	He	Ultra high purity
Oxygen	O <sub>2</sub>	10% in He
Nitric oxide	NO	1% in He
Propene	C <sub>3</sub> H <sub>6</sub>	3% in He



- |                        |                                  |                            |                    |
|------------------------|----------------------------------|----------------------------|--------------------|
| 1. Pressure Regulator  | 2. Gas Filter                    | 3. On-Off Valve            | 4. Flow meter      |
| 5. Three-way Valve     | 6. Reactor                       | 7. Furnace                 | 8. Catalyst Bed    |
| 9. Thermocouple        | 10. Variable Voltage Transformer | 11. Temperature Controller | 12. Sampling Valve |
| 13. Gas Chromatography | 14. Bubble Flow Meter            |                            |                    |

**Figure 3.2** Schematic diagram of the reaction line for NO and HC conversions analyzed by gas chromatographs equipped with molecular sieve 5A and porapak QS columns

## B. Apparatus

A flow diagram of the system for testing the catalytic activity is shown in Figure 3.2. A quartz flow reactor with 0.6 cm inside diameter was used in this experiment. Feed and effluent gases were analyzed by TCD gas chromatographs, SHIMADZU GC8-ATP and SHIMADZU GC-8AIT. An operating condition used in this experiment is given in Table 3.5. This section is divided into two parts including the catalyst activity and the nature of surface species

**Table 3.5** Operating conditions of gas chromatographs for the catalytic activity test

Gas Chromatograph	SHIMADZU GC8A-ATP	SHIMADZU GC8A-AIT
Detector	TCD	TCD
Packed column	Molecular sieve 5A	Porapak QS
Carrier gas	He (UHP)	He (UHP)
Flow rate of carrier gas	45 ml/min	85 ml/min
Injector temperature	100°C	110°C
Column temperature	60°C	80°C
Detector temperature	100°C	110°C
Current	80 mA	90 mA
Analyzed gas	O <sub>2</sub> , N <sub>2</sub> , CH <sub>4</sub> , CO	CH <sub>4</sub> , CO <sub>2</sub> , N <sub>2</sub> O, C <sub>3</sub> H <sub>6</sub> , SO <sub>2</sub>

## C. Procedure

### An experiment for studying catalyst activity behavior

- 0.4 g of a catalyst sample was packed in quartz tubular down flow reactor. The reactor was placed in the furnace.
- A gas mixture containing 1000 ppm NO, 1000 ppm C<sub>3</sub>H<sub>6</sub> and 5% O<sub>2</sub> diluted in helium at a total flow rate of 200 ml/min (GHSV of 16000 h<sup>-1</sup>) was used as a model exhaust gas to test the catalytic activity through temperature programmed

reaction. The reaction gases were introduced to the reactor whose temperature was raised from 50 to 700°C stepwise. At each step, the catalyst bed was held at constant temperature until steady state was reached. This was achieved within 20 min. The effluent gases were analyzed by TCD gas chromatographs as shown in table 3.5.

3. These chromatograms were compared with calibration curve to calculate the composition of gases in feeds and effluent gases.

### **An experimental set for studying the nature of surface species**

1. 0.4 g of a catalyst sample was packed in quartz tubular down flow reactor and the height of the catalyst bed was about 0.6 cm. The reactor was placed in the furnace and helium was introduced into the reactor in order to remove the remaining air out of the system.

3. The nature of surface species on the catalyst exposed to the reactants was investigated by an experiment consisting of three steps as follows:

a. Reaction step: A selected reactant gas mixture containing 1000 ppm NO, 1000 ppm C<sub>3</sub>H<sub>6</sub> and 5% O<sub>2</sub> diluted in helium at a total flow rate of 200 ml/min (GHSV of 16000 h<sup>-1</sup>) was used as a model exhaust gas to produce the surface species. This reactant gas mixture was introduced at a given temperature for 2 h. Samples of effluent gases were taken to measure a composition and analyzed by gas chromatograph every 10 min to check the steady state conversions of C<sub>3</sub>H<sub>6</sub> and NO at a dosing temperature. When a time on stream was equal to 2 h, the catalyst sample was immediately flushed with helium at the same temperature for 10 min and then cooled down to room temperature.

b. Temperature programmed desorption (TPD) step: After dosing the catalyst in the first step, it was continuously followed by temperature programmed desorption to remove as much of the adsorbed surface species as possible in the same apparatus. During TPD step, temperature was ramped at a constant 5°C/min from 100

to 800°C under 50 ml/min helium flow. The effluent gases were analyzed using two TCD GCs, one equipped with a molecular sieve 5A column for separating O<sub>2</sub>, N<sub>2</sub> and CO and a Porapak QS column for separating CO<sub>2</sub>, N<sub>2</sub>O and hydrocarbons. Peak areas were automatically determined using Shimadzu C-R6A integrator data system. The amount of surface species was calculated from tracers of releasing gases through calibration curves as described in Appendix C. Finally, the catalyst sample was cooled down to room temperature.

c. Temperature programmed oxidation (TPO) step: On completion of the TPD step, a TPO run using oxidizing gases such as 1% O<sub>2</sub> in He was carried out to determine if there were any residual carbonaceous materials on the catalyst. During TPO step, temperature was ramped at a constant 5°C/min from 100 to 800°C under 50 ml/min helium flow. The effluent gases were analyzed using two TCD GCs being the same as the TPD step.

4. It was remarked that an experiment to test a reactivity of the surface species was achieved by using temperature programmed oxidation with changing an oxidizing gases such as NO+O<sub>2</sub>.



## CHAPTER IV

### RESULTS AND DISCUSSION

In this research, the characteristic of surface species on the SCR of NO with propene in the presence of excess oxygen over Ag/Al<sub>2</sub>O<sub>3</sub> were investigated through temperature programmed techniques. The results and discussion in this chapter were separated into two main parts. In the first section, a basic characterization of a monometallic Ag/Al<sub>2</sub>O<sub>3</sub> catalyst is pronounced. Next, the catalyst activity and characterization of surface species are shown in section 4.2. To discuss the behavior of surface species, the reactivity and physical mixture method were used to study the nature of surface species.

#### 4.1 The Characterization of Ag/Al<sub>2</sub>O<sub>3</sub> Catalyst

Ag/Al<sub>2</sub>O<sub>3</sub> catalyst was first characterized to overview their properties and characteristics. XRD was used to measure the structure of Ag/Al<sub>2</sub>O<sub>3</sub> while the desorption of CO<sub>2</sub> was investigated through CO<sub>2</sub>-TPD.

##### 4.1.1 X-ray Diffraction Analysis

The crystallinity and structure of pure 2% and 10% Ag/Al<sub>2</sub>O<sub>3</sub> catalysts were analyzed by X-ray diffraction (XRD). The same XRD patterns of both are illustrated in Figure 4.1. These spectra are similar with XRD pattern of Al<sub>2</sub>O<sub>3</sub> [57] and reveal neither the presence of silver oxide nor metallic silver. This means that the silver particle size may be quite small. Bethke et al. [57] found that XRD of Ag/Al<sub>2</sub>O<sub>3</sub> catalysts exhibited the signal, which indicated the absence of Ag<sup>2+</sup> and small paramagnetic Ag<sup>0</sup> particles. Moreover, they use UV-Vis diffuse to determine the existent silver and they found that Ag/Al<sub>2</sub>O<sub>3</sub> catalyst contain small Ag<sub>2</sub>O particle isolated Ag<sup>+</sup> atoms.

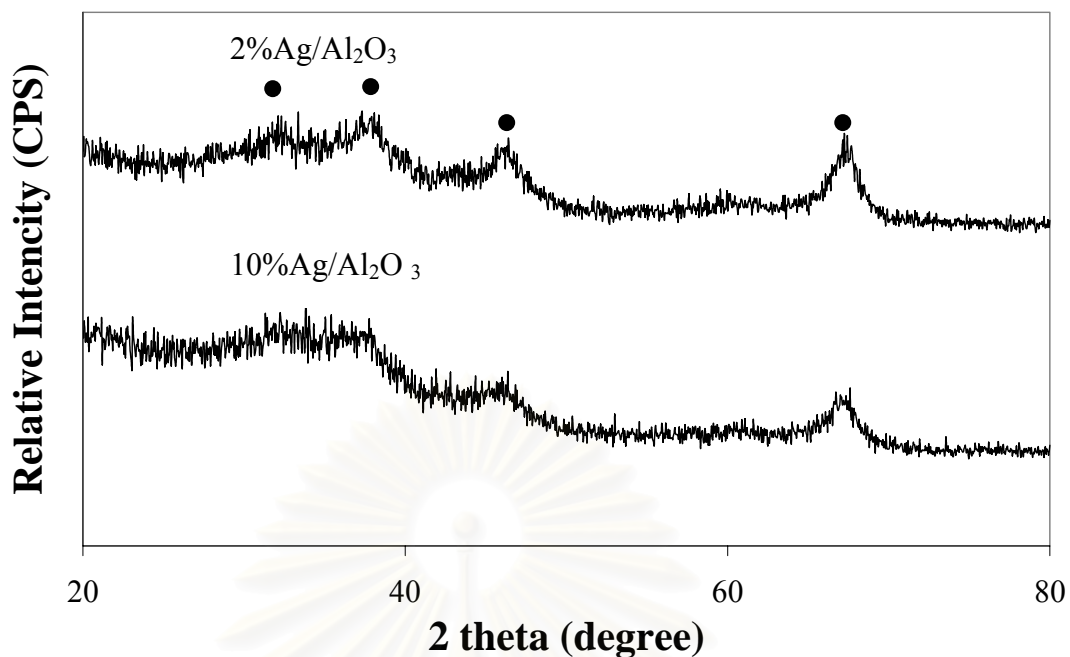


**Figure 4.1** X-ray diffraction pattern of 2% and 10%Ag/Al<sub>2</sub>O<sub>3</sub> catalysts: (●)  $\gamma$ -Al<sub>2</sub>O<sub>3</sub>.

#### 4.1.2 The Basicity by CO<sub>2</sub>-TPD

In this experiment, the desorption of CO<sub>2</sub> molecule was investigated by using CO<sub>2</sub>-TPD technique and this data do not show only basicity behavior but also give information regarding the temperature range for desorption of CO<sub>2</sub> molecule. Figure 4.2 exhibits CO<sub>2</sub>-TPD profile of Ag/Al<sub>2</sub>O<sub>3</sub> catalyst. This spectrum shows a peak with a maximum at 125°C and a shoulder at 100°C as well as a long tail, extending to 300 °C. It can be implied that a majority of basic sites on our Ag/Al<sub>2</sub>O<sub>3</sub> catalyst behaves the weak basic sites.

สถาบันวิทยบริการ  
จุฬาลงกรณ์มหาวิทยาลัย

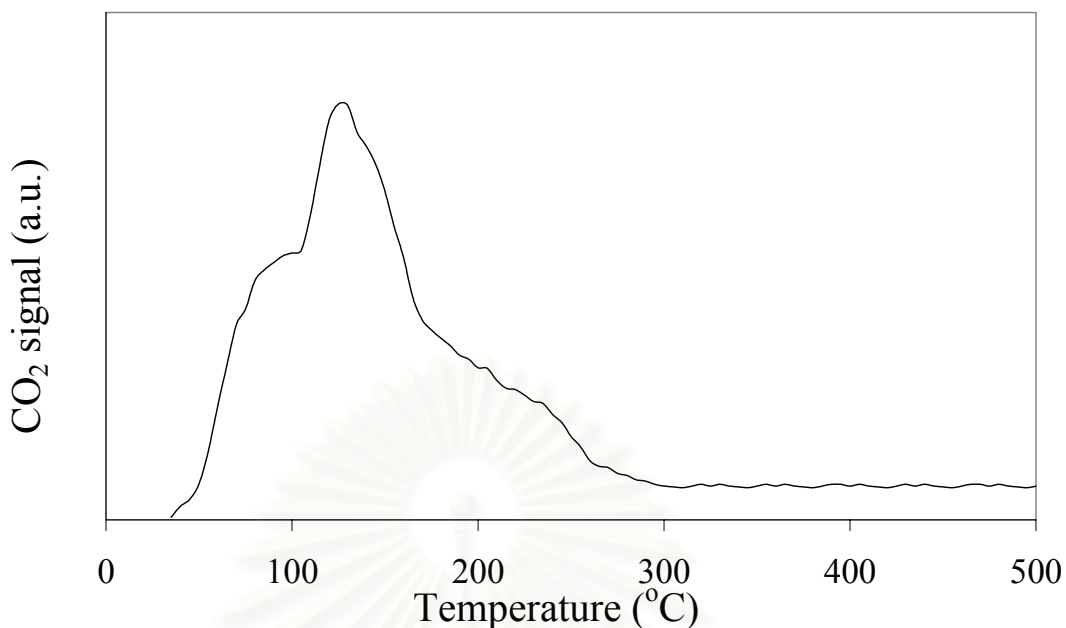


**Figure 4.2** Carbon dioxide TPD spectrum of Ag/Al<sub>2</sub>O<sub>3</sub> catalyst

#### 4.2 Evaluation of surface species

Before the behavior study of surface species, temperature programmed reaction (TPR) of propene and nitric oxide was made because these data were used to select the temperatures for production the surface species during the reaction steps in the next section. These results do not only show activity behavior but also give information regarding the temperature range. In this part, two concentrations of Ag/Al<sub>2</sub>O<sub>3</sub> catalysts were tested the catalytic activity measurement toward TPR.

TPR profiles involving C<sub>3</sub>H<sub>6</sub> and NO conversions versus the elevated temperature are shown in Figure 4.3 for the 2 wt% Ag/Al<sub>2</sub>O<sub>3</sub> and in Figure 4.4 for the 10 wt% Ag/Al<sub>2</sub>O<sub>3</sub>. The 2 wt% Ag/Al<sub>2</sub>O<sub>3</sub> is an effective catalyst but is active at a high temperature while the difference activity is observed over the 10 wt% Ag/Al<sub>2</sub>O<sub>3</sub>. This catalyst is active at a low temperature. The overall NO reduction conversion reaches a sharp maximum of approximately 90% at 450 °C and 50% at 350 °C for the 2 and 10 wt% catalysts, respectively. The main products are CO<sub>2</sub> and N<sub>2</sub>. No CO is both observed while N<sub>2</sub>O product occurs on only high-loading silver material while the other products such as NH<sub>3</sub> and NO<sub>2</sub> could not detect in this experimental. Meunier et al. [36] reported that the formation of various products (NO<sub>2</sub>, N<sub>2</sub>, N<sub>2</sub>O and NH<sub>3</sub>) was

observed. The peak for reduction to  $N_2$  occurs about 100 °C similar to the peak for total NO conversion so that there is some variation of selectivity to  $N_2O$  with changing temperature. It is approximately in the range of 15-50%. Both catalysts show coincidence of the onset of NO reduction and  $C_3H_6$  oxidation.

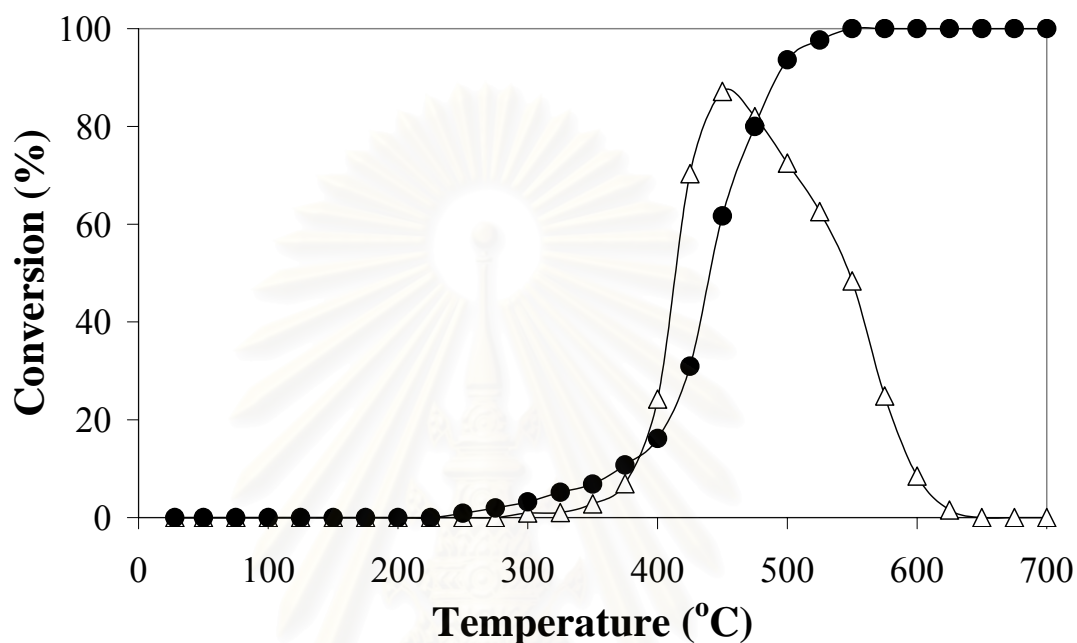


**Figure 4.3** The temperature programmed reaction profiles of 2 wt%  $Ag/Al_2O_3$  for the selective catalytic reduction of NO by  $C_3H_6$  under excess oxygen: (●)  $C_3H_6$  conversion and (△) total NO conversion.

Nevertheless, there is also some difference in the behavior patterns of both TPR profiles. Maximum  $NO_x$  conversion is coincident with 100%  $C_3H_6$  conversion for the 10 wt%  $Ag/Al_2O_3$  but not for the 2 wt%  $Ag/Al_2O_3$ . The low-loading silver shows occurrence of the maxima for total NO conversion at approximately 100 °C before combustion approaches to completion. These different activity patterns are related to the different of reaction mechanisms, which arise on different catalytic phase. Meunier et al. [36] found that the low-loading silver material exhibited high conversions to  $N_2$  whereas the high-loading sample predominantly yielded  $N_2O$ . They proposed that low-loading silver revealed the presence  $Ag^+$  species while high-loading silver showed the presence of oxidic species of silver (as isolate  $Ag^+$  and silver aluminates). This phenomenon is in agreement with the results reported several

authors [36, 77]. Finally, it is significantly noted that 2% Ag/Al<sub>2</sub>O<sub>3</sub> gives much more activity and selectivity than 10 % Ag/Al<sub>2</sub>O<sub>3</sub> catalysts.

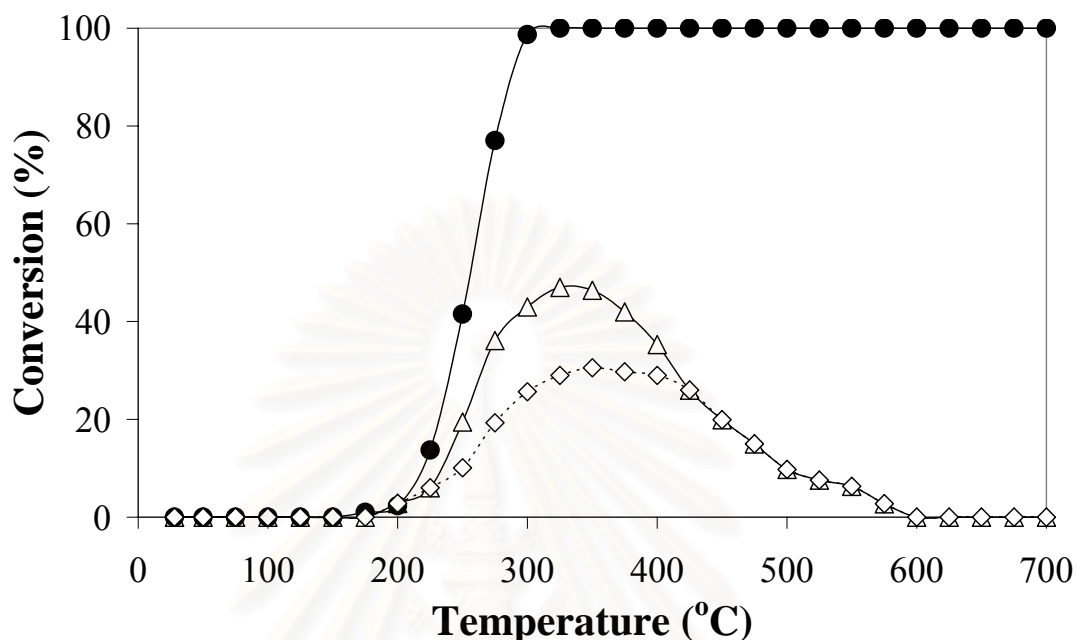


**Figure 4.4** The temperature programmed reaction profiles of 10 wt% Ag/Al<sub>2</sub>O<sub>3</sub> for the selective catalytic reduction of NO by C<sub>3</sub>H<sub>6</sub> under excess oxygen: (●) C<sub>3</sub>H<sub>6</sub> conversion, (△) total NO conversion to N<sub>2</sub> and N<sub>2</sub>O as well as (◇) NO conversion to N<sub>2</sub>O.

#### 4.2.2 The nature of surface species

In this part, temperature programmed techniques were undertaken to identify the active intermediate species and propose the possible reaction pathways in the C<sub>3</sub>H<sub>6</sub>-SCR of NO over Ag/Al<sub>2</sub>O<sub>3</sub> catalysts. Temperature programmed techniques consist three steps containing reaction step, temperature programmed desorption (TPD) and temperature programmed oxidation (TPO). It is remarked that in the first step the surface species were produced at the constant temperature. Afterwards, the TPD was carried out to remove the adsorbed surface species. Finally, the remaining surface species were removed in the TPO step. All compositions of the effluent gases in these experiments would be expected to provide some insight into the nature of the adsorbed species on the catalyst surface. However, the features of surface species on

the catalyst surface are carefully considered because the surface species do not behave only the intermediate species but also the spectator species.

To prevent elimination of all the intermediates by  $O_2$  during the production step of the surface species, in the TPD-TPO experiments, the surface species have to be introduced at a temperature above an onset temperature for  $C_3H_6$  oxidation, but below the temperature at which combustion goes to completion, that is, between 325 and 550 °C for the 2 wt%  $Ag/Al_2O_3$  and between 200 and 300 °C for the 10 wt%  $Ag/Al_2O_3$ . Because of this, the dosing temperatures of 370 °C and 210 °C in the first step of TPD-TPO experiment are used for the 2 wt%  $Ag/Al_2O_3$  and the 10 wt%  $Ag/Al_2O_3$ , respectively.

After exposure the Ag catalysts to a gas mixture of  $C_3H_6$ , NO and  $O_2$  at a given temperature, the  $C_3H_6$  and NO conversion of each system is equally approximately 60%. Figures 4.5 and 4.6 show gas evolution from surface of the 2 wt%  $Ag/Al_2O_3$  dosed with reactants ( $C_3H_6+NO+O_2$ ) at 370 °C for 2 h during TPD and TPO steps, respectively. It is noted that there appears gas evolution during TPD and TPO steps, unlike zeolite- and platinum-based catalysts as reported previously elsewhere [40,41]. The surface species on Pt formulation are almost totally released during TPD step whereas those on metal ion exchange ZSM-5 are necessarily removed by the oxidant on TPO step.

These effluent gases contained  $CO_2$ ,  $CH_4$  and  $N_2$  in the TPD step and only  $CO_2$  and  $N_2$  in the TPO step. Other species expected to be present such as NO,  $NO_2$  and  $NH_3$  were not observed in this experiment due to limitations of our analysis. Zuzaniuk et al. [37] reported production of  $NO_2$  and  $NH_3$  in oxidation of nitromethane and *tert*-butyl nitrite, which were assigned as models of possible intermediates. Considering the TPD profile, the effluent gases are obtained by decomposition process of some surface species, perhaps intermediates. For TPD step, as seen in Figure 4.5, a 600 °C  $CO_2$  peak occurs at about the same temperature as a  $CH_4$  peak. There is in addition a broad  $CO_2$  peak appearing at approximately 400 °C coincident with a very little  $N_2$  peak.

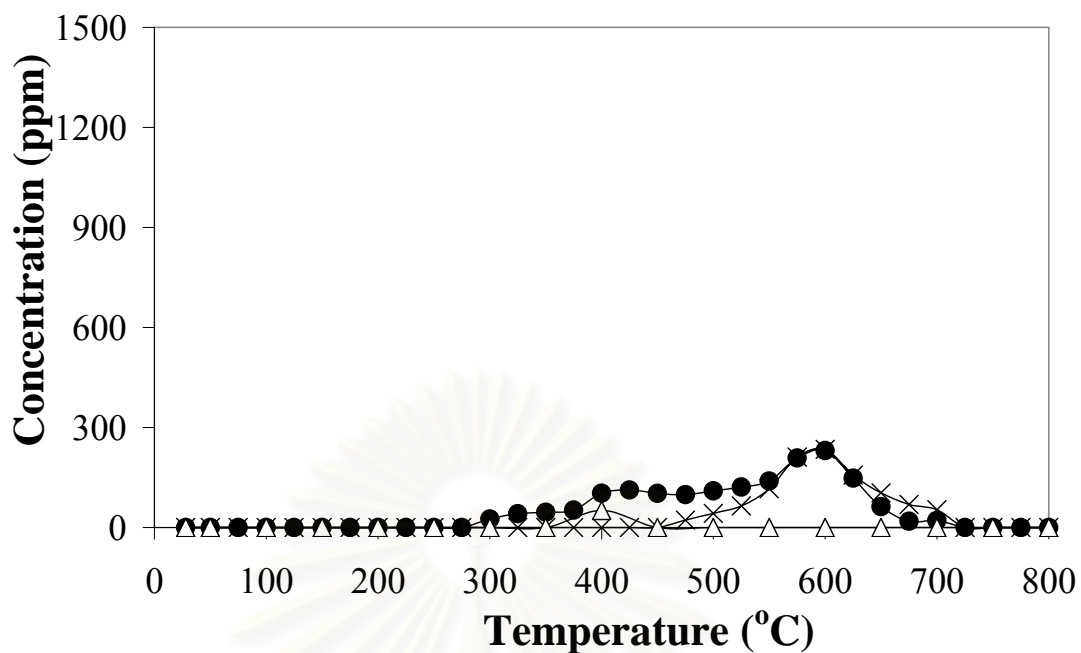


**Figure 4.5** The temperature programmed desorption profiles of 2 wt% Ag/Al<sub>2</sub>O<sub>3</sub> after dosing 1000 ppm C<sub>3</sub>H<sub>6</sub> + 1000 ppm NO + 5% O<sub>2</sub> at 370°C for 2 h: (△) N<sub>2</sub>, (●) CO<sub>2</sub> and (×) CH<sub>4</sub>.

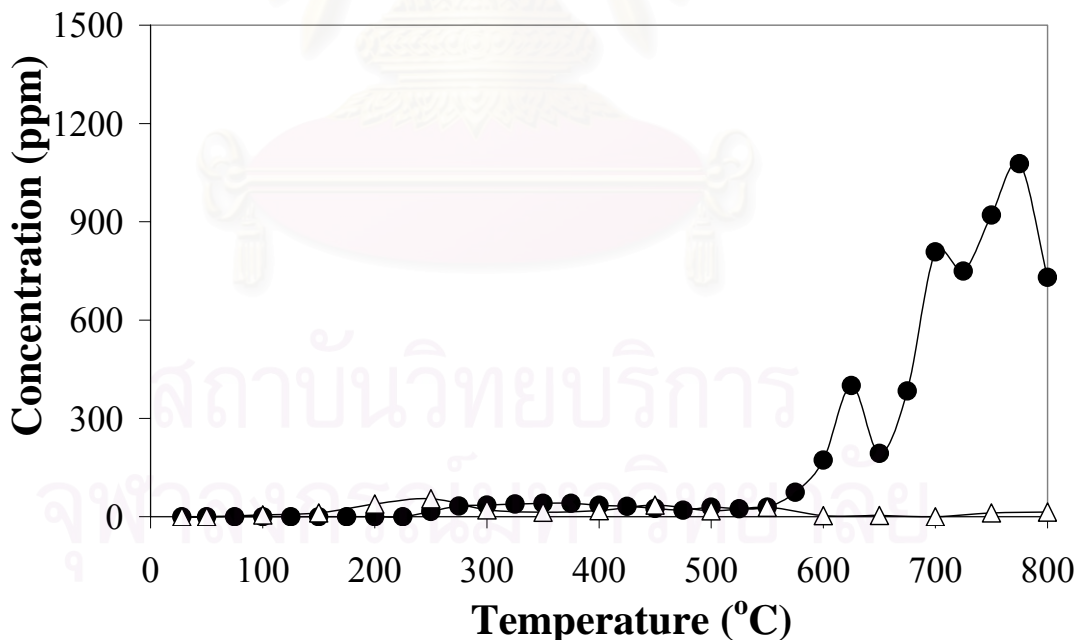


**Figure 4.6** The temperature programmed oxidation profiles of 2 wt% Ag/Al<sub>2</sub>O<sub>3</sub> by using 1% O<sub>2</sub> as the oxidizing gas after the two steps, reaction and TPD steps: (△) N<sub>2</sub> and (●) CO<sub>2</sub>.

In case of TPO surface species, this profile shows oxidation characteristic of the remaining deposits. It is also reminded that these deposits cannot decompose under He atmosphere at below 800 °C. Three large CO<sub>2</sub> peaks are centered at 625, 700 and 775 °C. There is in addition very small signal of CO<sub>2</sub> and N<sub>2</sub> at below 500°C, but probably significant.

It is speculated that each peak should be assigned to decomposition of at least one surface species, but possibly two may be involved. However, when there is a coincidence of peaks both probably arise from the same single surface species. Deconvolution of TPD profile suggests that at least two surfaces species on catalyst surface can decompose even in an inert gas. Since their structure and composition are as yet unknown, these species are designated as S<sub>TPDL</sub> and S<sub>TPDH</sub>. The former species is associated with the CO<sub>2</sub> and N<sub>2</sub> peaks at about 400 °C, while the latter species appears related to the CO<sub>2</sub> and CH<sub>4</sub> peaks at 600 °C. Nitrogen is present only in the structure of S<sub>TPDL</sub>. For TPD surface species, the existence of these surface species is in agreement with the observation by IR technique [78]. This results involves the observation of isocyanate (-NCO) and formate (CH<sub>3</sub>COO-) species on Ag/Al<sub>2</sub>O<sub>3</sub> in C<sub>3</sub>H<sub>6</sub>+NO+O<sub>2</sub> system. It was also found that surface isocyanate on Ag/Al<sub>2</sub>O<sub>3</sub> disappeared distinctly when flushed with He flow at 500 °C while the removal of formate species was observed over 500 °C. This is consistent with our discovery that only S<sub>TPDL</sub> can decompose under He atmosphere in the temperature range of 300-500 °C. In addition, only S<sub>TPDH</sub> decompose over 600 °C. As a consequence, it could be generally admitted that the species observed at low temperature indicate the formation of C<sub>w</sub>H<sub>x</sub>O<sub>y</sub>N<sub>z</sub> species resulting from the oxidation of with NO or the oxidation of the other species with NO while the species appeared at high temperature exhibit the formation of C<sub>x</sub>H<sub>y</sub>O<sub>z</sub> species resulting from partial oxidation of propene.

For TPO surface species, TPO profile shows at least three surfaces species being oxidized by O<sub>2</sub> at high temperature. To accommodate for discussion, we combine the three species to be only one group and designate a group of these species as S<sub>TPOH</sub>.



Because of the results of activity mentioned above, nature of the surface species on the high-loading Ag catalyst was additionally studied in order to fulfill our information. Gas evolutions during TPD and TPO experiments of the 10 wt% Ag/Al<sub>2</sub>O<sub>3</sub> exposed to a gas mixture of C<sub>3</sub>H<sub>6</sub>, NO and O<sub>2</sub> at 210 °C for 2 h are shown in Figures 4.7 and 4.8, respectively.

Clearly, there are some differences in TPD-TPO patterns compared to the low-loading Ag catalyst. The TPD surface species on the 10 wt% Ag/Al<sub>2</sub>O<sub>3</sub> are much more produced than that on the 2 wt% Ag/Al<sub>2</sub>O<sub>3</sub>. Considering gas evolution in the TPD profiles (see Figure 4.7), there are two CO<sub>2</sub> peaks at 325 and 575 °C as well as a shoulder at ca. 450 °C while N<sub>2</sub> and CH<sub>4</sub> show only one peak at 275 and 575 °C, respectively. The 575 °C carbon-containing species (coincidence of CO<sub>2</sub> and CH<sub>4</sub> peaks) seems to show the same characteristic of S<sub>TPDH</sub> on low-loading silver but much more production. The N<sub>2</sub> peak is a 125 °C shift from the experiment of the low-loading silver. This is relative with a shift of the 325 °C CO<sub>2</sub> peak although just 75 °C of the maximum CO<sub>2</sub> position is shifted. However, we think that these N<sub>2</sub> and CO<sub>2</sub> decompose from the same sort of surface species. Two possible reasons are pronounced to explain the shift of the N<sub>2</sub> and CO<sub>2</sub> peaks. First, these species are actually S<sub>TPDL</sub> but either their decomposition behavior or structural composition is changed. An example is change of the decomposition temperature of isocyanate species if this species occurs on the different catalyst surface. Over 2 wt% Ag/Al<sub>2</sub>O<sub>3</sub> the isocyanate species disappeared completely at about 500 °C [78] while it vanished definitely at just 350 °C on 0.8 wt% Pt/Al<sub>2</sub>O<sub>3</sub> [79]. The second reason is occurrence of new surface species definitely independent on S<sub>TPDL</sub>. Iglesias et al. [77] reported about the different of surface species for high and low silver loading. That significant difference was identification of cyanide species for the former on high silver loading, appearing initially at 300°C. We assign the species that contain with N and decompose during TPD step as S<sub>TPDL</sub>. This is relative with a shift of operating temperature that contain with N-containing compound can decompose to produce N<sub>2</sub> and CO<sub>2</sub> at low temperature when compare with TPD surface of low Ag loading. However, we found that the only shoulder of CO<sub>2</sub> for high loading appear at 400°C at which was the same temperature of S<sub>TPDL</sub> decomposition for low loading. Some literature [78] reported about the disintegration of aldehyde species that the

decomposition of this occurs at 425°C. We designate a species as  $S_{TPDM}$ . From the previous work [40,42], two relatively peaks at 325 and 525°C are also observed. There are two  $CO_2$  peaks at 350 and 500°C. These species are designated as  $C_xH_yO_zN_w$  and  $(C_1H_mO_n)_{HT}$ , respectively. The positions of both species are coincident with the two  $CO_2$  peaks of  $S_{TPDL}$  and  $S_{TPDH}$  species appearing in the TPD profile for the dosing reactants gases.

For TPO step, both different and similar surface species loading Ag were observed as shown in Fig.4.8. The surface species were oxidized and released both low and high temperature. At low temperature, the surface species is more produced than that appears in 2 wt% silver. We assign these species as  $S_{TPOL}$ .

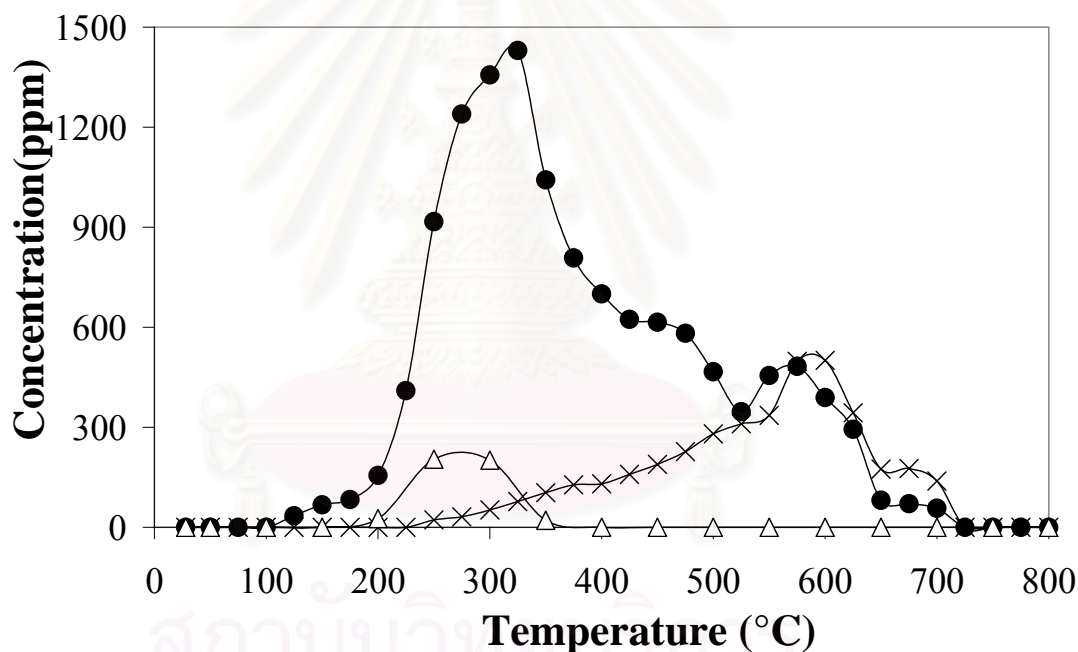


**Figure 4.7** The temperature programmed desorption profiles of 10 wt% Ag/ $Al_2O_3$  after dosing 1000 ppm  $C_3H_6$  + 1000 ppm NO + 5%  $O_2$  at 210°C for 2 h: ( $\Delta$ )  $N_2$ , ( $\bullet$ )  $CO_2$  and ( $\times$ )  $CH_4$ .

Certainly, the surface species may possible play a role to be either the intermediate species or the spectator species. For example, nitrite (-CN) and isocyanate species were proposed as the intermediates for the selective catalytic reduction of NO by hydrocarbon over Ag/ $Al_2O_3$  [65]. In addition, there is some work suggested that acetates were the catalytic intermediate for the selective catalytic

reduction of NO by n-hexane over Ag/Al<sub>2</sub>O<sub>3</sub> while nitrate species exhibited the behavior of spectator in this reaction [64]. Therefore, the surface species released in TPD and TPO steps need to be tested the reactivity with reactant under reaction condition. The species, which can be decomposing or oxidized at a relative temperature, is possible to be an intermediate. Hence, the reactivity of surface species that appear in TPD and TPO steps with oxidizing reactant gases was studied. The reactivity test was conducted by using TPO technique without or with TPD step. Before the reactivity tests, the surface species were produced by dosing a gases mixture of C<sub>3</sub>H<sub>6</sub>+NO+O<sub>2</sub> at 370 and 210 for 2% and 10% Ag/Al<sub>2</sub>O<sub>3</sub>, respectively. Temperature programmed oxidation with oxidizing reactant gases such as O<sub>2</sub> and NO+O<sub>2</sub> was used to test the reactivity.

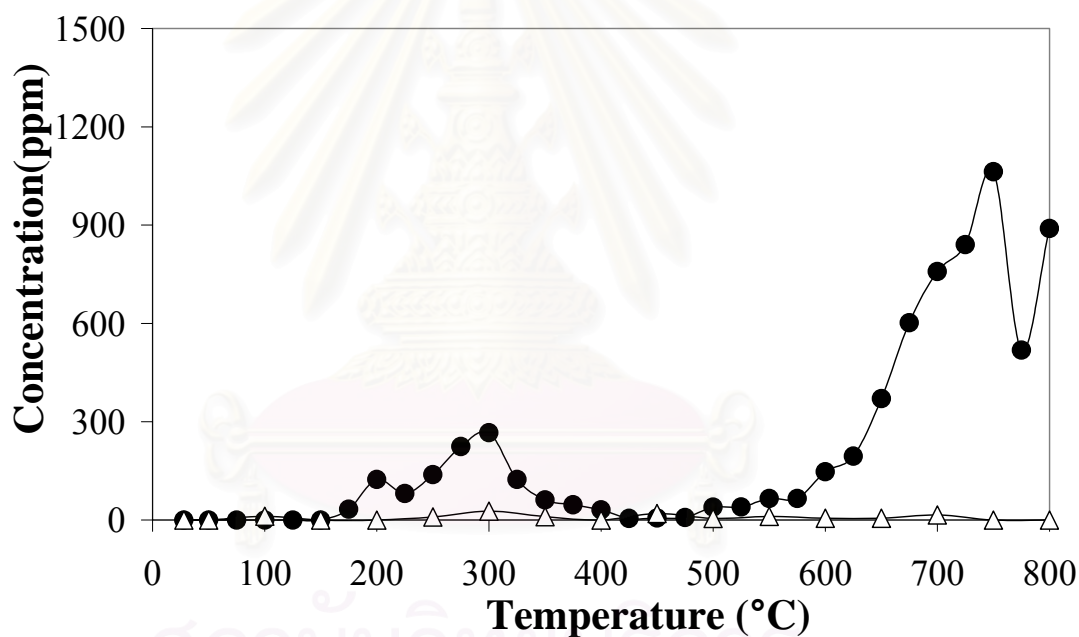


**Figure 4.8** The temperature programmed oxidation profiles of 10 wt% Ag/Al<sub>2</sub>O<sub>3</sub> by using 1% O<sub>2</sub> as the oxidizing gas after the two steps, reaction and TPD steps: (△) N<sub>2</sub> and (●) CO<sub>2</sub>.

To study the characteristics of TPD surface species, the TPO by O<sub>2</sub> without TPD technique was made. Figure 4.9 shows the traces of outlet gases obtained from the oxidation of surface species by O<sub>2</sub> over 2% Ag/Al<sub>2</sub>O<sub>3</sub> catalyst after exposed to C<sub>3</sub>H<sub>6</sub>+NO+O<sub>2</sub>. The effluent gases contain CO<sub>2</sub> and N<sub>2</sub>. It is found that the position of CO<sub>2</sub> peak addressed as S<sub>TPDL</sub> was unaffected with introducing O<sub>2</sub> as oxidizing gases

while the  $\text{CO}_2$  and  $\text{CH}_4$  peak addressed as  $S_{\text{TPDH}}$  disappeared. We speculate that  $S_{\text{TPDH}}$  should be oxidized by  $\text{O}_2$  and transformed to be  $\text{CO}_2$  and  $\text{N}_2$  centered at  $425^\circ\text{C}$ . This result indicates that  $S_{\text{TPDL}}$  species can decompose even in excess oxygen at the same temperature where decompose under helium atmosphere. On the other hand,  $S_{\text{TPDH}}$  is easily oxidized by  $\text{O}_2$ . The similar result was reported by Shimizu et al. [64]. They found that

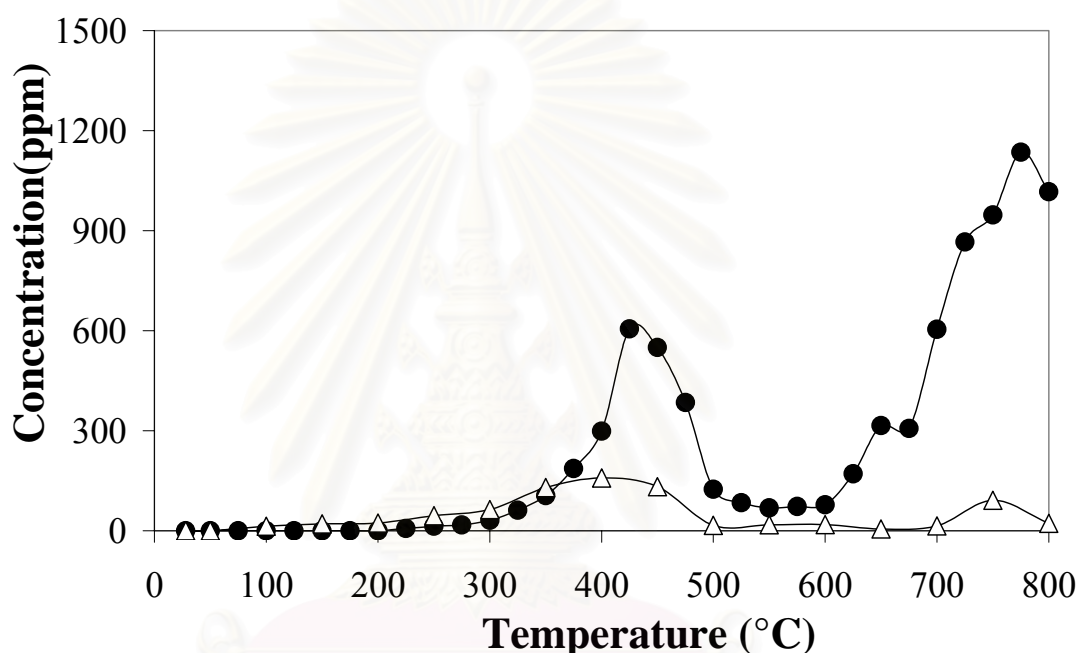


**Figure 4.9** The temperature programmed oxidation profiles of 2 wt%  $\text{Ag}/\text{Al}_2\text{O}_3$  by using 1%  $\text{O}_2$  as the oxidizing gas after dosing 1000 ppm  $\text{NO}$  + 1000 ppm  $\text{C}_3\text{H}_6$  + 5%  $\text{O}_2$  at  $370^\circ\text{C}$  for 2 h: ( $\Delta$ )  $\text{N}_2$  and ( $\bullet$ )  $\text{CO}_2$ .

Figures 4.10 and 4.11 show the effluent gases obtained from the oxidation of surface species by  $\text{NO}+\text{O}_2$  without and with TPD step over 2%  $\text{Ag}/\text{Al}_2\text{O}_3$  catalyst after exposed to  $\text{C}_3\text{H}_6+\text{NO}+\text{O}_2$ . When the oxidizing gas is changed to  $\text{NO}+\text{O}_2$ , the reactivity of  $S_{\text{TPDH}}$  and  $S_{\text{TPOH}}$  surface species was observed both reactivity tests.  $S_{\text{TPDH}}$  was oxidized with  $\text{NO}+\text{O}_2$  to produce  $\text{CO}_2$  at the lower temperature while  $\text{CO}_2$  at high temperature disappeared. From the above results, it indicates that the surface species decomposing at high temperature addressed as  $S_{\text{TPDH}}$  species is easily removed by both  $\text{O}_2$  and  $\text{NO}+\text{O}_2$ .

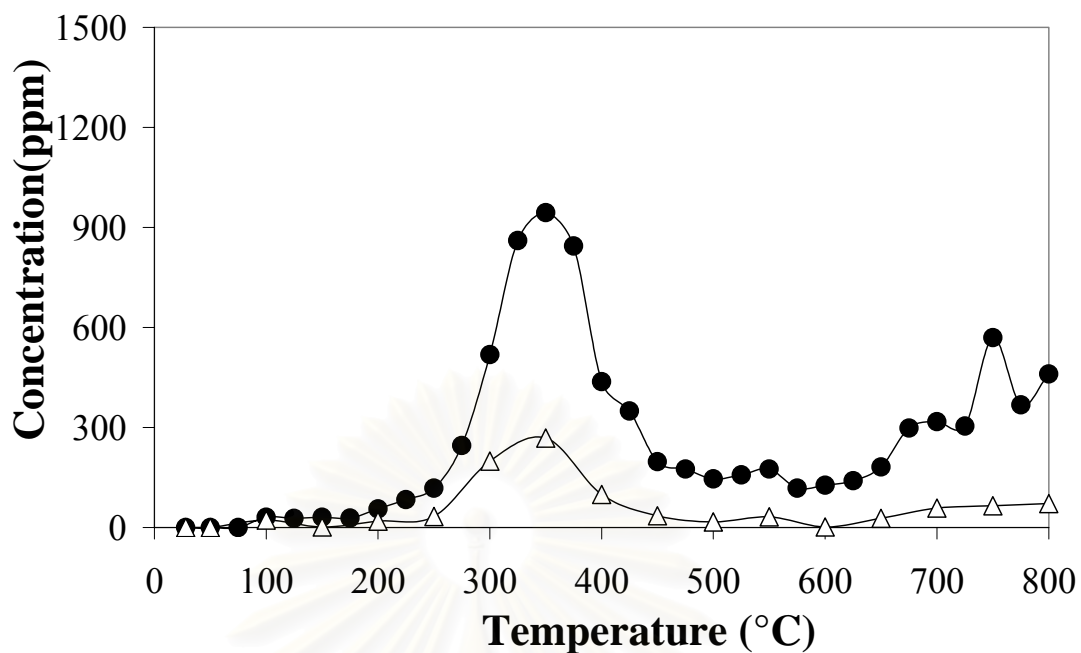


**Figure 4.10** The temperature programmed oxidation profiles of 2 wt% Ag/Al<sub>2</sub>O<sub>3</sub> by using 1% O<sub>2</sub>+1000 ppm. NO without TPD as the oxidizing gas after dosing 1000 ppm C<sub>3</sub>H<sub>6</sub> + 5% O<sub>2</sub> at 370°C for 2 h: (△) N<sub>2</sub> and (●) CO<sub>2</sub>.

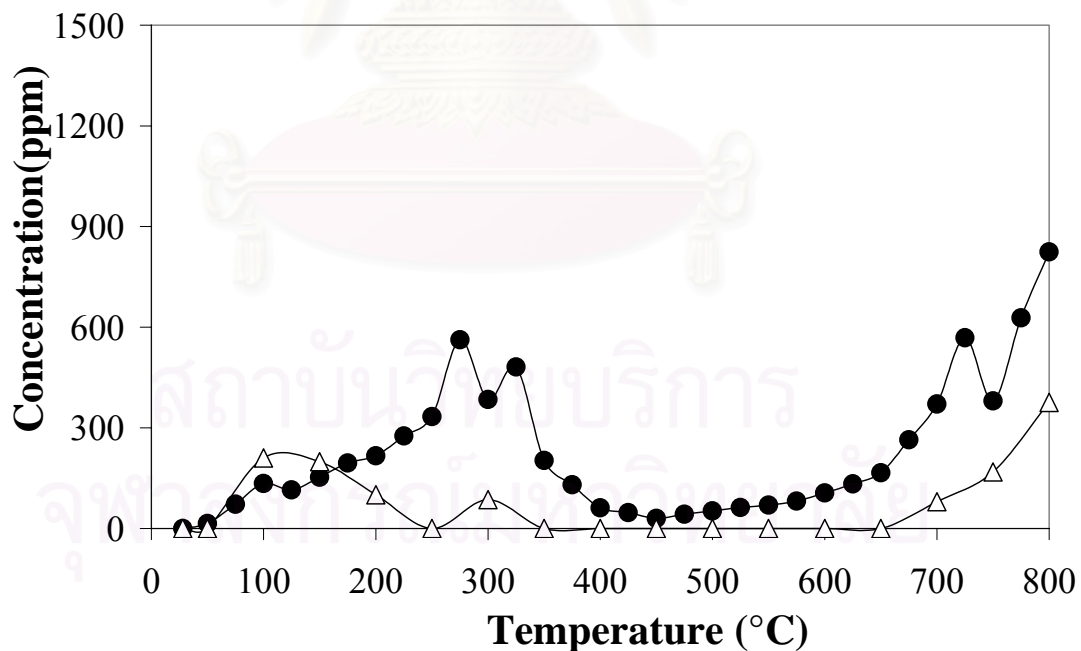


**Figure 4.11** The temperature programmed oxidation profiles of 2 wt% Ag/Al<sub>2</sub>O<sub>3</sub> by using 1% O<sub>2</sub>+1000 ppm. NO as the oxidizing gas after dosing 1000 ppm C<sub>3</sub>H<sub>6</sub> + 5% O<sub>2</sub> at 370°C for 2 h: (△) N<sub>2</sub> and (●) CO<sub>2</sub>.

For  $S_{\text{TPOH}}$  species, a large amount  $\text{CO}_2$  released at low temperature and disappearance of the  $\text{CO}_2$  peak at high temperature imply that this species are partially reactive with  $\text{NO}+\text{O}_2$ . However, the remainder of  $\text{CO}_2$  peak at high temperature was observed as seen in Figures 4.10 and 4.11. It is revealed that some of  $S_{\text{TPOH}}$  was not reactive with  $\text{NO}+\text{O}_2$ . It was remarked that after TPD technique  $S_{\text{TPOH}}$  species was oxidized by  $\text{NO}+\text{O}_2$  and appeared at the lower temperature where it was removed under  $\text{NO}+\text{O}_2$  without TPD. This indicates that the presence of the TPD surface species may be inhibit the reaction of TPO surface species.

The reactivity of  $S_{\text{TPOH}}$  is in agreement with the results of Shimizu et al. [30] and Meunier et al [34]. Shimizu et al. reported regarding the reactivity of acetate, which is produced via the partial oxidation hydrocarbon that the acetate, which was stable in  $\text{O}_2$  atmosphere, was reactive in  $\text{NO}+\text{O}_2$ . In addition, Meunier et al. suggested that nitrate species could still be observed over  $600^\circ\text{C}$ . It was remarked that the  $S_{\text{TPOH}}$  species after TPD step were readily reactive with  $\text{NO}+\text{O}_2$  and removed at the lower temperature where they were removed under  $\text{NO}+\text{O}_2$  without TPD. This indicates that the TPD species may inhibit the reaction of TPO surface species because the TPD species are much more easily reacted with oxidant gases than the TPO species.

Unfortunately, we can not determine from these experiments that whether  $S_{\text{TPOH}}$  is reacted with  $\text{NO}+\text{O}_2$  or not. The reactivity with reactants gas was not observed because the little amount of this species was released in TPO step at low temperature. From these results, the reactivity tests of surface species over 10%  $\text{Ag}/\text{Al}_2\text{O}_3$  were made to give the more information confirmed.

In case of 10% $\text{Ag}/\text{Al}_2\text{O}_3$ , the concentrations of carbon dioxide and nitrogen containing compounds removed during the oxidation steps by using  $\text{NO}+\text{O}_2$  as the oxidizing gases without and with TPD step are exhibited in Figures 4.12 and 4.13, respectively. The reactivity of surface species illustrated some similar results with 2% $\text{Ag}/\text{Al}_2\text{O}_3$ .

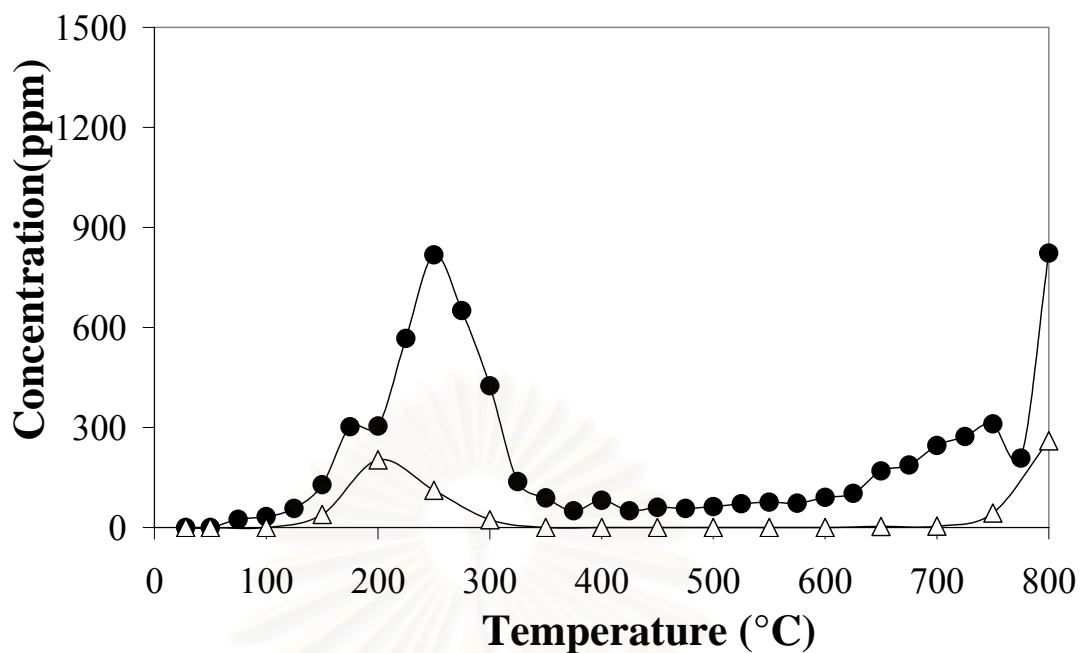


**Figure 4.12** The temperature programmed oxidation profiles of 10 wt% Ag/Al<sub>2</sub>O<sub>3</sub> by using 1% O<sub>2</sub>+1000 ppm. NO TPD as the oxidizing gas after dosing 1000 ppm C<sub>3</sub>H<sub>6</sub> + 5% O<sub>2</sub> at 210°C for 2 h: (△) N<sub>2</sub> and (●) CO<sub>2</sub>.

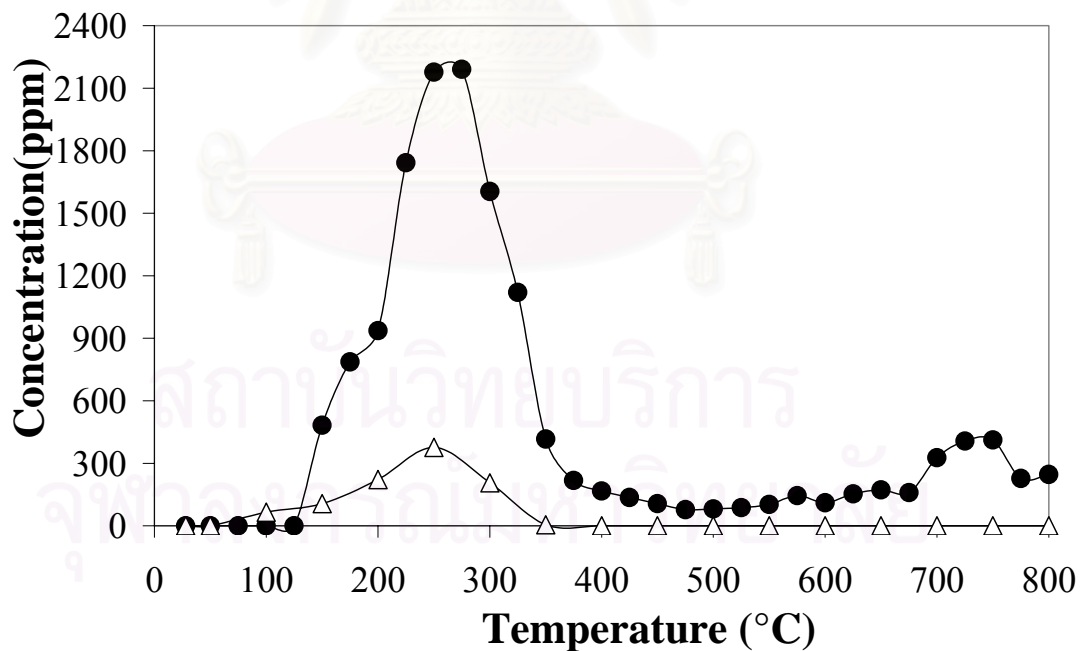


**Figure 4.13** The temperature programmed oxidation profiles of 10 wt% Ag/Al<sub>2</sub>O<sub>3</sub> by using 1% O<sub>2</sub>+1000 ppm. NO as the oxidizing gas after dosing 1000 ppm C<sub>3</sub>H<sub>6</sub> + 5% O<sub>2</sub> at 210°C for 2 h: (△) N<sub>2</sub> and (●) CO<sub>2</sub>.

Considering the reactivity of surface species at moderate ( $S_{TPDM}$ ) and high temperature (both  $S_{TPDH}$  and  $S_{TPOH}$  species), when  $NO+O_2$  were used as the oxidizing gases, the vanishing of carbon dioxide peak appeared both TPD profile (Figure 4.7) and TPO profile (Figure 4.8) was observed while a large amount of carbon dioxide peak much more produced at lower temperature ( $250^\circ C$ ) as shown in Figure 4.13, which is different from low loading silver.

From the above results described in section 4.2.2, the observation of five types of surface species indicates the complication in formation of surface species. We can speculate that all surface species involve the formation of  $N_2$  or  $CO_2$  in HC-SCR on  $Ag/Al_2O_3$  because these species are reacted with reactant gases in reaction temperature. However, there are only two surface species,  $S_{TPDL}$  and  $S_{TPOH}$ , regarding the production of  $N_2$ . Considering the behavior of two surface species,  $S_{TPDL}$  species can decompose or desorb while  $S_{TPOH}$  is oxidized with  $NO+O_2$  to produce  $N_2$ . And the temperature of decomposition or oxidation for both species can shift together with the reaction temperature. Therefore, it is predicted that there are at least two main reaction pathways dependent on characteristic of surface species and temperature of reaction. The parallel reaction mechanisms are decomposition and oxidation of surface species as shown in equation 4.1 as well as 4.2, respectively.



First,  $S_{TPDL}$  species decomposed or desorbed to produce nitrogen and carbon dioxide. This reaction occurs at moderate temperature. Second, the oxidations of  $S_{TPOH}$  species with  $NO+O_2$  and  $O_2$  are performed at low temperature while the remainder of  $S_{TPOH}$  species is oxidized with  $NO+O_2$  to produce nitrogen at high temperature.



#### 4.2.3 The nature study by using physical mixture of Ag/SiO<sub>2</sub> and Al<sub>2</sub>O<sub>3</sub>

Although the characteristic of surface species was investigated using the reactivity tests, but this methods does not show the appeared position of surface species that occur on metal active site or metal-support interface or support active site. In this section, the study of surface species was carried out on a physical mixture of Ag/SiO<sub>2</sub> and Al<sub>2</sub>O<sub>3</sub> on the assumption that SiO<sub>2</sub> is not active for the SCR reaction [76]. Before the study by using physical mixture, the activities and selectivities of these mixture systems are necessarily tested to consider the NO and C<sub>3</sub>H<sub>6</sub> conversions. If the similar patterns of TPR data with Ag/Al<sub>2</sub>O<sub>3</sub> are observed, the mixture of Ag/SiO<sub>2</sub> and Al<sub>2</sub>O<sub>3</sub> will be used to probe the behavior of surface species. Figure 4.15 shows temperature programmed reaction profiles of 2% Ag/SiO<sub>2</sub> and Al<sub>2</sub>O<sub>3</sub>. The conversions result in two parts separately. First, the maximum yield of nitrogen slightly decrease from 35% at 250 °C while the C<sub>3</sub>H<sub>6</sub> conversion rises together with NO conversion and reaches maximum at 300°C. This maximum conversion is 95%. The other, both NO and C<sub>3</sub>H<sub>6</sub> conversions increase again after the reductive conversion has been observed at 350°C. The overall NO reduction conversion reaches a sharp maximum of approximately 70% at 500°C. The peak for reduction to N<sub>2</sub>O occurs about 200-350 and 450-550°C.

The TPR profile over 10% Ag/SiO<sub>2</sub> and Al<sub>2</sub>O<sub>3</sub> is shown in Figure 4.16. Similar tendency with 2% silver is observed. The overall NO reduction conversion reaches a sharp maximum of approximately 10% and 50% at 200 and 500°C, respectively. In term of CO<sub>2</sub>, the first CO<sub>2</sub> peak appears at 200°C and reaches a constant maximum at 95% until the temperature increase to 350°C. The complete combustion of second CO<sub>2</sub> peak occurs at 500°C.

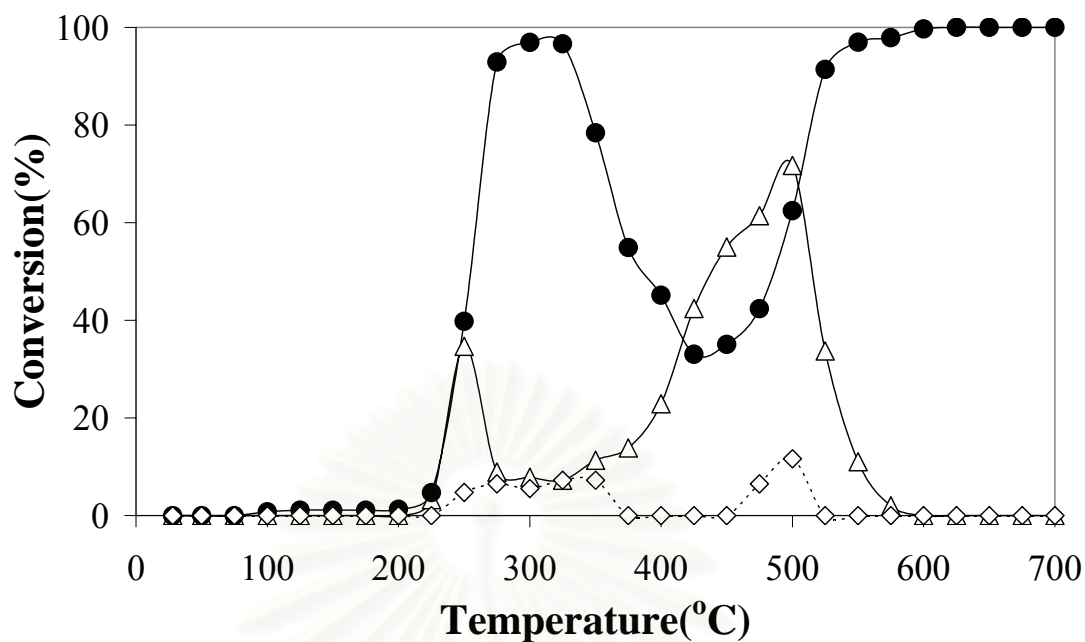


**Figure 4.14** The temperature programmed reaction profiles of 2 wt% Ag/SiO<sub>2</sub> and Al<sub>2</sub>O<sub>3</sub> for the selective catalytic reduction of NO by C<sub>3</sub>H<sub>6</sub> under excess oxygen: (●) C<sub>3</sub>H<sub>6</sub> conversion, (△) NO conversion and (◇) NO conversion to N<sub>2</sub>O.

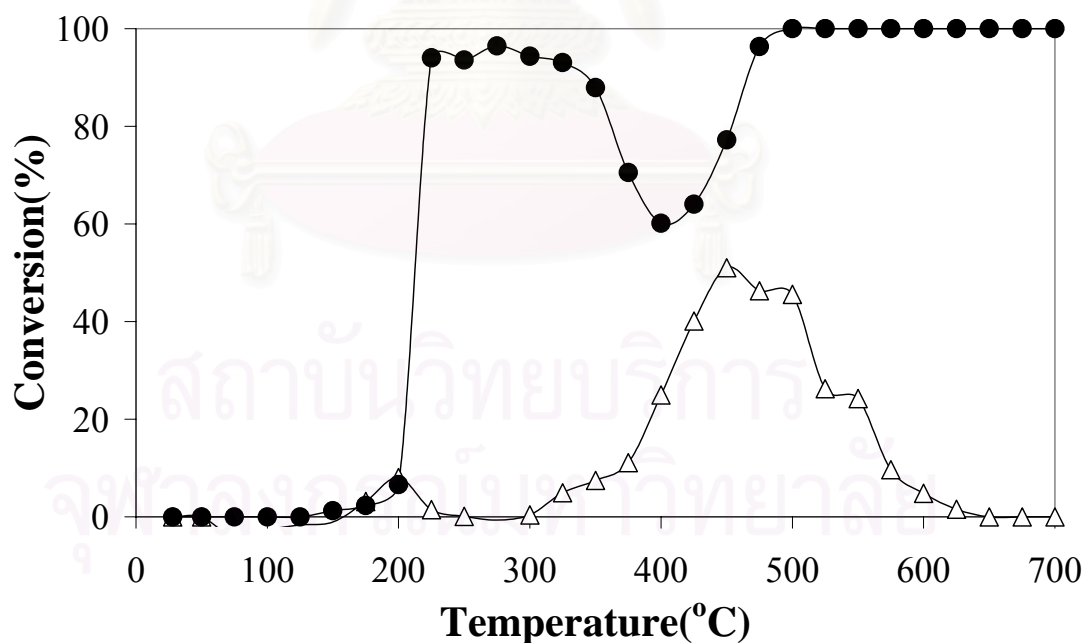


**Figure 4.15** The temperature programmed reaction profiles of 10 wt% Ag/SiO<sub>2</sub> and Al<sub>2</sub>O<sub>3</sub> for the selective catalytic reduction of NO by C<sub>3</sub>H<sub>6</sub> under excess oxygen: (●) C<sub>3</sub>H<sub>6</sub> conversion and (△) NO conversion

The comparisons of TPR results between Ag/Al<sub>2</sub>O<sub>3</sub> and the physical mixtures method show the different profile. The profile of TPR over Ag/Al<sub>2</sub>O<sub>3</sub> appears one while the physical mixtures show two characteristic. Hence, these methods not use to investigate the behavior of surface species. However, from both methods, the significant differentia between low and high silver loading is observed. The NO conversion for low silver loading reaches higher maximum than high silver loading. It indicates that the low silver loading promote NO reduction. In contrast, CO<sub>2</sub> from combustion over high loading much more produce than low loading silver and onset temperature over high loading shift to lower temperature. This result demonstrates that high loading is promoter for HC combustion. This behavior is in agreement with the results reported several work [36, 76].

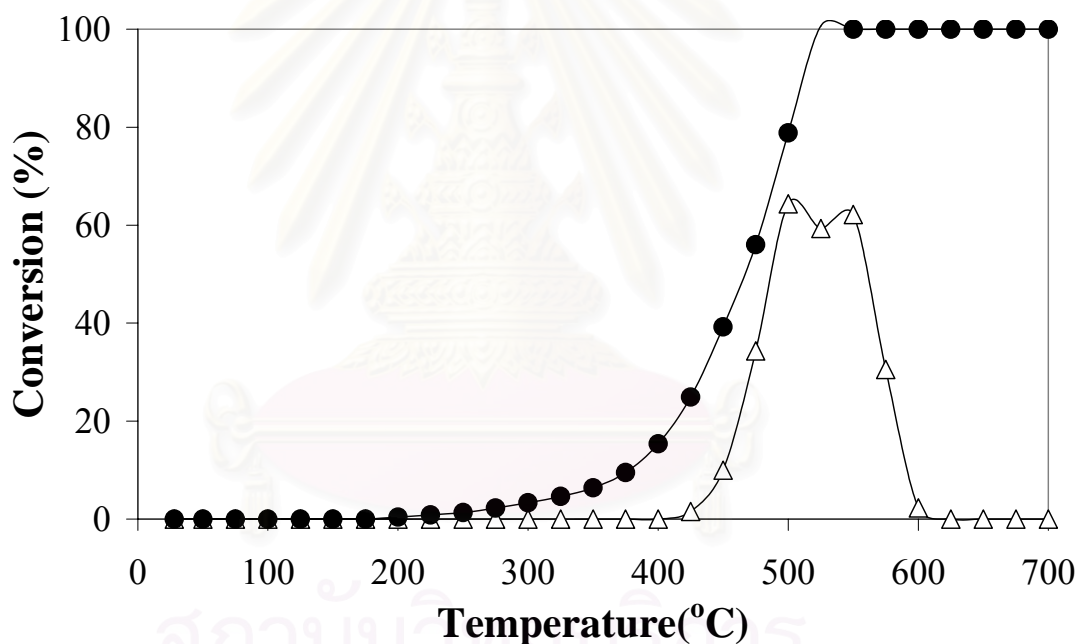


**Figure.4.16** The temperature programmed reaction profiles of Al<sub>2</sub>O<sub>3</sub> for the selective catalytic reduction of NO by C<sub>3</sub>H<sub>6</sub> under excess oxygen: (●) C<sub>3</sub>H<sub>6</sub> conversion and (△) NO conversion

In addition, we found that at high temperature (400-600°C) the NO conversion profile of SCR over physical mixture show the similar activity pattern with Al<sub>2</sub>O<sub>3</sub> as shown in Figure 4.16. The NO conversion over Al<sub>2</sub>O<sub>3</sub> catalyst appeared at temperature range from 350 to 600 °C. Another NO conversion at low temperature may occur over Ag/SiO<sub>2</sub>. To confirm this assumption, TPR of Ag/SiO<sub>2</sub> was made and

shown in Figure 4.17. It is noted that both NO and C<sub>3</sub>H<sub>6</sub> conversion appeared approximately 200-300°C show only effect of silver.

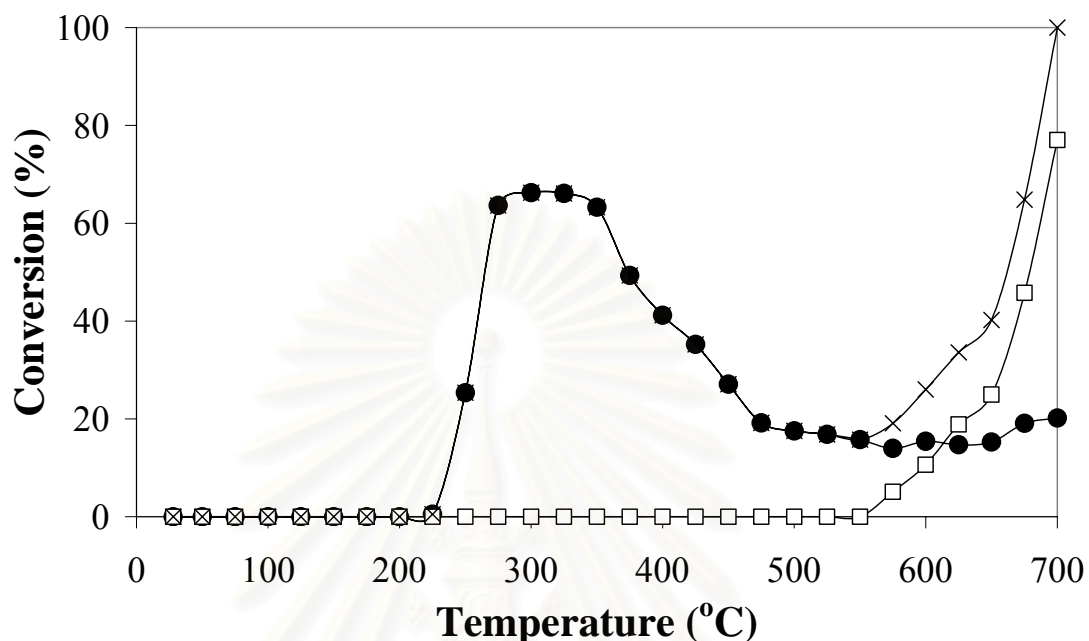


**Figure 4.17** The temperature programmed reaction profiles of 2 wt% Ag/SiO<sub>2</sub> for the selective catalytic reduction of NO by C<sub>3</sub>H<sub>6</sub> under excess oxygen: (●) C<sub>3</sub>H<sub>6</sub> conversion to CO<sub>2</sub>, (x) total C<sub>3</sub>H<sub>6</sub> conversion and (□) C<sub>3</sub>H<sub>6</sub> conversion to CO.

From the above result, temperature programmed technique was used to study the nature of surface species over Ag/SiO<sub>2</sub> catalyst to classify the occurred species over silver active site. The surface species have to be produced at a temperature 370 °C in the first step of TPD-TPO experiment. After dosing steps, the surface species occur both TPD and TPO steps. Figures 4.17 and 4.18 show gas evolution from surface of the 2 wt% Ag/SiO<sub>2</sub> dosed with reactants (C<sub>3</sub>H<sub>6</sub>+NO+O<sub>2</sub>) at 370 °C for 2 h during TPD and TPO steps, respectively. The released gases during TPD step consist CH<sub>4</sub> and a little CO<sub>2</sub> while no N<sub>2</sub> was detected. A little CO<sub>2</sub> group appears at 350°C while small CH<sub>4</sub> is observed at 750°C. From this result, it possible that the adsorbed HC species crack and produce CH<sub>4</sub> at high temperature. Considering the TPO profile, the effluent gases are obtained by decomposition process of some surface species, perhaps intermediates. Above 600 °C three CO<sub>2</sub> peak occurs at the same temperature as oxidation of S<sub>TPOH</sub> species over Ag/Al<sub>2</sub>O<sub>3</sub>. From the corresponding of this species.

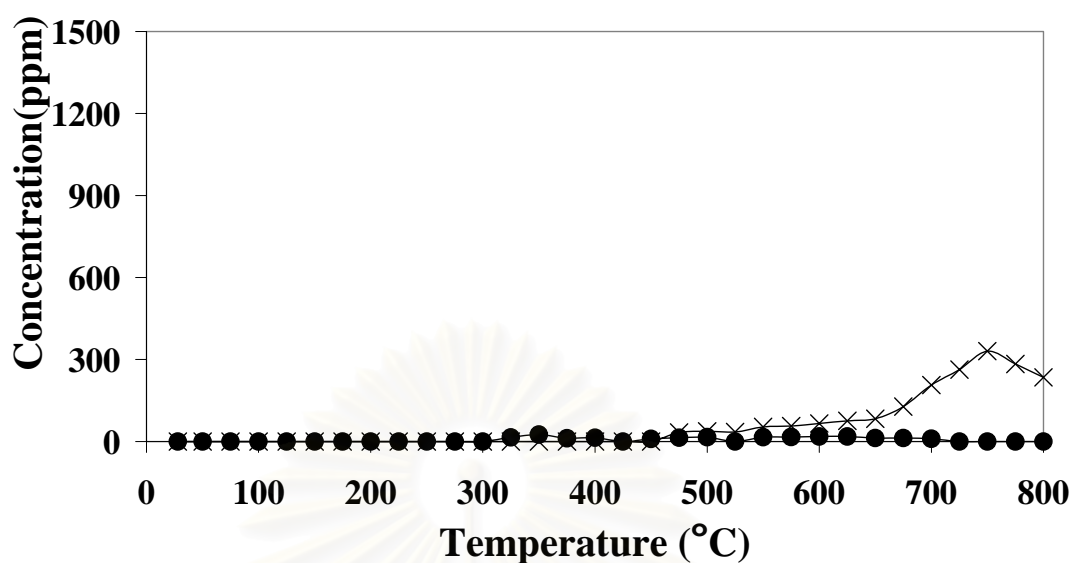


**Figure 4.18** The temperature programmed desorption profiles of 2 wt% Ag/SiO<sub>2</sub> and Al<sub>2</sub>O<sub>3</sub> after dosing 1000 ppm C<sub>3</sub>H<sub>6</sub> + 1000 ppm NO + 5% O<sub>2</sub> at 370°C for 2 h

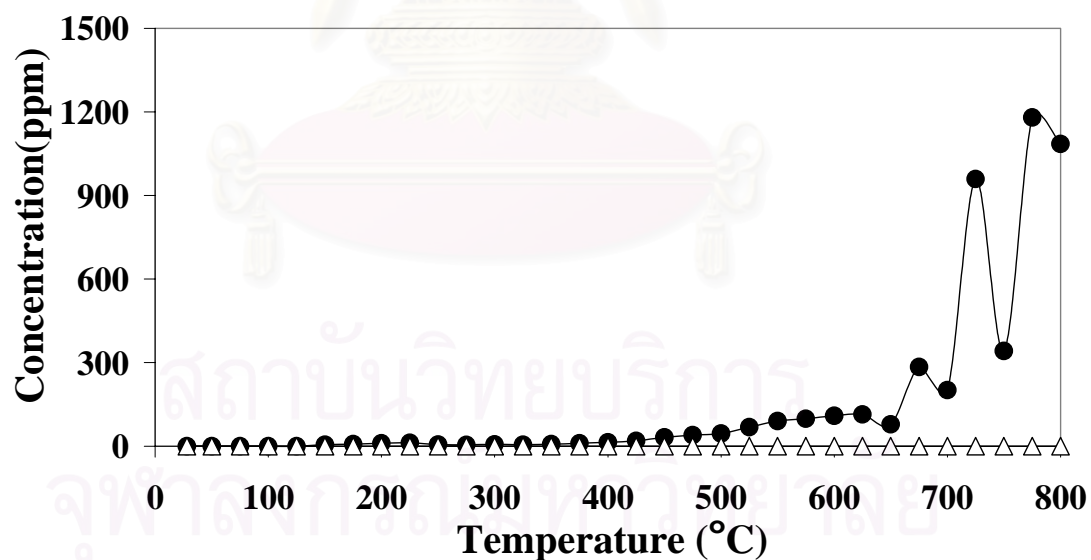


**Figure 4.19** The temperature programmed oxidation profiles of 2 wt% Ag/SiO<sub>2</sub> and Al<sub>2</sub>O<sub>3</sub> by using 1% O<sub>2</sub> as the oxidizing gas after dosing 1000 ppm C<sub>3</sub>H<sub>6</sub> + 5% O<sub>2</sub> at 370°C for 2 h

both Ag/SiO<sub>2</sub> and Ag/Al<sub>2</sub>O<sub>3</sub>, the characteristic study of this species over Ag/SiO<sub>2</sub> probably exhibit the behavior of this species over Ag/Al<sub>2</sub>O<sub>3</sub>. Hence, the reactivity of S<sub>TPOH</sub> species over Ag/SiO<sub>2</sub> was made

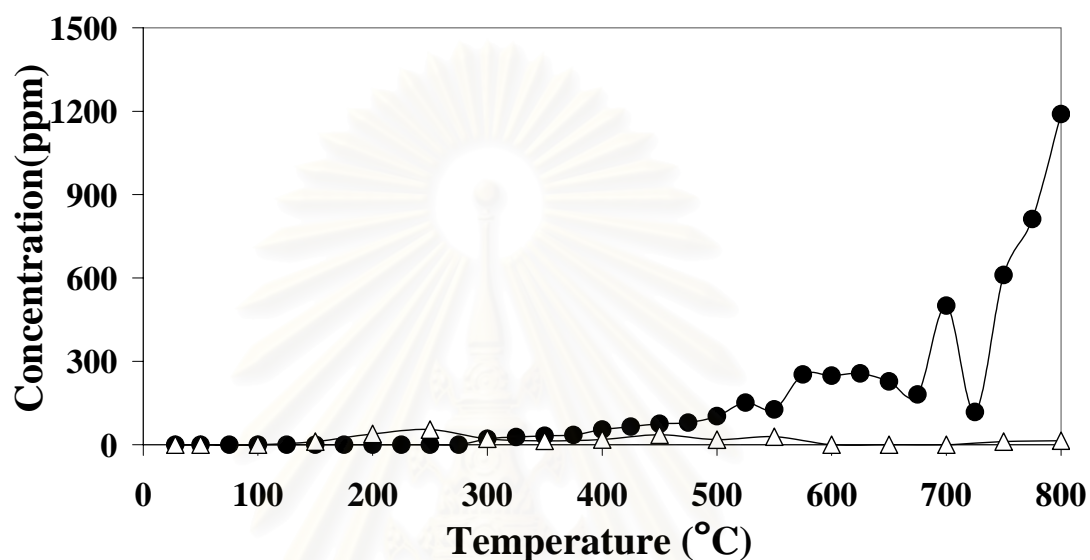


**Figure 4.20** The temperature programmed oxidation profiles of 2 wt% Ag/SiO<sub>2</sub> and Al<sub>2</sub>O<sub>3</sub> by using NO+O<sub>2</sub> as the oxidizing gas after dosing 1000 ppm C<sub>3</sub>H<sub>6</sub> + 5% O<sub>2</sub> at 370°C for 2 h.

The behavior of surface species over Ag/SiO<sub>2</sub> was tested by using the temperature programmed oxidation with NO+O<sub>2</sub> without TPD step. The reactivity of surface species shows in Figure 4.20. The observed groups of CO<sub>2</sub> peak above 500°C not shift to the lower temperature during the changing of oxidant gases. In contrast, the S<sub>TPOH</sub> over Ag/Al<sub>2</sub>O<sub>3</sub> reacted with NO+O<sub>2</sub> at low temperature. It may be possible that the adsorbed species on Ag/SiO<sub>2</sub> occurred only on silver metal active sites and then blocked these active sites, which used to form the adsorbed species while adsorbed species on Ag/Al<sub>2</sub>O<sub>3</sub> appeared both metal and support active sites.

**Table 4.1** Metal Active Sites Measurement of Silver

Sample	Metal Active Site
2 % Ag/Al <sub>2</sub> O <sub>3</sub>	2.50x10 <sup>19</sup>
2 % Ag/Al <sub>2</sub> O <sub>3</sub> after pretreat with time on stream and TPD	1.58x10 <sup>19</sup>
2 % Ag/SiO <sub>2</sub>	1.87x10 <sup>19</sup>
2 % Ag/ SiO <sub>2</sub> after pretreat with time on stream and TPD	0

To confirm this result, the measured metal active site by using N<sub>2</sub>O adsorption method was made. The metal active site of silver is shown in Table 4.1. After pretreated with reaction step and released TPD species, the remainder of silver active site over Ag/Al<sub>2</sub>O<sub>3</sub> is 1.58x10<sup>19</sup> while no silver active site remains for Ag/SiO<sub>2</sub> systems. It confirm that the formation of surface species over Ag/Al<sub>2</sub>O<sub>3</sub> occur on alumina active sites while the adsorbed surface species over Ag/ SiO<sub>2</sub> was formed on only silver active site. It is agreement with the results reported by Bio et al.[20]. They found that the surface species first adsorbed on silver active site and reacted with alumina active site to form the surface species on alumina active sites, then the surface species on alumina active sites was reacted with oxidizing gases to form N<sub>2</sub>.

From the observation regarding the reactivity test of S<sub>TPOH</sub>, this species first adsorbed on silver active sites and can react with NO+O<sub>2</sub> to produce carbon dioxide and nitrogen at low temperature, which is the same temperature of low temperature surface species appearing. Moreover, no S<sub>TPDL</sub> species appeared in case of Ag/SiO<sub>2</sub>. Therefore, it may be possible that the other surface species were produced from the reaction of S<sub>TPOH</sub> surface species with reactant gases. Shimizu et al. [30] found that partially oxidized hydrocarbon species, such as the acetate, can reduce nitrate to N<sub>2</sub> via N-containing organic species, Ag<sup>+</sup>-NCO and -CN adspecies. From this result, the experimental was performed by using the reaction with NO+O<sub>2</sub> of S<sub>TPOH</sub> species over 10%Ag/Al<sub>2</sub>O<sub>3</sub>. The S<sub>TPOH</sub> species was reacted with NO+O<sub>2</sub>+C<sub>3</sub>H<sub>6</sub> for 30 s at 210°C to form the new surface species which was investigated by using TPD step.

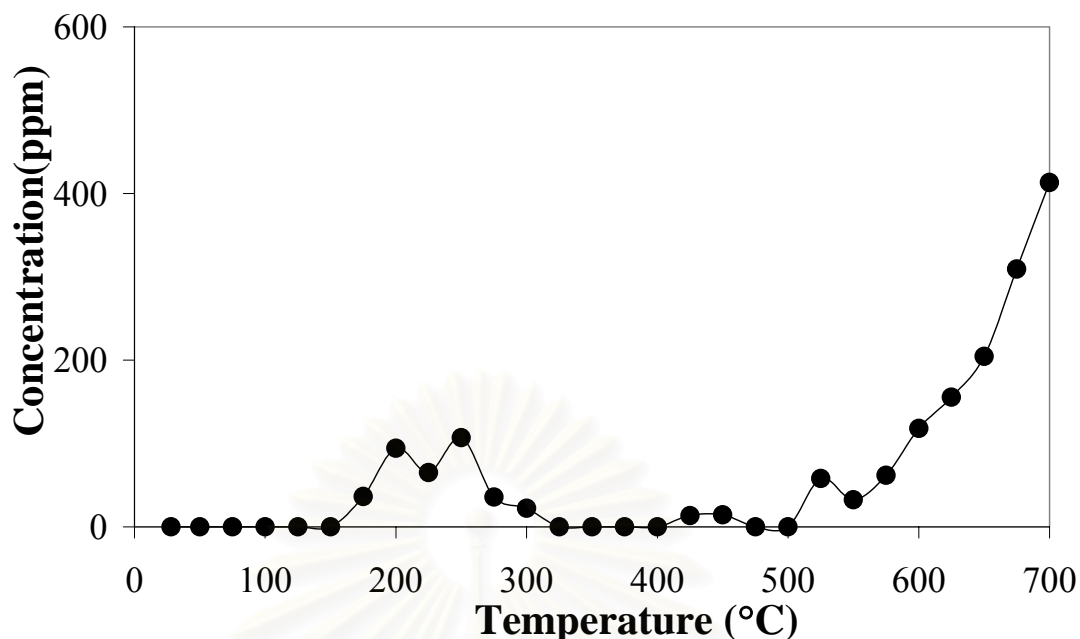


**Figure 4.21** The temperature programmed desorption profiles of  $S_{TPOH}$  surface species over 10 wt%  $Ag/Al_2O_3$  after dosing 1%  $O_2$  + 1000 ppm NO at 210°C for 30 s: (●)  $CO_2$ .

Figure 4.21 shows the effluent gas from temperature programmed desorption  $S_{TPOH}$  species over 10%  $Ag/Al_2O_3$  after expose to 1%  $O_2$  + 1000 ppm NO. The effluent gas consist carbon dioxide and no nitrogen was detected. The carbon dioxide appears both low temperature and high temperature which are close to the temperature of desorbed TPD species. .

However, from above result, the appeared TPD subsurface species may occur from the reaction of TPO surface species with oxidizing gases. Therefore, the other reaction mechanism is the oxidation of TPO surface species ( $S_{TPOH}$ ) with oxidizing gases to produce the other surface species. It is noted that in fact, the latter reaction mechanism may hardly occur on  $Ag/Al_2O_3$  due to its activity being preceded at low operating temperature in real condition.



## CHAPTER V

### CONCLUSIONS AND RECOMMENDATION

In this research, the reaction mechanism of the selective catalytic reduction of NO by hydrocarbon over Ag/Al<sub>2</sub>O<sub>3</sub> catalyst under lean-burn condition is proposed via the investigation of surface species produced on the catalyst surface. The conclusions of these results are summarized as follows:

1. The different activity between low and high silver is observed. Low silver loading promotes the NO reduction at high temperature while high silver loading shows the activity at low temperature.
2. There are five surface species, S<sub>TPDL</sub>, S<sub>TPDH</sub>, S<sub>TPOL</sub>, S<sub>TPOM</sub> as well as S<sub>TPOH</sub>, observed both TPD and TPO step. The conclusions of the reactivity of surface species to various oxidizing gases shown in table 5.1.

**Table 5.1** the reactivity of surface species with oxidizing gases

	S <sub>TPDL</sub>	S <sub>TPDH</sub>	S <sub>TPOL</sub>	S <sub>TPOM</sub>	S <sub>TPOH</sub>
O <sub>2</sub>	-	+	+	+	+
NO+O <sub>2</sub>	-	+	n/a	+	+

3. The reaction mechanisms for the production of N<sub>2</sub> over Ag/Al<sub>2</sub>O<sub>3</sub> consists two main pathways including the decomposition of S<sub>TPDL</sub> surface species and the oxidation of S<sub>TPOH</sub>.

4. From the reactivity study of surface species over Ag/Al<sub>2</sub>O<sub>3</sub> and Ag/SiO<sub>2</sub> found that the S<sub>TPOH</sub> surface species primary occurs on metal active sites. After that, this species can move to alumina active site and then reacted with NO+O<sub>2</sub> to form S<sub>TPDL</sub> species.

From this work, the recommendations for further study can be as follows:

1. To confirm the proposed mechanism for  $C_3H_6+NO+O_2$  reaction, the other techniques should be simultaneously used.
2. To employ extensively the investigation of surface species by an experimental set of three continuous steps for the prediction of reaction mechanism, other reactions should be tested, especially the reaction involving the ambiguous mechanism.
3. To develop the catalytic performance of  $Ag/Al_2O_3$  catalyst, the detailed information about the effect of metal particle size should be profoundly studied.



สถาบันวิทยบริการ  
จุฬาลงกรณ์มหาวิทยาลัย

## REFERENCES

1. De Nevers, N. Air pollution control engineering. New York: McGraw-Hill, 1995.
2. Ronald, M.H. Catalytic abatement of nitrogen oxides-stationary applications. Catal. Today 53 (1999): 519-523.
3. Cohn, G., Steele, D., and Anderson, H. U.S. Patent 2,975,025, 1961.
4. Jan, K., Paolo, F., and Neal, H. Automotive catalytic converters: current status and some perspectives. Catal. Today 77 (2003): 419-449.
5. Obuchi, A., Kaneko, I., Oi, J., Ohi, A., Ogata, A., Bamwenda, G.R., and Kushiyama, S. A practical scale evaluation of catalysts for the selective reduction of NO<sub>x</sub> with organic substances using a diesel exhaust. Appl. Catal. B 15 (1998): 37-47.
6. Li, Z., and Flytzani-Stphanopoulos, M. Selective catalytic reduction of nitric oxide by methane over cerium and silver ion-exchanged ZSM-5 zeolite. Appl. Catal. A 165 (1997): 15-34.
7. Shimizu, K., Satsuma A., and Hattori, T. Catalytic performance of Ag-Al<sub>2</sub>O<sub>3</sub> catalyst for selective catalytic reduction of NO by higher hydrocarbons. Appl. Catal. B 25 (2000): 239-247.
8. Otsuka, K., Takahashi, R., Amakawa, K., and Yamanaka, I. Partial oxidation of light alkanes by NO<sub>x</sub> in the gas phase. Catal. Today 45 (1998): 23-28.
9. Miyadera, T. Alumina –supported silver catalysts for the selective reduction of nitric oxide with propene and oxygen-containing organic compounds. Appl. Catal. B 2 (1993): 119-205.
10. Masuda, K., Tsujimura, K., Shinoda, K. and Kato, T. Silver-promoted catalyst for removal of nitrogen oxides from emission of diesel engines. Appl. Catal. 8 (1996): 33-40.
11. Radtke, F., Koepfel, R. A., Minardi, E. G., and Baiker, A. Catalytic reduction of nitrogen oxides by olefins in the presence of oxygen over copper/alumina: Influence of copper loading and formation of byproducts. J. Catal. 167 (1997): 127-141.

12. Takagi, K., Kobayashi, T., Mizushima, T., Kakuta, N., Abe, A., and Yoshida, K. Selective reduction of NO on Ag/Al<sub>2</sub>O<sub>3</sub> catalyst prepared from boehmite needles. Catal. Today 45 (1998): 123-127.
13. Torre-Abreu, C., Ribeiro, M.F., Henriques, C., and Ribeiro, F.R. Influence of cocation on catalytic activity of CuMOR catalysts for NO SCR by propene. Effect of water presence. Catal. Lett. 43 (1997): 25-29.
14. Haneda, M., Kintaichi, Y., Inaba, M., and Hamada, H. Catalytic performance of silver- and indium-supported TiO<sub>2</sub>-ZrO<sub>2</sub> binary oxide for the selective reduction of nitrogen monoxide with propene. Appl. Surf. Sci. 121/122 (1997): 391-395.
15. Jen, H.W. Study of nitric oxide reduction over silver/alumina catalysts under lean conditions: Effects of reaction condition and support. Catal. Today 42 (1998): 37-44.
16. Seker, E., Cavataio, J., Gulari, E., Lorptionpaiboon, P., and Osuwan, S. Nitric oxide reduction by propene over silver/alumina and silver-gold/alumina catalysts: effect of preparation methods. Appl. Catal. A 183 (1999): 121-134.
17. Furusawa, T., Seshan, K., Lercher, J.A., Lefferts, L., and Aika, K. Selective reduction of NO to N<sub>2</sub> in presence of oxygen over supported silver catalysts. Appl. Catal. B 37 (2002): 205-216.
18. Bethke, K.A., Kung, M.C., Yang, B., Shah, M., Alt, D., Li, C., and Kung, H.H. Metal-oxide catalysts for lean NO<sub>x</sub> reduction. Catal. Today 26 (1995): 169-183.
19. Angelidis, T.N., Christoforou S., Bongiovanni, A., and Kruse, N. On the promotion by SO<sub>2</sub> of the SCR process over Ag/Al<sub>2</sub>O<sub>3</sub>: influence of SO<sub>2</sub> concentration with C<sub>3</sub>H<sub>6</sub> versus C<sub>3</sub>H<sub>8</sub> as reductant. Appl. Catal. B 39 (2002): 197-204.
20. Bion, N., Saussey, J., Haneda, M., and Daturi, M. Study by in situ FTIR spectroscopy of the SCR of NO<sub>x</sub> by ethanol on Ag/Al<sub>2</sub>O<sub>3</sub>-Evidence of the role of isocyanate species. J. Catal. 217 (2003): 47-58.
21. Abe, A., Aoyama, N., Sumiya S., Kakuta, N., and Yoshida, K. Effect of SO<sub>2</sub> on NO<sub>x</sub> reduction by ethanol over Ag/Al<sub>2</sub>O<sub>3</sub> catalyst. Catal. Lett. 51 (1998): 5-9.

22. Aoyama, N., Yosida, K., Abe, A., and Miyadera, T. Characterization of highly active silver catalyst for NO<sub>x</sub> reduction in lean-burning engine exhaust. Catal. Lett. 43 (1997): 249-253.
23. Sumiya, S., Saito, M., He, H., Feng, Q., Takezawa, N., and Yoshida, K. Reduction of lean NO<sub>x</sub> by ethanol over Ag/Al<sub>2</sub>O<sub>3</sub> catalysts in the presence of H<sub>2</sub>O and SO<sub>2</sub>. Catal. Lett. 50 (1998): 87-91.
24. Delahay, G., Coq, B., Ensuque, E., and Figuers, F. Catalytic behavior of Cu/ZrO<sub>2</sub> and Cu/ZrO<sub>2</sub>(SO<sub>4</sub><sup>2-</sup>): in the reduction of nitric oxide by decane in oxygen-rich atmosphere. Catal. Lett. 39 (1996): 105-109.
25. Pasel, J., Speer, V., Albrecht, C., Richter, F., and Papp, H. Metal doped sulfated ZrO<sub>2</sub> as catalyst for the selective catalytic reduction (SCR): of NO with propane. Appl. Catal. B 25 (2000): 105-113.
26. Satokawa, S., Shibata, J., Shimisu, K., Satsuma, A., and Hattori, T. Promotion effect of H<sub>2</sub> on the low temperature activity of the selective reduction of NO by light hydrocarbon over Ag/Al<sub>2</sub>O<sub>3</sub>. Appl Catal. B 42 (2003): 179-186.
27. Halasz, I., and Brenner, A. Selectivity-determining role of C<sub>3</sub>H<sub>8</sub>/NO ratio in the reduction of nitric oxide by propane in presence of oxygen over ZSM-5 zeolites. Catal. Lett. 51 (1998): 195-206.
28. Satokawa, S., Yamaseki, K., and Uchida, H. Influence of low concentration of SO<sub>2</sub> for selective reduction of NO by C<sub>3</sub>H<sub>6</sub> in lean-exhaust conditions on the activity of Ag/Al<sub>2</sub>O<sub>3</sub> catalyst. Appl. Catal. B 34 (2001): 299-306.
29. Eranen, K., Lindfors, L.E., Klingstedt, F., and Murzin, D.Y. Continuous reduction of NO with octane over a silver/alumina catalyst in oxygen-rich exhaust gases: combined heterogeneous and surface-mediate homogeneous reactions. J. Catal. 219 (2003): 25-40.
30. Ukisu, Y., and Miyadera, T. Infrared study of catalytic reduction of lean NO<sub>x</sub> with alcohols over alumina-supported silver catalyst. Catal. Lett. 39 (1996): 265-267.
31. Kameoka, S., Chafik, T., Ukisu, Y., and Miyadera, T. Reactivity of surface species with NO, O<sub>2</sub> and NO+O<sub>2</sub> in selective reduction of NO<sub>x</sub> over Ag/Al<sub>2</sub>O<sub>3</sub> and Al<sub>2</sub>O<sub>3</sub> catalyst. Catal. Lett. 55 (1998): 211-215.

32. Shimizu, K., Kawabata, H., Satsuma, A., and Hattori, T. Formation and reaction of surface acetate on  $\text{Al}_2\text{O}_3$  during reaction by  $\text{C}_3\text{H}_6$ . Appl. Catal. B 19 (1998): L87-L92.
33. Kameoka, S., Chafik, T., Ukisu, Y., and Miyadera, T. Role of organic nitro compounds in selective reduction of  $\text{NO}_x$  with ethanol over different supported silver catalysts. Catal. Lett. 51 (1998): 11-14.
34. Meunier, F.C., Breen, J.P., Zuzaniuk, V., Olsson, M., and Ross, J.R.H. Mechanistic aspects of the selective reduction of NO by propene over alumina and silver-alumina catalysts. J. Catal. 187 (1999): 493-505.
35. Shimizu, K., Kawabata, H., Satsuma, A., and Hattori, T. Role of acetate and nitrates in the selective catalytic reduction of NO by propene over alumina catalyst as investigated by FTIR. J. Phys. Chem. B 103 (1999): 5240-5245.
36. Meunier, F.C., Zuzaniuk, V., Breen, J.P., Olsson, M., and Ross, J.R.H. Mechanistic differences in the selective reduction of NO by propene over cobalt- and silver-promoted alumina catalysts: kinetic and in situ DRIFTS study. Catal. Today 59 (2000): 287-304.
37. Zuzaniuk, V., Meunier, F.C., and Ross, J.R.H. Differences in the reactivity of organo-nitro and nitrio compounds over  $\text{Al}_2\text{O}_3$ -based catalysts active for the selective reduction of  $\text{NO}_x$ . J. Catal. 202 (2001): 340-353.
38. Satsuma, A., and Shimizu, K. In situ FT/IR study of selective catalytic reduction of NO over alumina-based catalysts. Pro. Energ. Combust. 29 (2003): 71-84.
39. Angelidis, T.N., and Tzitzios, V. Promotion of the catalytic activity of a  $\text{Ag}/\text{Al}_2\text{O}_3$  for  $\text{N}_2\text{O}$  decomposition by the addition of Rh. A comparative activity and kinetic study. Ind. Eng. Chem. Res. 42 (2003): 2996-3000.
40. Praserttham, P., Chaisuk, C., Panit, A., and Kriwattanawong, K. Some aspects about the nature of surface species on Pt-based and MFI-based catalysts for the selective catalytic reduction of NO by propene under lean-burn condition. Appl. Catal. B 38 (2002): 227-241.
41. Isarangura na ayuthaya, S., Mongkolsiri, N., Praserttham, P., and Silveston, P.L. Carbon deposits effects on the selective catalytic reduction of NO over zeolite using temperature programmed oxidation technique. Appl. Catal. B 42 (2003): 1-12.

42. Chaisuk, C., and Praserthdam, P. The role of surface species on the SCR of NO by C<sub>3</sub>H<sub>6</sub> under lean-burn conditions over platinum catalyst. React. Kinet Catal. Lett. 78 (2003): 99-105.
43. Srihiranpullo, S., Praserthdam, P., and Mongkhonsi, T. Deactivation of the metal and acidic function for Pt, Pt-Sn and Pt-Sn-K using physically mixed catalysts. Korean J. Chem. Eng. 17 (2000): 548-552.
44. Held, W., Konig, A., Richter, T., and Puppe, L. Catalytic NO<sub>x</sub> reduction in net oxidizing exhaust gas. SAE 900496, 1990
45. Iwamoto, M. Heterogeneous catalysis for removal of NO in excess oxygen progress in 1994. Catal. Today 29 (1996): 29-35.
46. Obuchi, A., Ohi, A., Nakamura, M., Ogata, A., Mizuno, K. and Ohuchi, H. Performance of platinum-group metal catalysts for the selective reduction of nitrogen oxides by hydrocarbons. Appl. Catal. B 2 (1993): 71-80.
47. Hamada, H., Kintaichi, Y., Sasaki, M., and Ito, T. Selective reduction of nitrogen monoxide with propane over alumina and HZSM-5 zeolite: Effect of oxygen and nitrogen dioxide intermediate. Appl. Catal. 70 (1991): L15-L20
48. Hamada, H., Kintaichi, Y., Sasaki, M., and Ito, T. Transition metal-promoted silica and alumina catalysts for the selective reduction of nitrogen monoxide with propane. Appl. Catal. 75 (1991): L1-L8.
49. Sato, S., Yu-u, Y., Yahiro, H., Mizuno, N., and Iwamoto, M. Cu-ZSM-5 zeolite as highly active catalyst for removal of nitrogen monoxide from emission of diesel engines. Appl. Catal. 70 (1991): L1-L5.
50. Torikai, Y., Yahiro, H., and Mizuno N. Enhancement of catalytic activity of alumina by copper addition for selective reduction of nitrogen monoxide by ethane in oxidizing atmosphere. Catal. Lett. 9 (1991): 91-96.
51. Luo, M., Yuan, X., and Zheng, X. Catalyst characterization and activity of Ag-Mn, Ag-Co and Ag-Ce composite oxides for oxidation of volatile organic compounds. Appl. Catal. A 175 (1998): 121-129.
52. McCarty, J.G., Gusman, M., Lowe, D.M., Hildenbrand, D.L. and Lau, H. Stability of supported metal and supported metal oxide combustion catalysts. Catal. Today 47 (1999): 5-17.
53. Chajar, Z., Denton, P., de Bernard, F. B., Primet, M., and Praliaud, H. Influence of silver on the catalytic activity of Cu-ZSM-5 for NO SCR by propane:

- Effect of the presence of water and hydrothermal agings. Catal. Lett. 55 (1998): 217-222.
54. Martínez-Arias, A., Fernández-García, M., Iglesias-Juez, A., Anderson, J.A., Conesa, J.C., and Soria, J. Study of the lean NO<sub>x</sub> reduction with C<sub>3</sub>H<sub>6</sub> in the presence of water over silver/alumina catalysts prepared from inverse microemulsion. Appl. Catal. B 28 (2000): 29-41.
  55. Meunier, F.C., and Ross, J.R.H. Effect of ex situ treatments with SO<sub>2</sub> on the activity of a low loading silver-alumina catalyst for the selective reduction of NO and NO<sub>2</sub> by propene. Appl. Catal. B 24 (2000): 23-32.
  56. Meunier, F.C., Ukropec, R., Stapton, C., and Ross, J.R.H. Effect of the silver loading and some other experimental parameters on the selective reduction of NO with C<sub>3</sub>H<sub>6</sub> over Al<sub>2</sub>O<sub>3</sub> and ZrO<sub>2</sub>-based catalysts. Appl. Catal. B 30 (2001): 163-172
  57. Bethke, K.A., and Kung, H.H. Supported Ag catalysts for the lean reduction of NO with C<sub>3</sub>H<sub>6</sub>. J. Catal. 172 (1997): 93-102.
  58. Shimizu, K., Satsuma, A., and Hattori, T. Selective catalytic reduction of NO by hydrocarbons on Ga<sub>2</sub>O<sub>3</sub>/Al<sub>2</sub>O<sub>3</sub> catalysts. Appl. Catal. B 16 (1998): 319-326.
  59. Hamada, H. Selective reduction of NO by hydrocarbons and oxygenated hydrocarbons over metal oxide catalysts. Catal. Today 22 (1994): 21-40.
  60. Haneda, M., Kintaichi, Y., and Hamada, H. Enhanced activity of metal oxide-doped Ga<sub>2</sub>O<sub>3</sub>-Al<sub>2</sub>O<sub>3</sub> for NO reduction by propene. Catal. Today 54 (1999): 391-400.
  61. Burch, R., Halpin, E., and Sullivan, J.A. A comparison of the selective catalytic reduction of NO<sub>x</sub> over Al<sub>2</sub>O<sub>3</sub> and sulphated Al<sub>2</sub>O<sub>3</sub> using CH<sub>3</sub>OH and C<sub>3</sub>H<sub>8</sub> as reductants. Appl. Catal. B 17 (1998): 115-129.
  62. Delahay, G., Ensuque, E., Coq, B., and Figuéras, F. Selective catalytic reduction of nitric oxide by *n*-decane on Cu/sulfated-zirconia catalysts in oxygen rich atmosphere: effect of sulfur and copper contents. J. Catal. 175 (1998): 7-15.
  63. Sadykov, V., Baron, S., Matyshak, V., Alikina, G., Bunina, R., Rozovskii A., Lunin, V., Lunina, E., Kharlanov, A., and Ivanova, A. A role of surface nitrite and nitrate complexes in NO<sub>x</sub> selective catalytic reduction by hydrocarbons under oxygen excess. Catal. Lett. 37 (1996): 157-162.



64. Shimizu, K., Shibata, J., Yosida, H., Satsuma A., and Hattori, T. Silver-alumina catalysts for selective reduction of NO by higher hydrocarbon: structure of active sites and reaction mechanism. Appl. Catal. B 30 (2001): 151-162.
65. Shimizu, K., Shibata, J., Satsuma, A., and Hattori, T. Mechanistic causes of the hydrocarbon effect on the activity of Ag-Al<sub>2</sub>O<sub>3</sub> catalyst for the selective reduction of NO. Phys. Chem. Chem. Phys. 3 (2001): 880-884.
66. Yan, J.Y., Kung, H.H., Sachtler, W.M.H., and Kung, M.C. Synergistic effect in lean NO<sub>x</sub> reduction by CH<sub>4</sub> over Co/Al<sub>2</sub>O<sub>3</sub> and H-zeolite catalysts. J. Catal. 175 (1998): 294-301.
67. Meunier, F., Breen, J., and Ross, J.R.H. New insights into the origin of NO<sub>2</sub> in the mechanism of the selective catalytic reduction of NO by propene over alumina. Chem. Com. 3 (1999): 259-260.
68. Hamada, H., Kintaichi, Y., Inaba, M., Tabata, M., Yoshinari, T., and Tsuchida, H. Role of supported metals in the selective reduction of nitrogen monoxide with hydrocarbons over metal/alumina catalysts. Catal. Today 29 (1996): 53-57.
69. Tanaka, T., Okuhara, T., and Misono, M. Intermediacy of organic nitro and nitrite surface species in selective reduction of nitrogen monoxide by propene in the presence of excess oxygen over silica supported platinum. Appl. Catal. B 4 (1994): L1-L9.
70. Smits, R.H.H., and Iwasawa, Y. Reaction-mechanisms for the reduction of nitric-oxide by hydrocarbon on Cu-ZSM5 and related catalysts. Appl. Catal. B 6 (1995): L201-L207.
71. Yokoyama, C., and Misono, M. Catalytic reduction of nitrogen-oxides by propene in the presence of oxygen over cerium ion-exchanged zeolites 2. Mechanistic study of role of oxygen and doped metals. J. Catal. 150 (1994): 9-17.
72. Cowan, A., Cant, N., Haynes, B., and Nelson, P. The catalytic chemistry of nitromethane over Co-ZSM5 and other catalysts in connection with the methane-NO<sub>x</sub> SCR J. Catal. 176 (1998): 329-343.
73. Obuchi, A., Wogerbauer, C., Koppel, R., and Baiker, A. Reactivity of nitrogen containing organic intermediates in the selective catalytic reduction of NO<sub>x</sub> with organic compounds: A model study with tert-butyl substituted nitrogen compounds. Appl. Catal. B 19 (1998): 9-22.

74. Sumiya, S., He, H., Abe, A., Takezawa, N., and Yoshida, K. Formation and reactivity of isocyanate (NCO): species on Ag/Al<sub>2</sub>O<sub>3</sub>. J. Chem. Soc. Faraday Tran. 94 (1998): 2217-2219.
75. Kameoka, S., Ukisu, Y., and Miyadera, T. Selective catalytic reduction of NO<sub>x</sub> with CH<sub>3</sub>OH, C<sub>2</sub>H<sub>5</sub>OH and C<sub>3</sub>H<sub>6</sub> in the presence of O<sub>2</sub> over Ag/Al<sub>2</sub>O<sub>3</sub> catalyst: Role of surface nitrate species. Phys.Chem. Chem. Phys. 2 (2000): 367-372.
76. Burch, R., Breen, J.P., and Meunier, A., F.C. A review of the selective reduction of NO<sub>x</sub> with hydrocarbons under lean-burn conditions with non-zeolitic oxide and platinum group metal catalysts. Appl. Catal. B 39 (2002): 283-303.
77. Iglesias-Juez, A., Hungría, A.B., Martínez-Arias, A., Fuerte, A., and Fernández-García, M. Nature and catalytic role of active silver species in the lean NO<sub>x</sub> reduction with C<sub>3</sub>H<sub>6</sub> in the presence of water. J. Catal. 217 (2003): 310-323.
78. Chafik, T., Kameoka, S., Ukisu, Y., and Miyadera, T. In situ diffuse reflectance fourier transform spectroscopy study of surface species involved in NO<sub>x</sub> reduction by ethanol over alumina-supported silver catalyst. J. Mol. Catal. A 136 (1998): 203-211.
79. Captain, D.K., and Amiridis, M.D. In situ FTIR studies of the selective catalytic reduction of NO by C<sub>3</sub>H<sub>6</sub> over Pt/Al<sub>2</sub>O<sub>3</sub>. J. Catal. 184 (1999): 377-389.



## APPENDICES

สถาบันวิทยบริการ  
จุฬาลงกรณ์มหาวิทยาลัย

## APPENDIX A

**SPECIFICATION OF ALUMINA SUPPORT (Al<sub>2</sub>O<sub>3</sub>) TYPE NKH-3****Table A.1** Chemical composition of alumina support type NKH-3

Chemical Composition	Weight percent
Al <sub>2</sub> O <sub>3</sub>	60-70
SiO <sub>2</sub>	30-35
Fe <sub>2</sub> O <sub>3</sub>	0.3-0.5
TiO <sub>2</sub>	0.5-0.7
CaO	0.1-0.2
MgO	0.2-0.4
Na <sub>2</sub> O	0.3-0.4
K <sub>2</sub> O	0.2-0.3
ZrO <sub>2</sub> + HfO <sub>2</sub>	0.03-0.04

**Table A.2** Physical properties of alumina support type NKH-3

Physical properties	
Bulk Density (g/ml)	1.3-1.5
Apparent Specific Gravity	3.1-3.3
Packing Density (lb/ft <sup>3</sup> )	20-25
Pore Volume (ml/g)	1.0-1.3
Surface Area (m <sup>2</sup> /g)	340-350

## APPENDIX B

### CALIBRATION CURVES

The thermal conductivity detectors (TCD) independently connected with two gas chromatographs (SHIMADZU GC-8ATP and SHIMADZU GC-8AIT) were used to analyze the concentration of the sampling gases in the catalytic activity test and an experimental set for studying the nature of surface species. The calibration curves of oxygen, nitrogen and carbon monoxide are obtained from TCD of GC 8ATP whereas those of oxygen, methane, carbon dioxide, nitrous oxide, propene, propane and sulfur dioxide are obtained from TCD of GC 8AIT. It is noted that the operating condition of gas chromatograph for making the calibration curves is maintained to be similar to that for testing the reaction. These calibration curves are given in Figures B.1-B.10.

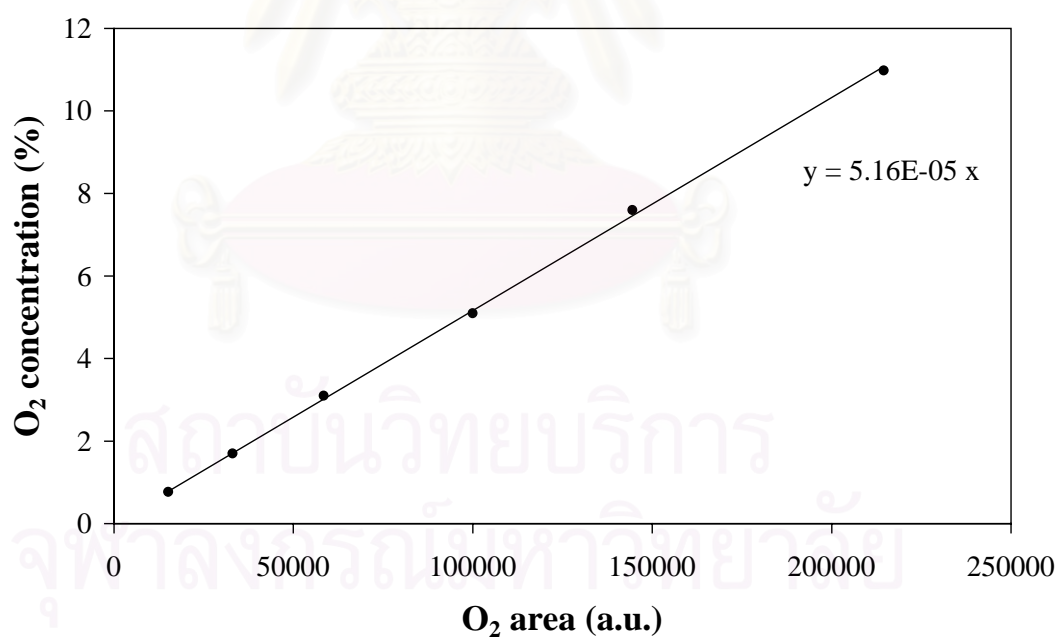


**Figure B.1** The calibration curve of oxygen from TCD of GC 8ATP

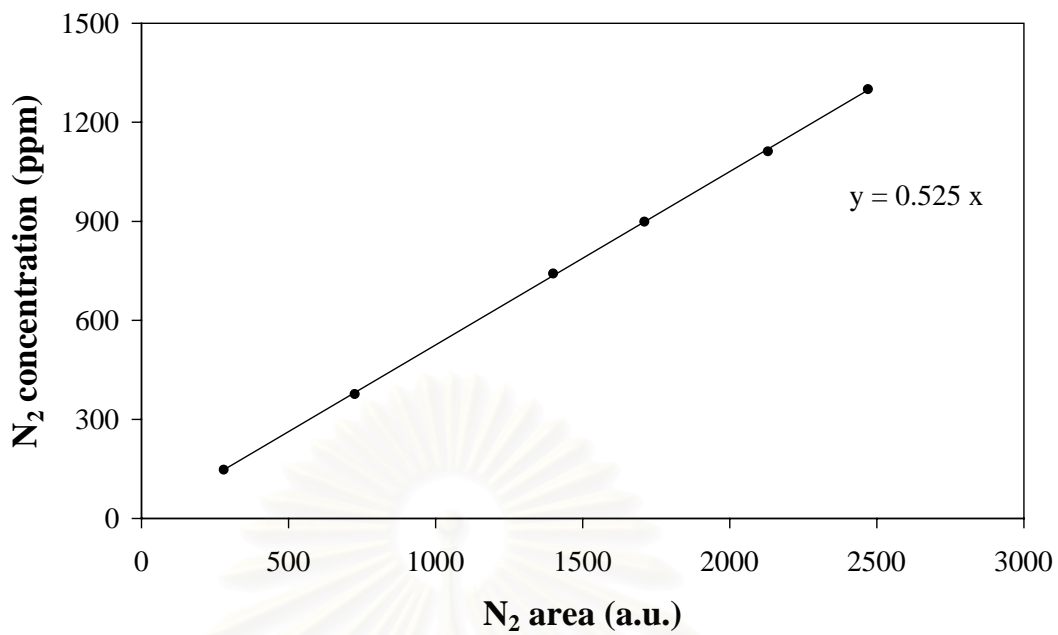


**Figure B.2** The calibration curve of nitrogen

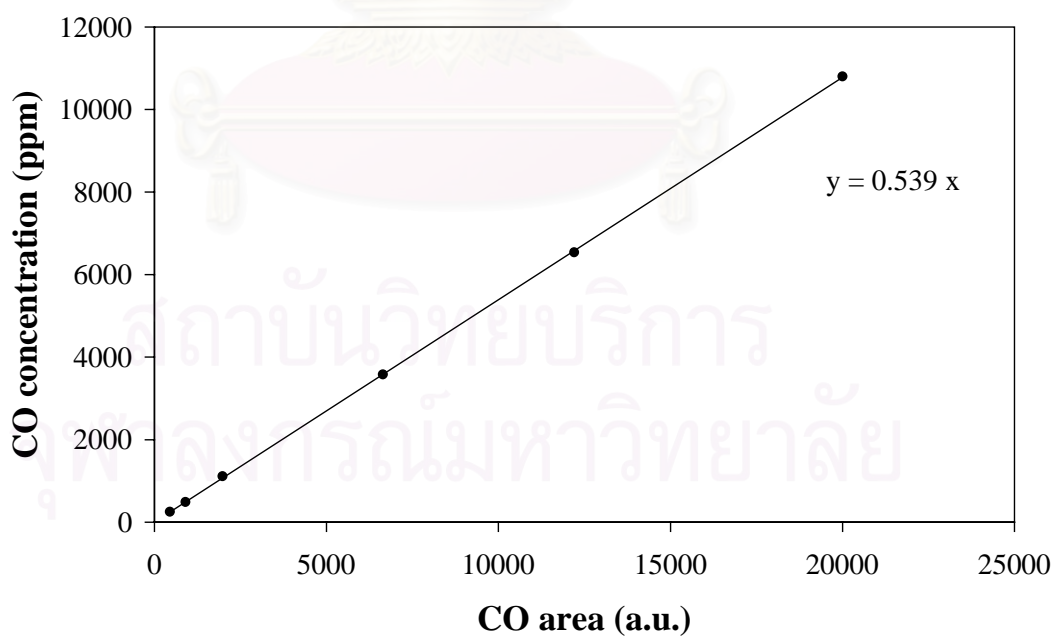


**Figure B.3** The calibration curve of carbon monoxide

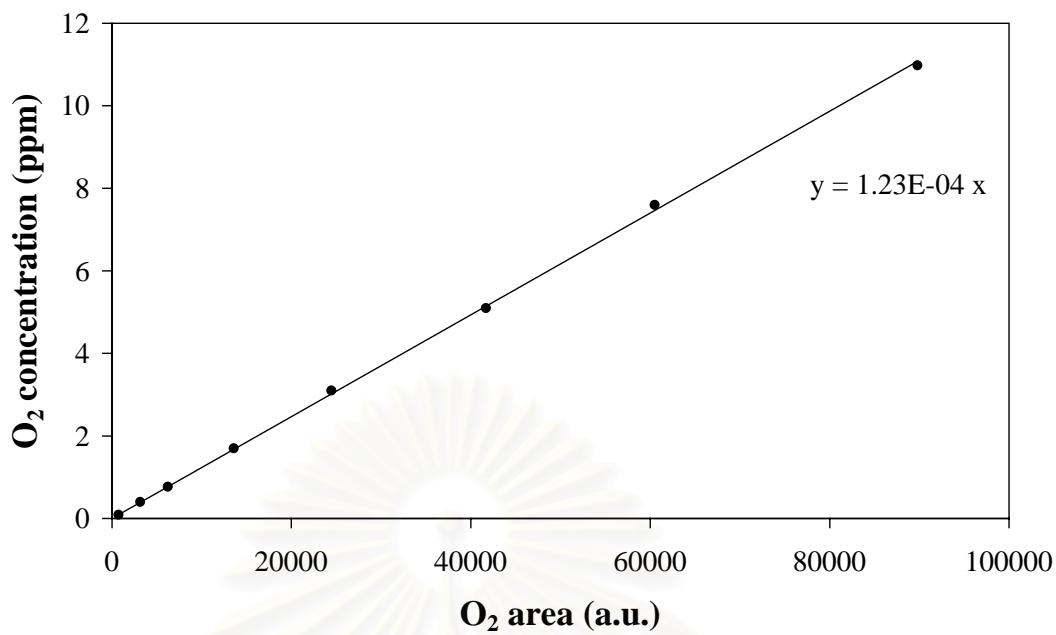


**Figure B.4** The calibration curve of oxygen from TCD of GC 8AIT

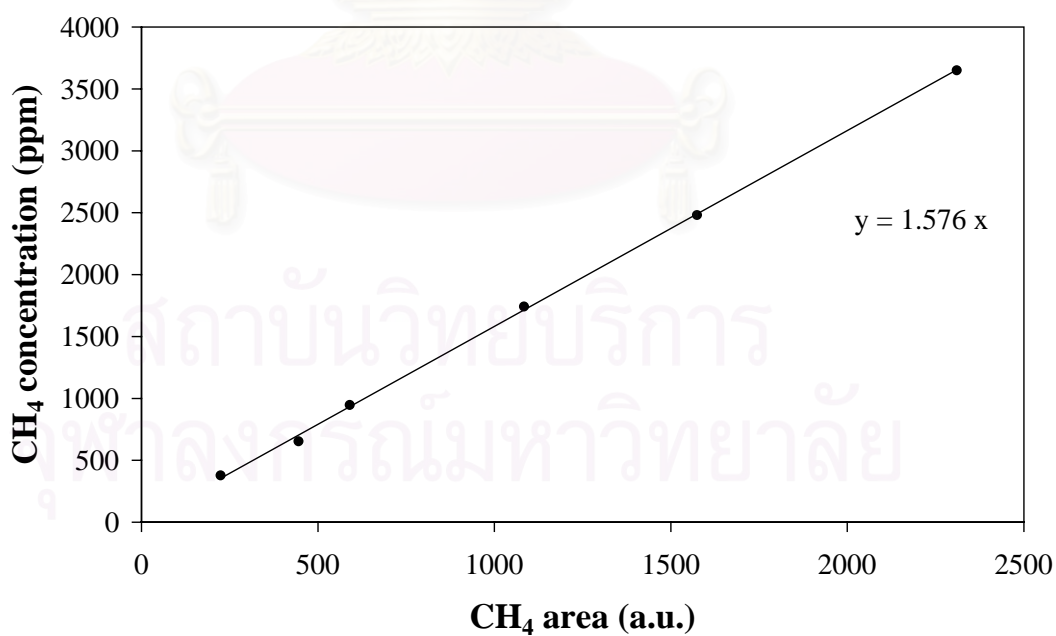


**Figure B.5** The calibration curve of methane

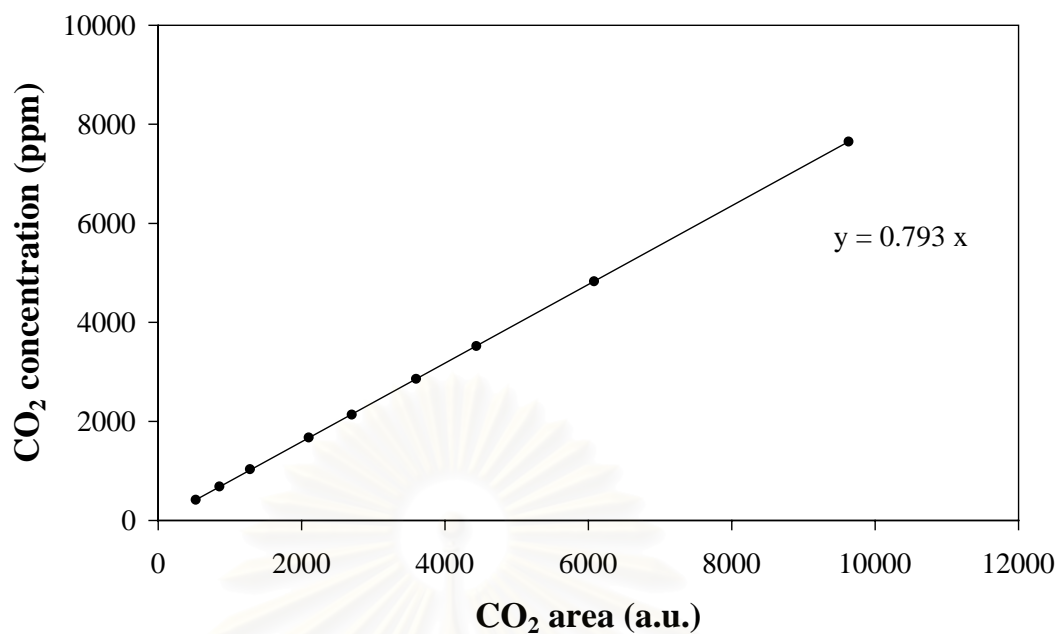


**Figure B.6** The calibration curve of carbon dioxide

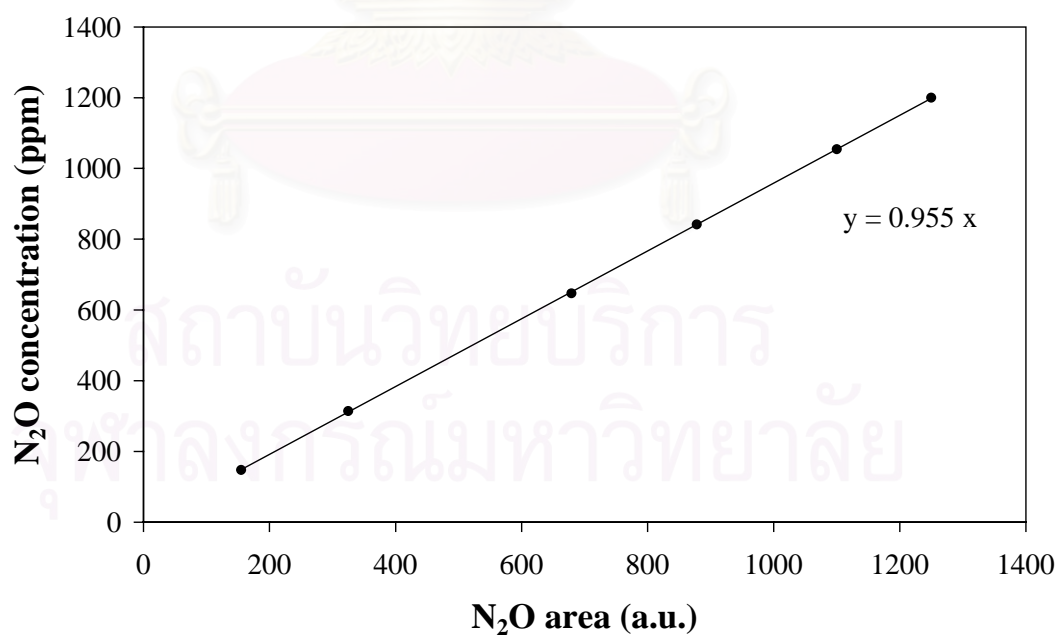


**Figure B.7** The calibration curve of nitrous oxide



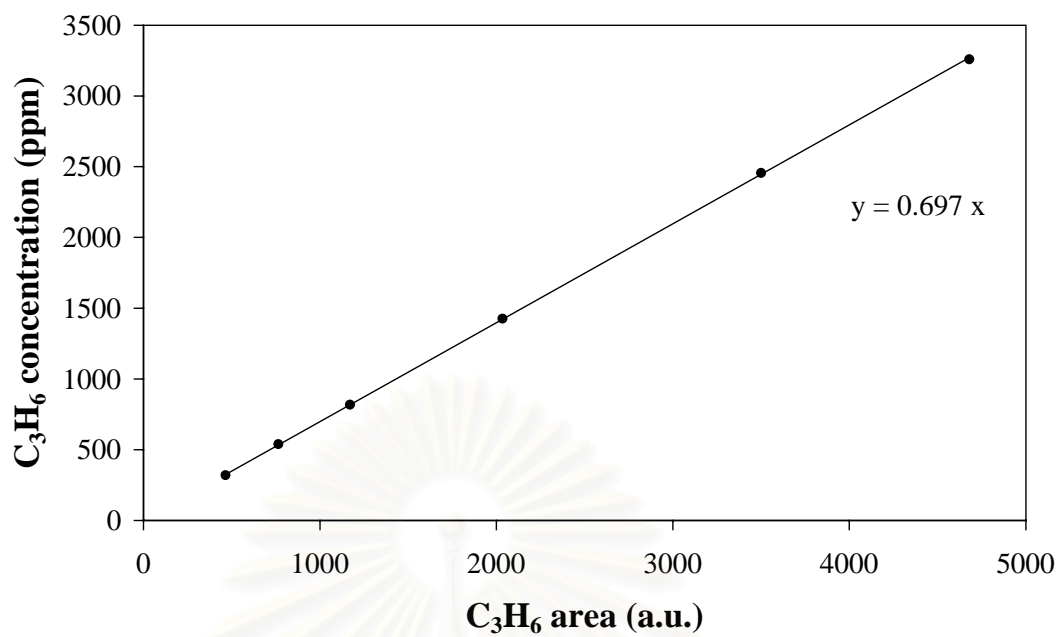


**Figure B.8** The calibration curve of propene

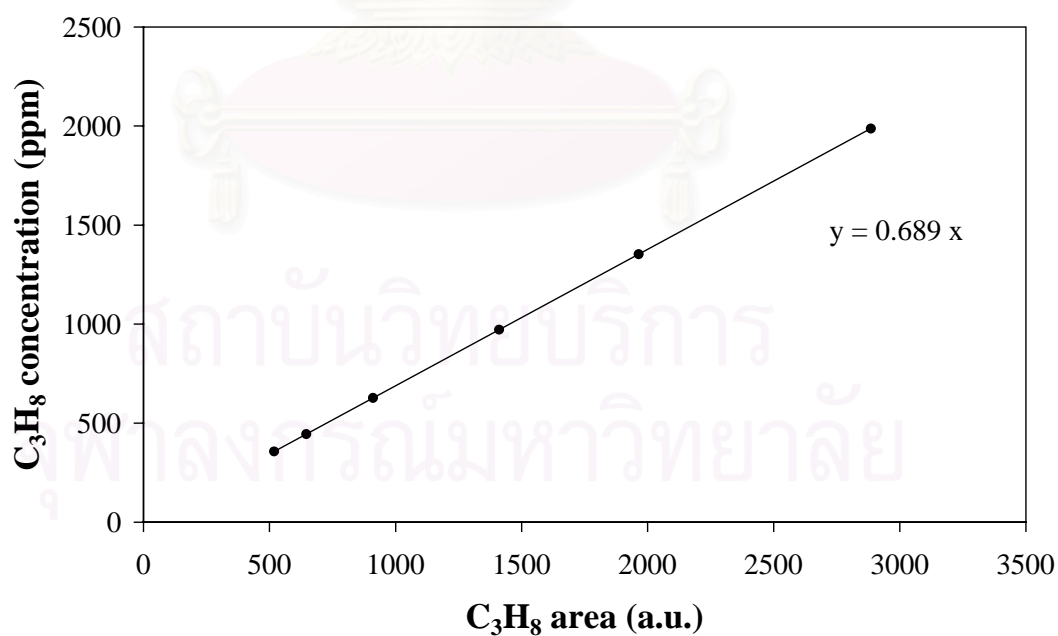


**Figure B.9** The calibration curve of propane

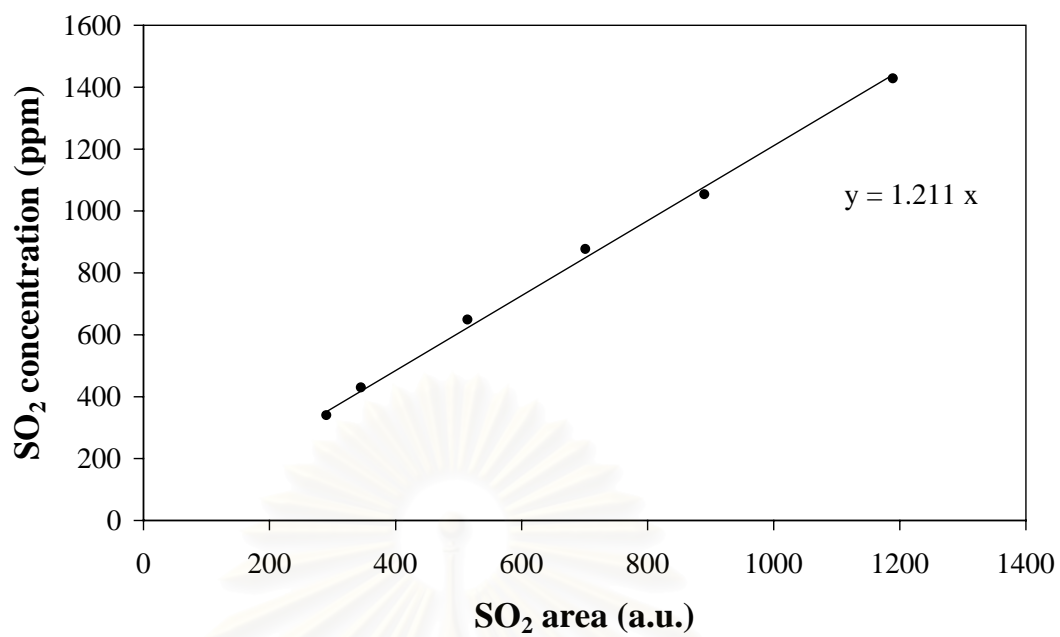


**Figure B.10** The calibration curve of sulfur dioxide

สถาบันวิทยบริการ  
จุฬาลงกรณ์มหาวิทยาลัย

## APPENDIC C

### CALCULATION OF CATALYST PREPARATION

The example of calculation shown is for 2wt% Ag/Al<sub>2</sub>O<sub>3</sub> catalyst. The alumina support weight used for all preparation was 2.0 g.

Based on catalyst 100 g, in order to prepare 2wt% Ag/Al<sub>2</sub>O<sub>3</sub>, the catalyst is composed of

Silver	2	g.
Alumina support	98	g.

The silver compound used is silver nitrate (AgNO<sub>3</sub>), which has a molecular weight 169.87 g, and the molecular weight of silver is 107.87 g.

The cluculation of the amount of each ingredient for required composition of the 2% wt Ag/Al<sub>2</sub>O<sub>3</sub> catalyst is shown as follows:

For 2.0 g. of alumina support used:

- Silver amount

In 100 g of 2% Ag/Al<sub>2</sub>O<sub>3</sub> catalyst has silver = 2 g

In 100 g of 2% Ag/Al<sub>2</sub>O<sub>3</sub> catalyst has alumina = 98 g

If used support 2 g required silver = 0.0408 g

Silver Nitrate (AgNO<sub>3</sub>) 169.87 g has Silver = 107.87 g

Silver 0.0408 g requires Silver Nitrate = 0.3499 g

If used Ag/Al<sub>2</sub>O<sub>3</sub> 2 % requires Silver Nitrate = 0.3499 g

## APPENDIC D

### CALCULATION OF SILVER METAL ACTIVE SITE ON CATALYST

The weight of catalyst used	=	w	g.
Area of N <sub>2</sub> O peak afte adsorption	=	A	unit.
Average area of 50 µl. standard N <sub>2</sub> O peak	=	B	unit.
Amounts of N <sub>2</sub> O asorbed on catalyst	=	Σ(B-A)	unit.
Volume of N <sub>2</sub> O adsorbed on catalyst	=	[Σ(B-A)/B] x50	µl.
Volume of gas 1 mole at 30°C	=	24.86 x 10 <sup>6</sup>	µl.
Mole of N <sub>2</sub> O asorbed on catalyst	=	[[Σ(B-A)/B]x[50/24.86x10 <sup>6</sup> ]]	

1 mole is 6.02x10<sup>23</sup> molecule

Then, molecule of N<sub>2</sub>O adsorbed on catalyst

$$= 2.01 \times 10^{-6} \times [\Sigma(B-A)/B] \times 6.02 \times 10^{23}$$

1 molecule of N<sub>2</sub>O reacts with 2 molecule of silver metal as the equation



Metal active site =  $1.21 \times 10^{18} \times [\Sigma(B-A)/B]/w$  molecule of Ag<sup>0</sup>/g.cat.

สถาบันวิทยบริการ  
 จุฬาลงกรณ์มหาวิทยาลัย

## VITAE

Mr. Natthayak Kiattisirikul was born on 8th October, 1980, in Ayutthaya province, Thailand. He received her Bachelor degree of Science with a major in Chemical Engineering from Chulalongkorn University in March 1996. Since June 1, 1999, he has been studying for his master degree of Engineering from the department of Chemical Engineering, Chulalongkorn University.



สถาบันวิทยบริการ  
จุฬาลงกรณ์มหาวิทยาลัย